ATMOSPHERIC AND SURFACE CONTROL ON EVAPOTRANSPIRATION

ATMOSPHERIC AND SURFACE CONTROL ON EVAPOTRANSPIRATION DURING SOYBEAN MATURATION

by

WILLIAM G. BAILEY, B.Sc.

A Thesis

Submitted to the School of Graduate Studies

in Partial Fulfilment of the Requirements

for the Degree

Doctor of Philosophy

McMaster University

December 1977

DOCTOR OF PHILOSOPHY (1977)
(Geography)

McMASTER UNIVERSITY
Hamilton, Ontario

TITLE: Atmospheric and Surface Control on Evapotranspiration during Soybean Maturation

AUTHOR: William G. Bailey, B.Sc. (University of Toronto)

SUPERVISOR: Professor J.A. Davies

NUMBER OF PAGES: xiv, 162

ABSTRACT

Procedures to calculate hourly and daily evapotranspiration from vegetated surfaces in the absence of lysimetric or micrometeorological measurements are few. A need for physically-based evapotranspiration models to account for atmospheric and surface control on the process is recognized. The micrometeorological investigation described in this study is a response to this need.

During the growing season of 1974, a measurement program was conducted to study atmospheric and surface control on hourly and daytime evapotranspiration. Data collected include net radiation and soil heat flux densities; vertical profiles of temperature, vapour pressure and windspeed; soil moisture; and leaf stomatal resistance.

The combination model which combines equations dealing with the energetics of evapotranspiration and turbulent transfer was employed in the study of hourly evaporative relationships. In the variant of the model used, atmospheric and surface controls on the process are explicitly considered through the deployment of an aerodynamic resistance to water vapour exchange and a surface resistance to water vapour efflux. Hourly estimates of aerodynamic resistance to water vapour exchange were computed from wind profile data. The combination model was insensitive to aerodynamic resistance errors. Hence, simple parameterization of surface roughness and zero plane displacement could be used with single level windspeed measurements to evaluate aerodynamic resistance. Also stability correction could be ignored

for practical applications.

Bulk stomatal resistance was evaluated by residual from the combination model on an hourly basis. Comparison was made with independent estimates developed from stomatal resistance and leaf area index measurements. After canopy development was sufficient to dominate surface energetics, the agreement between the estimations was good. Leaf stomatal and bulk stomatal resistances were found to vary in response to irradiance, soil moisture availability and the vapour pressure deficit of the air. However, the relationship found for the latter is not well defined.

For days when canopy development was sufficient to dominate surface energetics, daytime evapotranspiration totals normalized by equilibrium evapotranspiration are linearly related to soil moisture availability when volumetric soil moisture is below 0.12 mm^3 H_2O/mm^3 soil. With soil moisture above this threshold limit, evapotranspiration proceeds at a potential rate. These results may prove useful in computing daytime evapotranspiration from cropped surfaces.

ACKNOWLEDGEMENTS

This study was supported by grants from the National Research Council of Canada and the Atmospheric Environment Service. Their support is appreciated.

I wish to express sincere gratitude to my supervisor Dr. J.A. Davies for his guidance and assistance throughout the course of this investigation. Also, I would like to acknowledge the helpful advice of Dr. W.R. Rouse and Dr. G.P. Harris, the other members of my supervisory committee. I am most grateful to Dr. G. Collin of the Horticultural Experiment Station, Simcoe, Ontario for providing the experimental site. I wish to record special thanks to Dr. J.T.A. Proctor of the Horticultural Experiment Station for his helpful advice, guidance and assistance throughout the field program. In particular, I am most grateful to Mr. P.F. Mills for his most able assistance during preparations for the field experiment; to Ms. J.E. Barton for her excellent assistance during the field program; to Mr. G. Davis for his assistance during phases of the data collection program; to the staff of the Atmospheric Environment Service Simcoe First Class Station for providing hourly weather observations; to Mr. N. Baumgartner of the Land Resource Science Department, University of Guelph, for providing soil moisture characteristi curves for the experimental site; and to Mrs. C. Moulder for typing the manuscript. My gratitude also extends to Mr. A.M. Sawchuck, Mr. F.D. Barlow and Dr. D.S. Munro for many meaningful discussions which occurred

during my graduate studies.

Special thanks are due to Ms. A.L.M. Skretkowicz, who participated in the collection and analysis of the field data, for her excellent assistance and undaunted optimism. Finally, I am indebted to my family for providing me with the opportunity to pursue my education.

TABLE OF CONTENTS

LIST OF ILLUSTRATIONS

LIST OF TABLES

CHAPTER ONE

INTRODUCTION

The need for procedures to calculate evapotranspiration from vegetation has been long recognized in water and energy balance studies. Satisfactory schemes, in the absence of lysimetric or micrometeorological measurements, are few. Any realistic evapotranspiration model must include parameters to account for atmospheric and surface control on the process. This requirement may be met through the use of the physically-based combination model. First proposed by Penman (1948) for potential evapotranspiration, it has been revised by Penman and Schofield (1951), Slatyer and McIlroy (1961), Monteith (1965) and Tanner and Fuchs (1968) for actual evapotranspiration. The model combines equations dealing with the energetics of evapotranspiration and turbulent transfer such that meteorological information at only one height is needed. However, surface controls on the process must be independently specified.

One of the variants of the combination model, proposed by Monteith (1965) with amendments by Thom (1972), explicitly includes atmospheric and surface control through an aerodynamic resistance to water vapour transfer and a surface resistance to water vapour efflux. Although simple, with a surface resistance representing the restriction to water vapour efflux by the complex physiological and structural characteristics of a plant canopy, it has been used successfully in the study of evapotranspiration from agricultural and forest surfaces (Black et al., 1970;

Monteith et al., 1965; Szeicz and Long, 1969; Szeicz et al., 1969; Szeicz et al., 1973; Tan and Black, 1976). These workers have shown that the surface resistance is related to physiological processes; in essence, it is a bulk stomatal resistance which is approximately equal to the stomatal resistance of all leaves acting in parallel. Although the combination model provides an excellent tool for the analysis of atmospheric and surface evaporative relationships, many researchers have been frustrated in its use for predictive application by the inability to accurately account for bulk stomatal resistance variability. A limited number of researchers, however, have been successful in inferring stomatal response to environmental parameters (Brady et al., 1975; Szeicz et al., 1973; Tan and Black, 1976). Still, little is known about stomatal behaviour for most vegetated surfaces, particularly throughout a growing season.

Although greater knowledge about the process of evapotranspiration, particularly surface control, is being sought, a requirement for simple methods to provide daily totals for application in agriculture, hydrology and other disciplines is acknowledged. Daily totals of evapotranspiration can be derived by accumulating hourly measurements or estimates; however, the necessity also exists for an approach which would utilize simple meteorological data.

During the growing season of 1974, a micrometeorological study was undertaken in southwestern Ontario. The investigation was directed towards the study of atmospheric and surface control on hourly and daytime evapotranspiration. This thesis describes the results of this investigation. The study aims:

(1) to evaluate aerodynamic and bulk stomatal resistances on an hourly basis throughout the growing season and to relate them to environmental parameters; and

(2) to evaluate relationships between daytime evapotranspiration and environmental parameters.

The results from the latter may prove useful in computing evapotranspiration from cropped surfaces.

CHAPTER TWO

THEORETICAL FRAMEWORK

In this chapter, the underlying theory of the energy balance and combination model approaches to evaluating evapotranspiration is presented. The latter is used in the study of atmospheric and surface control on evapotranspiration and underlies the approaches that will be used to estimate daily evapotranspiration.

A. The Energy Balance Approach

For a vegetated surface, following the conservation of energy principle, the energy balance can be expressed as

$$Q^* + \mathrm{div}Q_H + \mathrm{div}\lambda Q_E = Q_H + \lambda Q_E + Q_G + Q_P + Q_S + Q_V \qquad (2.1)$$

in which Q^* is the net radiation flux density, $\mathrm{div}Q_H$ and $\mathrm{div}\lambda Q_E$ are the horizontal divergences of sensible and latent heat, Q_H, λQ_E and Q_G are the vertical heat flux densities of sensible, latent and soil heat, and Q_P, Q_S and Q_V are the flux densities stored by net photosynthesis, net storage of sensible heat and latent heat in the air and net heat storage in the phytomass.

This energy balance equation is applicable to any atmosphere-surface volume containing plant matter as it accounts for storage and horizontal as well as vertical flux densities. For practical

applications, it is customary to simplify this equation by neglecting some of the terms.

The horizontal divergence of sensible and latent heat flux densities between the soil surface ($z = 0$) and a reference height z_R are given by

$$\mathrm{div}Q_H = \int_0^{z_R} \frac{\partial(\rho C_p u\theta)}{\partial\chi}\,dz \simeq \rho C_p z_R \bar{u}\frac{\partial\bar{\theta}}{\partial\chi} \qquad (2.2)$$

and

$$\mathrm{div}\lambda Q_E = \int_0^{z_R} \frac{\partial}{\partial\chi}\left(\frac{\rho C_p u e}{\gamma}\right) dz \simeq \frac{\rho C_p z_R \bar{u}}{\gamma}\frac{\partial\bar{e}}{\partial\chi} \qquad (2.3)$$

in which ρ is the density of air, C_p is the specific heat of air at constant pressure, γ is the psychrometric constant[1], u is horizontal windspeed, θ is air temperature, e is vapour pressure, z is height and χ is horizontal distance. The terms with an overbar are average values for the layer from the soil surface to height z_R. In both approximations, ρ and $\bar{u}$ are assumed independent of χ. With $\bar{u} = 2\ \mathrm{m\ s^{-1}}$, $z_R = 2$ m and $\theta = 293$ K, $\mathrm{div}Q_H$ becomes significant for $\frac{\partial\bar{\theta}}{\partial\chi} \geq 10^{-2}\ \mathrm{K\ m^{-1}}$. Similarly, $\mathrm{div}\lambda Q_E$ becomes significant for $\frac{\partial\bar{e}}{\partial\chi} \geq 1\ \mathrm{Pa\ m^{-1}}$. Hence, the horizontal divergence of sensible and latent heat flux densities will be negligible only if windspeeds are exceptionally low or if the horizontal gradients of temperature and vapour pressure are small.

1. The psychrometric constant $\gamma = \frac{C_p P}{\lambda\varepsilon}$ in which P is atmospheric pressure, λ is the latent heat of vapourization of liquid water and ε is the ratio of the molecular weight of water to the mean molecular weight of dry air. When P = 100 kPa, $\gamma = 66\ \mathrm{Pa\ K^{-1}}$.

For micrometeorological investigations, it is customary to consider the energy balance at a location above a homogeneous surface of substantial extent where the vertical flux densities are constant with height and where the terms $\partial\bar{\theta}/\partial\chi$ and $\partial\bar{e}/\partial\chi$ can be neglected. Constancy of flux density with height is a characteristic which defines the atmospheric boundary layer. The depth of this layer is a function of the distance (fetch) from the leading edge defining surface characteristic change. There is general agreement that the ratio of the boundary layer height to fetch is at least 1:100. A measurement site should therefore be selected in the midst of a large uniform surface to allow measurement to be made within a boundary layer of convenient depth. In this investigation, it is assumed that sufficient horizontal homogeneity existed, such that $\partial\bar{\theta}/\partial\chi$ and $\partial\bar{e}/\partial\chi$ can be neglected and that only the vertical flux densities required assessment. The theoretical limitation of this assumption when canopy coverage is incomplete during early stages of crop development is acknowledged.

The energy flux density from the net storage of sensible and latent heat in the air from the soil surface to a reference height z_R is given by

$$Q_S = Q_{SH} + Q_{SV} \tag{2.4}$$

where

$$Q_{SH} = \int_0^{z_R} \rho Cp \frac{\partial\theta}{\partial t}\, dz \simeq \rho Cp z_R \frac{\partial\theta}{\partial t} \tag{2.5}$$

and

$$Q_{SV} = \int_0^{z_R} \frac{\rho Cp}{\gamma} \frac{\partial e}{\partial t} dz \simeq \frac{\rho Cp}{\gamma} \frac{\partial e}{\partial t} \quad (2.6)$$

in which $\partial\theta/\partial t$ and $\partial e/\partial t$ are the temporal rates of change of temperature and vapour pressure respectively. Setting z_R = 2 m and assuming $\frac{\partial \theta}{\partial t}$ = 5 K h^{-1} and $\frac{\partial e}{\partial t}$ = 100 Pa h^{-1}, Q_{SH} and Q_{SV} are respectively 3.5 Wm^{-2} and 1.0 Wm^{-2}. These terms will be negligible for hourly periods and can be neglected.

The energy flux density from net heat storage in the phytomass layer between the soil surface and the top of the plant canopy CH is given by

$$\dot{Q}_V = \int_0^{CH} \rho_v c_v \frac{\partial \theta_v}{\partial t} dz \quad (2.7)$$

where ρ_v, c_v and θ_v are respectively, the density, specific heat and temperature of the vegetation. Introducing m_v as $\int_0^{CH} \rho_v dz$, assuming that c_v is approximately 70% of the specific heat of water (Thom, 1975) and setting $\frac{\partial \theta_v}{\partial t}$ = 5 K h^{-1}, $\dot{Q}_v$ is 4 Wm^{-2} per kg m^{-2} of vegetal matter. Assuming m_v = 2 kg m^{-2}, a value representative of a fully matured annual agricultural crop, Q_v is only 8 Wm^{-2}, which is negligible.

The net photosynthesis of a plant community per unit area of ground is the gross rate of photosynthesis of the community minus its respiration losses. The energy flux density stored by net photosynthesis is the energy equivalent of net CO_2 assimilation. Assuming the specific energy fixation for CO_2 in net photosynthesis is 10^4 J g^{-1} (Lemon, 1967) and employing the maximum rates of net photosynthesis for cultivated crops (2 to 4 g m^{-2} h^{-1} depending on species (Šesták, Čatský and Jarvis, 1971)),

Q_P reaches maximum values between 6 and 11 Wm^{-2}. However these rates of net photosynthesis would be achieved only during periods of high irradiance, hence Q_P is almost always negligible in comparison with Q^*. As such it can be neglected.

Neglecting $\mathrm{div}Q_H$, $\mathrm{div}\lambda Q_E$, Q_P, Q_S and Q_V, the energy balance equation reduces to

$$Q^* - Q_H - \lambda Q_E - Q_G = 0 \quad . \tag{2.8}$$

This is solved for λQ_E by introducing the Bowen ratio $\beta = Q_H/\lambda Q_E$ and the mass transfer equations

$$Q_H = -\rho Cp \; K_H \frac{\partial \theta}{\partial z} \tag{2.9}$$

and

$$\lambda Q_E = -\frac{\rho Cp}{\gamma} K_W \frac{\partial e}{\partial z} \tag{2.10}$$

in which K_H and K_W are the eddy diffusivities for heat and water vapour and $\partial\theta/\partial z$ and $\partial e/\partial z$ are the vertical gradients of temperature and vapour pressure. Therefore:

$$\lambda Q_E = \frac{Q^* - Q_G}{1 + \gamma \frac{K_H}{K_W} \frac{\partial \theta/\partial z}{\partial e/\partial z}} \simeq \frac{Q^* - Q_G}{1 + \gamma \frac{\Delta\theta}{\Delta e}} \quad . \tag{2.11}$$

In this equation, the eddy diffusivities for heat and water vapour are assumed equal (Swinbank and Dyer, 1967; Dyer, 1967).

Hence, λQ_E can be evaluated from measurements of Q^*, Q_G and temperature and vapour pressure at a minimum of two levels in the boundary layer.

B. The Combination Model Approach

1. Theoretical framework

The combination model combines the energy balance approach of evaluating evapotranspiration with turbulent transfer theory. Its success rests in the height integration of turbulent transfer functions between the surface and the height of measurement.

The mass transfer equations for sensible and latent heat (equations 2.9 and 2.10), in which molecular exchange has been neglected, can be re-arranged and integrated with height to give

$$Q_H = \rho Cp \frac{[\theta(0) - \theta(z)]}{\int_0^z \frac{dz}{K_H}} \qquad (2.12)$$

and

$$\lambda Q_E = \frac{\rho Cp}{\gamma} \frac{[e(0) - e(z)]}{\int_0^z \frac{dz}{K_W}} \qquad (2.13)$$

in which $\theta(0)$ and $e(0)$ are mean surface temperature and vapour pressure and $\theta(z)$ and $e(z)$ are the temperature and vapour pressure at height z. These expressions are analogous to Ohm's Law, where a property flux density is equal to a concentration difference divided by an aerodynamic

resistance, if by definition $r_{aH} = \int_0 \frac{dz}{K_H}$ and $r_{aV} = \int_0 \frac{dz}{K_W}$. Hence

$$\lambda Q_E = \frac{\rho Cp}{\gamma} \frac{[e(0) - e(z)]}{r_{aV}} \qquad (2.14)$$

and

$$Q_H = \rho Cp \frac{[\theta(0) - \theta(z)]}{r_{aH}} \qquad (2.15)$$

in which r_{aH} and r_{aV} are aerodynamic resistances for heat and water vapour exchange.

Practical application of these flux density expressions is restricted by difficulties in assessing $\theta(0)$ and $e(0)$ accurately and easily. Monteith (1965) suggested an extension of Ohm's Law to overcome these. Initially he considered water efflux from a single leaf. The efflux from a sub-stomatal pore at vapour pressure e_i will move across the potential difference $e_i - e_0$, where e_0 is the vapour pressure at the leaf surface, against a stomatal resistance r_s. Hence:

$$\lambda Q_E = \frac{\rho Cp}{\gamma} \frac{[e_i - e_0]}{r_s} . \qquad (2.16)$$

He then assumed that the vapour pressure at the stomatal wall is at saturation defined by the temperature of the wall θ_i, so that e_i can be replaced by $e_s(\theta_i)$ and that within a thin leaf, the temperature of the stomatal wall and the leaf surface θ_0 are approximately equal. Hence $e_i = e_s(\theta_i) = e_s(\theta_0)$ and equation 2.16 becomes

$$\lambda Q_E = \frac{\rho Cp}{\gamma} \frac{\left[e_s(\theta_o) - e_o\right]}{r_s} \quad (2.17)$$

Equation 2.17 can be applied to a plant canopy if soil surface evaporation is negligible. However r_s, θ_o and e_o must be re-defined. r_s is replaced by r_{ST}, a bulk stomatal resistance representing the physiological resistance of the components of the vegetation to water vapour efflux, and θ_o and e_o are replaced by $\theta(0)$ and $e(0)$. Hence:

$$\lambda Q_E = \frac{\rho Cp}{\gamma} \frac{\left[e_s\left[\theta(0)\right] - e(0)\right]}{r_{ST}} \quad (2.18)$$

The two surface terms, $\theta(0)$ and $e(0)$, are eliminated from equation 2.18 using equations 2.8, 2.14 and 2.15 and the slope of the saturation vapour pressure-temperature curve ($S = de_s(\theta)/d\theta$) evaluated at the mean of $\theta(0)$ and $\theta(z)$ (or simply $\theta(z)$ if $\theta(0)$ is unknown). This yields Monteith's form of the combination model:

$$\lambda Q_E = \frac{S(Q^*-Q_G) + \rho Cp\left[e_s\left[\theta(z)\right] - e(z)\right]/r_{aH}}{S + \gamma(r_{aV}+r_{ST})/r_{aH}} \quad (2.19)$$

Thom (1972) has suggested a further simplification for equation 2.19. Since $K_H = K_W$, the aerodynamic resistances for heat and water vapour can be assumed equal. Therefore

$$\lambda Q_E = \frac{S(Q^*-Q_G) + \rho Cp\left[e_s\left[\theta(z)\right] - e(z)\right]/r_{aVH}}{S + \gamma + \gamma \frac{r_{ST}}{r_{aVH}}} \quad (2.20)$$

where $r_{aVH} (= r_{aV} = r_{aH})$ is the aerodynamic resistance for heat and water vapour exchange.

Hence, with direct measurements of Q^* and Q_G and single level measurements of $\theta(z)$ and $e(z)$, λQ_E can be computed if r_{aVH} and r_{ST} are known. Attention will now be given to these latter terms which reflect atmospheric and surface control on evapotranspiration.

2. Aerodynamic resistance

The mass transfer equation for momentum flux density τ is

$$\tau = \rho K_M \frac{\partial u}{\partial z} \quad , \tag{2.21}$$

in which K_M is the eddy diffusivity of momentum and $\partial u/\partial z$ is the vertical gradient of windspeed. Re-arranging and integrating with respect to height, an aerodynamic resistance for momentum exchange can be defined as

$$r_{aM} = \int_0^z \frac{dz}{K_M} = \frac{u(z)}{u^{*2}} \tag{2.22}$$

in which $u^* (= \sqrt{\tau/\rho})$ is the friction velocity.

u^* can be evaluated from a wind profile model. Under conditions of neutral equilibrium, when turbulent mixing is entirely mechanical with no buoyancy effects, the vertical gradient of windspeed in the constant flux layer is given by

$$\frac{\partial u}{\partial z} = \frac{u^*}{kz} \tag{2.23}$$

where k is von Karman's constant (0.41). Integrating with respect to height

$$u(z) = \frac{u^*}{k} \ln\left(\frac{z+z_o}{z_o}\right) , \qquad (2.24)$$

in which z_o is a surface roughness parameter. As vegetation displaces the wind profile upwards by a length d known as the zero plane displacement, equation 2.24 is amended:

$$u(z) = \frac{u^*}{k} \ln\left(\frac{z-d+z_o}{z_o}\right) . \qquad (2.25)$$

Both of the surface parameters z_o and d are determined from the analysis of wind profiles in neutral equilibrium.

Combining equation 2.25 with 2.22 yields an expression for r_{aM} which can be determined solely from wind profiles in neutral equilibrium:

$$r_{aM} = \frac{\left[\ln\left(\frac{z-d+z_o}{z_o}\right)\right]^2}{k^2\, u(z)} . \qquad (2.26)$$

When the atmosphere departs from a state of neutral equilibrium due to buoyancy effects, the vertical gradient of windspeed must be adjusted by a stability correction factor for momentum ϕ_M:

$$\frac{\partial u}{\partial z} = \frac{u^*}{kz}\, \phi_M . \qquad (2.27)$$

Integrating with respect to height, and allowing for d,

$$u(z) = \frac{u^*}{k}\left[\ln\left(\frac{z-d+z_o}{z_o}\right) + \int_d^z \frac{\phi_M - 1}{z}\, dz\right] . \qquad (2.28)$$

The aerodynamic resistance for momentum transfer then becomes

$$r_{aM} = \frac{\left[\ln\left(\frac{z-d+z_o}{z_o}\right) + \Phi_M\right]^2}{k^2\, u(z)} \qquad (2.29)$$

in which $\Phi_M = \int_d^z \frac{\phi_M - 1}{z}\, dz$.

Dyer (1974) reviewed empirical functions for ϕ_M. Using the gradient form of the Richardson number as a measure of atmospheric stability

$$R_i = \frac{g\,(\partial\theta_{v*}/\partial z)}{\bar{\theta}_{v*}(\partial u/\partial z)^2} \simeq \frac{g}{\bar{\theta}}\,\Delta z\,\frac{\Delta\theta}{(\Delta u)^2} \qquad (2.30)$$

in which θ_{v*} is virtual potential temperature, he suggested for the unstable case, $R_i < 0$,

$$\phi_M = (1-16R_i)^{-\frac{1}{4}} \qquad (2.31)$$

and for the stable case, $R_i > 0$,

$$\phi_M = (1-5R_i)^{-1} . \qquad (2.32)$$

Knowing ϕ_M, r_{aM} is evaluated from equation 2.29 using a numerical integration procedure to obtain Φ_M and wind profile analysis estimates of z_o and d.

Thom (1972) has shown that an aerodynamic resistance for momentum exchange is inappropriate for heat and mass exchange. The mass transfer equations for momentum and a property flux density F can be expressed as

$$\tau = \frac{\rho u(z)}{r_{aM}} \qquad (2.33)$$

and

$$F = \frac{x(m) - x(z)}{r_f} \qquad (2.34)$$

where $x(m) - x(z)$ is the potential difference between the mean surface concentration $x(m)$ and a concentration at height z which is opposed by an aerodynamic resistance r_f. Since $r_{aM} = u(z)/u^{*2}$ and $r_f = \frac{1}{u^*}\left[\frac{x(m) - x(z)}{F/u^*}\right]$:

$$r_f - r_{aM} = \frac{1}{u^*}\left[\frac{x(m) - x(z)}{F/u^*}\right] - \frac{u(z)}{u^{*2}} \qquad (2.35)$$

In aerodynamically rough flow, momentum is destroyed at a surface by pressure forces or bluff body effects which have no counterpart in heat or mass transfer. As such, a resistance to a property flux r_f can be equated to r_{aM} by the inclusion of an additional resistance to account for the absence of bluff-body influences r_b:

$$r_f = r_{aM} + r_b \qquad (2.36)$$

Thom (1972) has suggested that as a first approximation r_b can be assigned a value of $6.266u^{*-2/3}$ for both heat and water vapour exchange in agricultural crops. Therefore, for aerodynamic resistances to heat and water vapour exchange, the following serves as a first approximation:

$$r_{aVH} = r_{aV} = r_{aH} = r_{aM} + 6.266\ u^{*-2/3} \quad . \tag{2.37}$$

Arising from this discussion of aerodynamic resistances, three aspects will be investigated in this study:

(i) The magnitude of errors in z_o and d determinations and the possible significance of these in evaluating aerodynamic resistance requires careful examination. Accurate evaluation of z_o and d is difficult over tall rough surfaces as great variability in parameter estimates can exist as a consequence of profile form and windspeed measurement errors. Since only profiles from neutral equilibrium can be employed for determining z_o and d, model estimates are often used, particularly where application to non-neutral cases is required. As such, the influence of such estimations employed in resistance evaluation must be determined.

(ii) The inclusion of a stability correction factor in aerodynamic resistance computation necessitates a stability measure requiring vertical gradients of temperature and windspeed. If the role of a stability correction factor in resistance evaluation is minor, r_{aM} and r_b can be determined solely from wind profile measurements. Hence an examination of the significance of stability correction in

r_{aVH} determination is merited.

(iii) The inclusion of a resistance to compensate for the absence of bluff-body influences in r_{aVH} must be examined to determine the magnitude of r_b over the range of influential environmental parameters.

3. Bulk stomatal resistance

Computation of λQ_E using the combination approach presented in equation 2.20 requires reliable estimates of r_{ST}. Retrospective evaluation of r_{ST} as a residual in equation 2.20 is possible if all other components are known. However, several difficulties exist in this approach. The first is that bare soil evaporation must be negligible. If it is not, r_{ST} will not reflect plant physiological control on water efflux. Second, r_{ST} determined by this approach is only of diagnostic value, and cannot be used predictively. Last, all errors in the components in equation 2.20 will reside in the calculated residual.

Validation of equation 2.20 is possible only if r_{ST} is evaluated independent of prior knowledge of the evapotranspiration regime. If r_{ST} is a bulk stomatal resistance representing the physiological resistance of the components of the vegetation to water vapour efflux, then independent measurements of leaf stomatal resistance r_L can be employed in estimating r_{ST}. Visualizing adaxial and abaxial leaf surfaces as parallel conductors of water vapour, adaxial and abaxial resistances, r_{AD} and r_{AB} respectively, can be weighted by leaf area index to estimate bulk stomatal resistance:

$$\frac{1}{r_{ST(P)}} = \frac{LAI}{r_L} = \frac{LAI}{r_{AD}} + \frac{LAI}{r_{AB}} \qquad (2.38)$$

The successful application of equation 2.38 however encounters several obstacles. The first is that bare soil evaporation losses must be negligible. If they are not, r_{ST} derived from equation 2.38 will not be representative of surface evapotranspiration losses. Second, spatial and temporal sampling problems are encountered in obtaining representative readings of r_{AD} and r_{AB} for a plant community. Third, LAI is tedious and difficult to measure, particularly in developing crops. Despite these limitations, this approach provides the only available method for r_{ST} assessment which is independent of prior knowledge of λQ_E.

The above discussion suggests that several items are worthy of examination.

(i) The concepts used to derive equation 2.20 explicitly involve the assumption that a physiologically based resistance model can be used to represent water vapour efflux from a plant canopy. If this is the case, it should be possible to use r_{ST} evaluated from field measurements of leaf resistance to provide reliable estimates for latent heat flux density computations using equation 2.20. This requires field validation.

(ii) Even though reliable estimates of r_{ST} may be obtainable from field measurements of stomatal response, it is apparent that the determination of r_{ST} from environmental parameters is desirable for application in routine evaluations of λQ_E. A number of researchers (Brady et al., 1975; Szeicz et al., 1973; Tan and Black, 1976) have been successful in this context but further investigation is merited.

C. Daily Totals of Actual, Potential and Equilibrium Evapotranspiration

1. Potential evapotranspiration

Potential evapotranspiration is the evaporative water loss from freely transpiring vegetation which is limited only by energy availability. The combination model expression of Monteith (1965) for actual evapotranspiration (equation 2.20) can be modified to provide an expression for potential evapotranspiration λQ_{PE}. This modification, presented by Monteith (1965) and employed by Davies (1972) and Szeicz and Long (1969), incorporates the assumption that the bulk stomatal resistance $r_{ST} = 0$ and the surface vapour pressure is at saturation defined by surface temperature when water in non-limiting. Hence, λQ_{PE} is

$$\lambda Q_{PE} = \frac{S(Q^*-Q_G) + \rho Cp\left[e_s\left[\theta(z)\right] - e(z)\right]/r_{aVH}}{S + \gamma} . \qquad (2.39)$$

In the application of this expression, three difficulties arise. First, the assumption regarding $r_{ST} = 0$ may not be valid. If it is not, inflated values of λQ_{PE} would be obtained. Second, the net available energy (Q^*-Q_G) present during non-potential conditions may not be representative of the potential case as a consequence of surface drying influences on surface albedo, emissivity and soil thermal diffusivity. Third, during non-potential conditions, the vapour pressure deficit of the air $\left[e_s\left[\theta(z)\right] - e(z)\right]$ will not be consistent with that which would be found during potential conditions. Rather, the inflated values of $\left[e_s\left[\theta(z)\right] - e(z)\right]$ will result in overestimations of λQ_{PE}.

A model which overcomes these limitations has been presented by

Priestley and Taylor (1972). Based on empirical evidence, they advocate the simple expression

$$\lambda Q_{PE} = \alpha \frac{S}{S+\gamma} (Q^*-Q_G) \quad . \qquad (2.40)$$

The proportionality constant α was shown by Priestley and Taylor for non-advective conditions to range from 1.08 ± 0.01 (daily value and standard error of the mean) to 1.34 ± 0.05 for a number of diverse surfaces with an overall average of 1.26.

Examination of equation 2.40 reveals that several generalizations can be made. Advective influences, unless specifically accounted for, will result in inflated α values. If Q_G is neglected in equation 2.40, as is the case in several studies (Kanemasu et al., 1976; Rosenthal et al., 1977; Tanner and Jury, 1976), a smaller α will be otained if daytime Q^* is used rather than 24 hour Q^*. Daytime Q^* is larger than that for 24 hours but 24 hour evapotranspiration losses will be slightly larger than daytime losses except for cases with heavy dewfall. If Q_G is incorporated, this general trend will be followed, however the differences will be dependent upon the magnitude of Q_G on a daytime and 24 hour basis.

An α = 1.26 for daytime observations was found for several crops by Davies and Allen (1973) as well as for arctic sedge meadow and shallow lakes by Stewart and Rouse (1976(a); 1976(b)). An α = 1.28 for well irrigated potatoes in non-advective conditions was found by Jury and Tanner (1975) when employing 24 hour data but when daytime values were used α decreased to 1.07. When advective conditions prevailed, increases

in α were noted. Tanner and Jury (1976) in succeeding investigations employed $\alpha = 1.35 \pm 0.10$. Kanemasu et al. (1976) found $\alpha = 1.28$ and 1.45 for sorghum and soybeans respectively using 24 hour periods with moderate advection. Rosenthal et al. (1977), based on the findings of Kanemasu et al. (1976) and Tanner and Jury (1976), employed $\alpha = 1.35$ for daily investigations on corn. On a daytime basis, McNaughton and Black (1973) found $\alpha = 1.05$ for Douglas fir forest.

Acknowledging the many different experimental procedures employed and the wide range of surface types and local climates, the variability found in α by workers is not unduly large for either daytime or 24 hour periods. However, the variation is sufficient to merit experimental determinations for specific crop and site conditions.

2. Equilibrium evapotranspiration

Combining equations 2.20 and 2.18, a revised expression of the combination model can be derived:

$$\lambda Q_E = \frac{S}{S+\gamma}(Q^*-Q_G) + \frac{\rho C_p}{r_{aV}} \frac{\left\{\left[e_s\left[\theta(z)\right] - e(z)\right] - \left[e_s\left[\theta(0)\right] - e(0)\right]\right\}}{(S+\gamma)} \quad (2.41)$$

An equilibrium rate of evapotranspiration is defined when $\left[e_s\left[\theta(z)\right] - e(z)\right] = \left[e_s\left[\theta(0)\right] - e(0)\right]$, that is when the saturation deficits at the surface and at height z are equal:

$$\lambda Q_{ES} = \frac{S}{S+\gamma}(Q^*-Q_G) \quad (2.42)$$

This rate can occur in two very different environments: in a saturated

environment when both deficits are zero and in a drier environment when they are equal but greater than zero. Both Slatyer and McIlroy (1961) and Monteith (1965) acknowledged these possibilities but anticipated that equation 2.42 would have limited application. However, Denmead and McIlroy (1970), Davies (1972), Stewart and Rouse (1976(a)), Rouse and Stewart (1972) and Wilson and Rouse (1972) found that equation 2.42 provided satisfactory estimates from fairly dry surfaces. Hence, its application appears to be more general than originally anticipated.

3. Generalized evapotranspiration models

Priestley and Taylor, in addition to proposing a simple model for estimating potential evapotranspiration, considered the influence of surface moisture depletion on evapotranspiration rates. They replaced the proportionality constant α in equation 2.40 with a variable α' and showed that its value decreases in response to increased surface dryness once potential conditions ceased to exist. This scheme was adopted by Davies and Allen (1973) for describing the response of ryegrass to soil moisture depletion. They found that daytime α' decreased from a maximum value of 1.26 in response to surface dryness once surface soil moisture fell below a threshold limit. Hence, experimental determination of α' and soil moisture may provide a simple means of evaluating actual daily values of evapotranspiration for a variety of surface types.

CHAPTER THREE

EXPERIMENTAL PROCEDURE

A. Experimental Site and Observation Period

Field measurements were made during the 1974 growing season (early June to late September) at the Ontario Ministry of Agriculture's Horticultural Experiment Station ($42^{\circ}51'N$, $80^{\circ}16'W$) located near Simcoe, Ontario. The site was a flat (slope $\leq 2^{\circ}$), rectangular plot (216 x 122 m) of soybeans (Glycine max (L.) Harosoy 63) (Figure 3.1). To the east and south, the plot was bounded by dirt road. Gravel roads defined the northern and western boundaries. Beyond the study plot boundaries, most of the land was cropped. Field laboratories were located on the eastern edge of the study plot.

B. Instrumentation and Field Program

1. Energy balance measurements

Net radiation and soil heat flux densities were measured directly. Turbulent heat flux densities were evaluated from hourly average Bowen ratio determinations derived from dry-bulb and wet-bulb temperatures at four levels in the constant flux boundary layer.

a. Net radiation flux density

Net radiation flux density was measured with a net pyrradiometer (Swissteco Pty. Ltd., Type S-1) mounted approximately 1.25 m above the

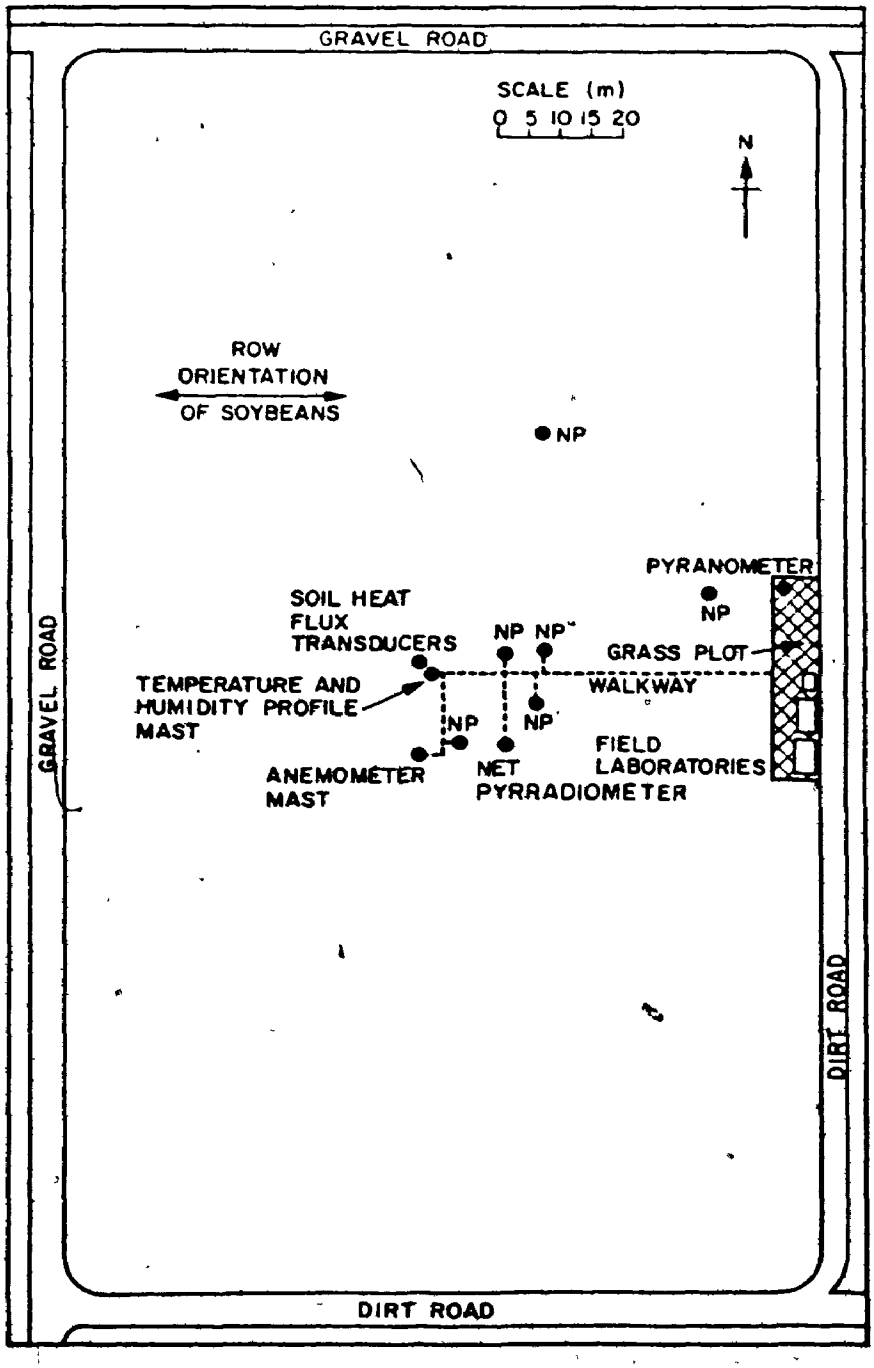

Figure 3.1. Experimental site plan. Closed circles with subscript (●NP) denote location of neutron probe access tubes.

top of the developing soybean canopy. This sensor consists of a wire-wound, plated (copper-constantan) thermopile in which one set of junctions is in thermal contact with an upfacing plate while another is in contact with a plate which faces the ground. The thermopile receivers are enclosed within a pair of polyethylene hemispheres. To avoid shadows cast by the supporting mast, the sensor was positioned facing south. It was purged continuously with a controlled rate of nitrogen gas to inflate the polyethylene hemispheres, to prevent internal condensation and to equalize convective heat loss from each of the thermopile surfaces.

The characteristics of the sensor and its calibration details are listed in Appendix Nine.

b. Soil heat flux density

Soil heat flux density was measured with eight transducers (Middleton Pty. Ltd.) wired in series. These were suspended by wires on an aluminum frame to maintain them in the same horizontal plane 50 mm below the surface. Four sensors were located beneath the crop rows and four beneath the inter-row spaces. Pre-season and post-season calibrations indicated that the manufacturer's calibration could be accepted with confidence.

A method suggested by van Wijk (1963) to compensate for vertical heat flux divergence in the soil between the sensors and the surface was used. The surface soil heat flux was obtained from

$$Q_G = Q_{G_z} + C \frac{\Delta \overline{\theta}_{o-z}}{\Delta t} \Delta z \qquad (3.1)$$

where Q_{G_z} is the soil heat flux density at depth z and C and $\bar{\theta}_{o-z}$ are the heat capacity and mean soil temperature between the surface and depth z. $\bar{\theta}_{o-z}$ was obtained from temperature measurements made with five thermocouples wired in series and set at constant depth intervals between the surface and the heat flux transducers.

The heat capacity of the soil was determined from

$$C = C_m X_m + C_o X_o + C_w X_w + C_a X_a \qquad (3.2)$$

in which C is heat capacity, X is volume fraction and the subscripts m, o, w and a denote mineral matter, organic matter, water and air. Neglecting C_a since it is small and using values of $C_m = 1.93 \times 10^6 Jm^{-3} K^{-1}$, $C_o = 2.51 \times 10^6 Jm^{-3} K^{-1}$ and $C_w = 4.19 \times 10^6 Jm^{-3} K^{-1}$ (De Vries, 1963):

$$C = (1.93 X_m + 2.51 X_o + 4.19 X_w) \times 10^6 \quad . \qquad (3.3)$$

Based on previous investigations at Simcoe (Wilson and McCaughey, 1971), values of $X_m = 0.459$ mm^3 mineral matter / mm^3 soil and $X_o = 0.024$ mm^3 organic matter / mm^3 soil were used. Hence:

$$C = (0.9461 + 4.19 X_w) \times 10^6 \quad . \qquad (3.4)$$

The average moisture content in the top 50 mm layer of soil was determined twice a day by gravimetric analysis. The morning samples were used in calculating C for the period 0100 to 1200 EST and the afternoon samples for the period 1300 to 2400 EST. Further details on the

soil moisture sampling program are given in a later section.

c. Temperature and humidity profiles

Ventilated dry-bulb and wet-bulb psychrometry was used to determine temperature and humidity profiles. The successful application of this method depends on accurate temperature probes, adequate radiation shielding and proper ventilation. Thermopile thermometers based on a design by Lourence and Pruitt (1969), with modification by the author, were used to measure dry and wet-bulb temperature.

(i) Thermopile thermometer construction

Five-junction thermopiles constructed from #30 awg copper-constantan thermocouple wire were used. The junctions were soldered in series and insulated with heat-shrink tubing and coated with acrylic resin. Each thermopile was potted within a length of thin walled (0.254 mm) stainless steel tubing (4.763 mm OD) which was then filled with polyester resin. Individual wires were led back through plastic tubing to a reference sensor of the same construction. This tubing was sealed onto the stainless steel probes, ensuring that the entire thermopile was waterproof.

The reference and wet-bulb probes were 220 mm in length whereas the dry-bulb probes were 310 mm. This additional length in the latter allowed it to be positioned ahead of the wet-bulb in the sensor housing. Thus the dry-bulb was unaffected by the environment of the wet-bulb.

(ii) Thermopile thermometer calibration

The individual thermopile thermometers were calibrated against a

set of precision platinum resistance thermometers (Rosemount Engineering Company, Model 104MB16CCXA, Bridge Model 414L, precision ± 0.015 K) following the field study, over the temperature range 273 to 303 K. An ice-point reference chamber was used as a reference source for the thermopiles during the calibration as it was throughout the field program. From the calibration data, polynomial regression relationships were obtained for each probe

$$T = a_0 + a_1 m + a_2 m^2 \qquad (3.5)$$

where T is temperature, m is the sensor electromotive output in mV and a_0, a_1 and a_2 are regression coefficients.

To minimize systematic deviations between sensors due to sensor housing differences, probe alignment and other features of the measurement system not accounted for in the laboratory calibration procedure, sensors were periodically intercompared in-situ during the field program. The results from this provided for the evaluation of correction constants. Temperatures were multiplied by these after the application of equation 3.5. The correction constants together with the polynomial regression equations for each probe are presented in Table 3.1.

(iii) Thermopile thermometer time constant

For a temperature sensor, the time constant depends on instrument size and aspiration rate. The time constant of the thermometers was experimentally determined to be approximately 80 s. When covered with wicking and attached to a distilled water reservoir, the time constant of the wet-bulb was found to decrease to approximately 57 s.

TABLE 3.1. Thermopile Thermometer Calibration and Correction Constants

SENSOR	FUNCTION	CALIBRATION CONSTANTS			CORRECTION CONSTANTS
		a_o	a_1	a_2	
01	LEVEL 1[1] - θ	273.78416	5.15131	-0.03436	0.9858
02	LEVEL 1 - θ_w	273.14682	5.24361	-0.03461	0.9999
03	LEVEL 2 - θ	273.22075	5.18926	-0.02990	1.0005
04	LEVEL 2 - θ_w	273.45168	5.21092	-0.03257	0.9961
05	LEVEL 3 - θ	273.21760	5.20112	-0.03267	1.0000
06	LEVEL 3 - θ_w	273.21354	5.21848	-0.03544	0.9998
07	LEVEL 4 - θ	273.18090	5.18487	-0.02801	1.0034
08	LEVEL 4 - θ_w	273.22499	5.16983	-0.02716	1.0011
09	LEAF TEMPERATURE	273.79593	2.71025	-0.01276	1.0000

1. Level i denotes the sensor level closest to the surface, with level 4 being furthest from the surface.

(iv) Sensor housing and aspiration

The sensor housings used in this study were based on a design by Lourence and Pruitt (1969) which was intended to:

(1) eliminate temperature errors arising from the absorption of radiation by the probes,

(2) supply water to the wet-bulb at a rate which is in equilibrium with evaporation from it (to avoid erroneous wet-bulb temperatures), and

(3) maintain a ventilation rate > 3 m s^{-1}, which is in accordance with the requirements of aspirated wet-bulb psychrometry (Bindon, 1965; Tanner, 1963).

The sensor housing consisted of two concentric shields, a T-junction, a water reservoir, and a ventilation unit. Both shields were covered with aluminized mylar on the outside with mylar on the inside of the outer shield and flat black paint on the inside of the inner shield. The outer shield was constructed of insulation foam tubing (55.56 mm OD with 4.76 mm wall) to which a hood was added. The mouth was inclined at 60 degrees to the horizontal to assist in shielding the interior from direct sunlight. The inner shield was capped by a hemispheric dome, with an aluminized mylar exterior and a flat black inner surface. This dome served to further shield the sensing probes from direct sunlight. The aperature between the dome and the inner shield was such that it maintained an outer perimeter area equal to the cross-sectional area of the inner shield. The inner shield was made from thin walled nylon tubing, with small holes drilled near the downstream end to allow purging of the air between the inner and outer shields. Both temperature sensors

were centre positioned inside the inner shield.

A standard PVC T-junction (38.10 mm OD) supported the inner shield. The outer shield was supported by a plastic sleeve, fitted over one end of the T-junction. A perspex plug, to hold the dry-bulb and wet-bulb probes in place, was inserted into the opposite end. Holes of appropriate diameter were drilled in the plug to allow the passage of a wick.

Perspex tubing covered with aluminized mylar (200 mm in length and 38.10 mm OD with 3.18 mm wall) was used for a water reservoir. It was fixed to the cross-arm by an adjustable clamp. Water was conducted by wicking within a plastic tube to the wet-bulb sensor. Each unit was aspirated by a 115 V ac fan (Rotron Mfg. Co., NTO 120) attached to the cross-arm. All exterior surfaces were painted white or covered with aluminized mylar to minimize heating by global solar radiation.

(v) Field installation and operation

The four cross-arms to which the housing were attached were fitted to a 2 m PVC pipe with cast metal T-junctions (Figure 3.2). The spacing between cross-arms was 0.25 m. This unit formed an outer sleeve around a metal mast. A clamp on the mast was used to fix the height of the sleeve above the ground. It was serated to allow the sleeve to be rotated so that sensors could be directed into the wind. This aided in the maintainence of sensor aspiration > 3 m s^{-1}. Throughout the study, the lowest level in the sensor array was maintained between 0.25 and 0.50 m above the canopy top.

The ice-point reference chamber used for thermopile reference

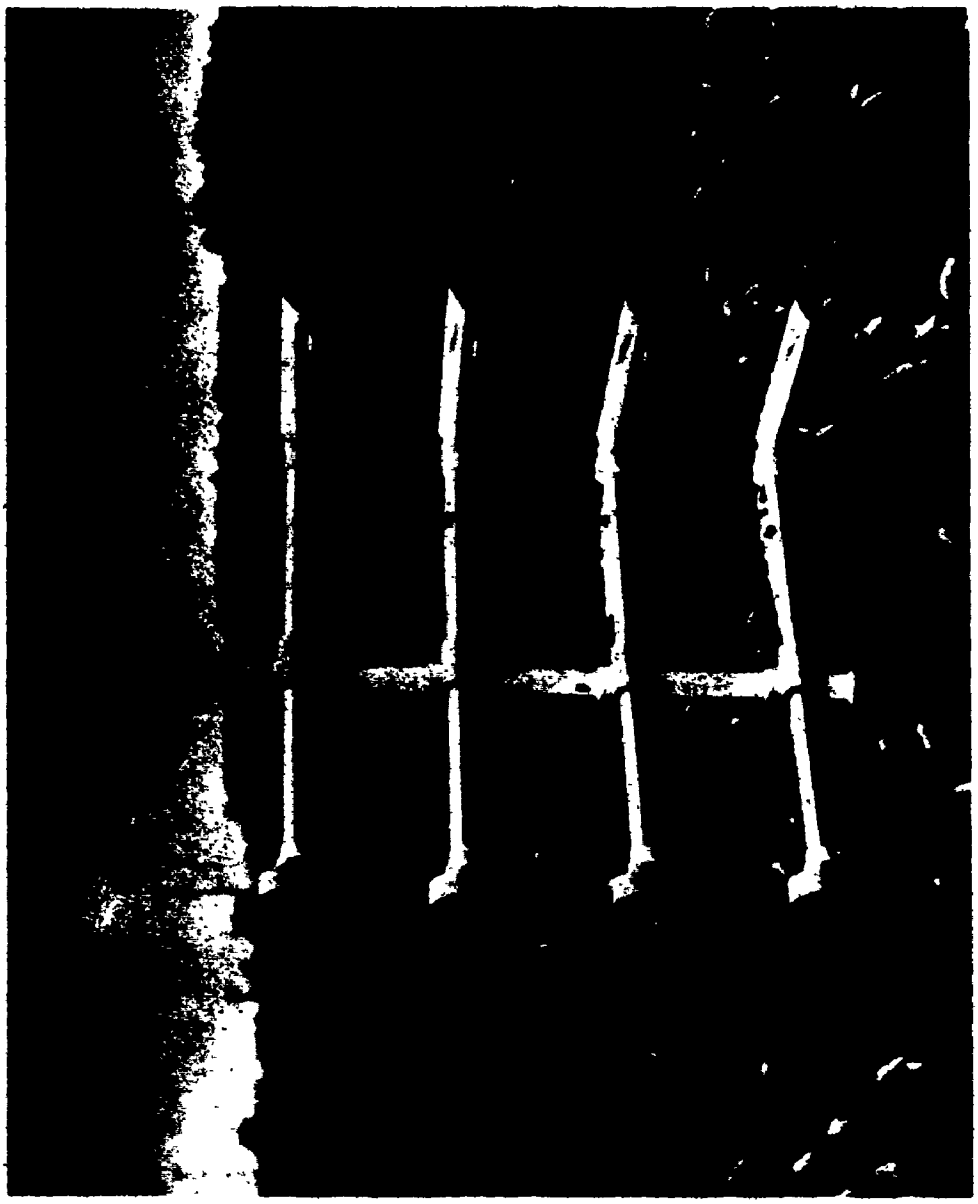

Figure 3.2. Temperature and humidity profile mast.

purposes was located 5 m from the mast in a half-sunken, louvered white container. This provided a naturally ventilated, all weather shelter for the chamber. In routine inspection of the temperature and humidity sensors, particular attention was paid to the orientation of the sensors, the level of the sensors above the canopy and the wet-bulb feed system. Replacement of the wet-bulb wicking was carried out every two days. Care was taken in the handling of the wicking so as not to contaminate its surface. Prior to the field study, the wicking was washed in a mild detergent solution, carefully rinsed and dried. This was an attempt to both increase and standarize the capillary flow characteristics of the material.

The temperature and humidity mast was located in the centre of the study plot. This position of optimum fetch from all directions (Figure 3.3) was selected as the study required long-term operation without regard to wind direction.

2. Soil moisture measurements

Soil moisture was measured by gravimetric and neutron moderation techniques.

Gravimetric samples were taken twice daily (0815 to 0845 EST and 1745 to 1815 EST) at 5 depths (0 to 0.01 m, 0.01 to 0.02 m, 0.02 to 0.055 m, centred at 0.10 m and centred at 0.25 m) in 3 locations. These samples were weighed in their fresh state and then dried at 378 K for 24 hours. Re-weighing then followed. With knowledge of the sample container weight, the mass of the soil solids and the soil water could be established. Volumetric soil moisture X_w was then evaluated as

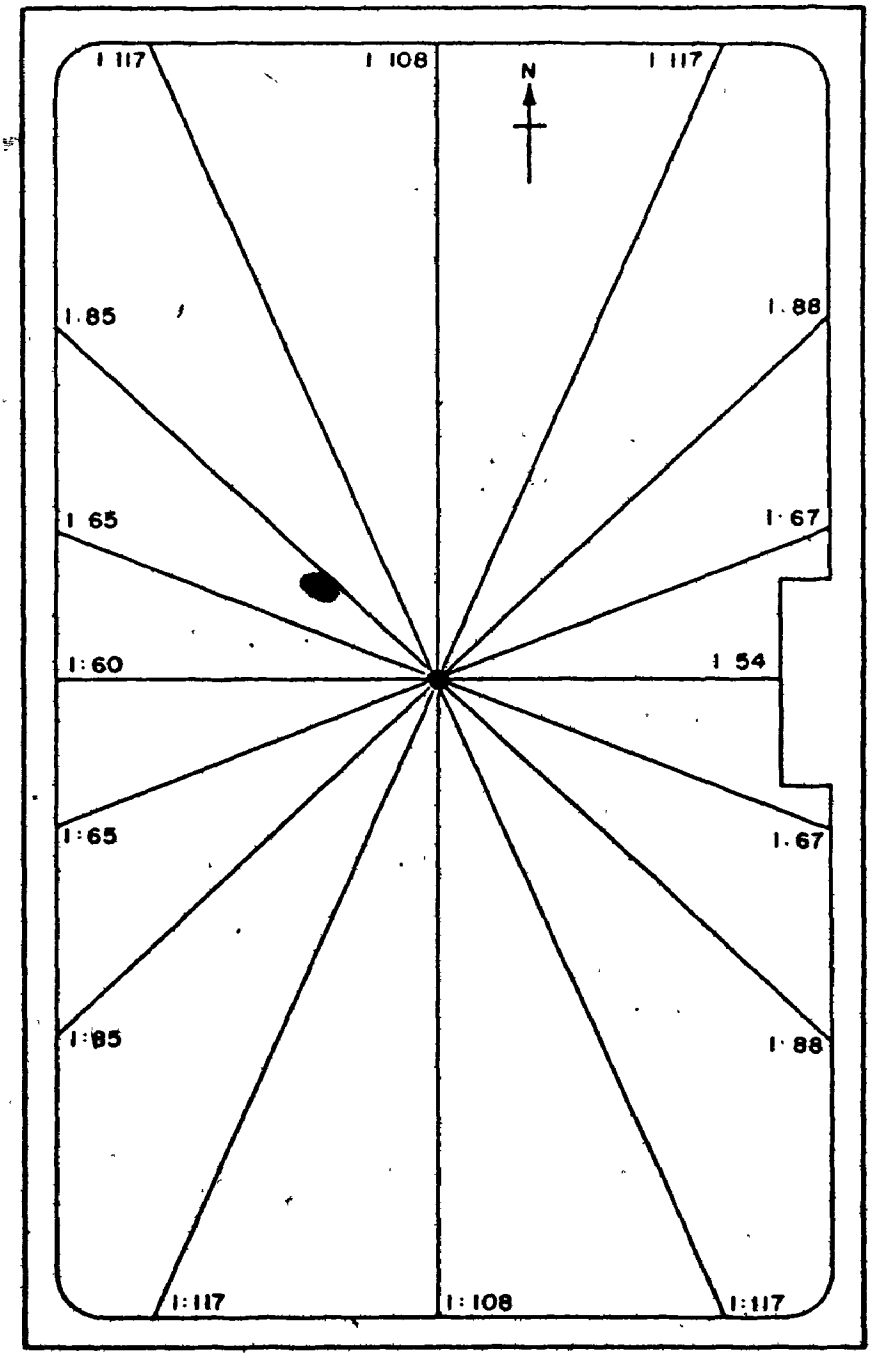

Figure 3.3. Height:fetch ratios for temperature and humidity profile mast.

$$X_w = \frac{m_w}{m_s} \rho_s \qquad (3.6)$$

where m_w and m_s are the masses of the soil water and soil solids and ρ_s is the bulk density of the soil. The bulk density values used in equation 3.6 were derived from independent analysis of ρ_s with depth.

Neutron moderation measurement of soil moisture was done daily (0800 to 0900 EST) when possible. In this technique, a probe is lowered down an access tube to a desired depth. Fast neutrons emitted from this source into the soil are slowed by collisions with other particles. Modification by hydrogen nuclei, mainly in the form of water, is more efficient than other elements in the soil. The density of the resultant cloud of slow neutrons is a function therefore of volumetric soil moisture. This cloud is monitored by a detector in the probe in the form of radioactive counts per unit time. The number of counts registered is linearly related to volumetric soil moisture. Field calibration of the sensor indicated that the manufacturer's (Nuclear-Chicago Corp.) calibration could be accepted with confidence.

Neutron moderation measurements were made at six sites. At each site, measurements at 11 depths were taken (0.25, 0.30, 0.35, 0.40, 0.50, 0.60, 0.75, 1.00, 1.25, 1.50 and 1.75 m). Access tubes were made from thin-walled aluminum (1.80 m in length with 41.28 mm OD and 0.84 mm wall). Rubber stoppers were cemented into the bottom of the tube and placed on the top to prevent internal moisture accumulation. The precautions noted by Wilson (1971) were observed during the installation of the tubes and the use of the sensing unit.

3. Wind profile measurements

Four lightweight cup anemometers (C.W. Thornthwaite Associates) were mounted on one mast at the same heights as the temperature and humidity sensors. These anemometers operate on the principle of a shutter interrupted light beam which generates an electric current when incident upon a photocell. Each anemometer cup revolution causes the photocell current to vary through one cycle. This in turn increments a counter. The number of counts per unit time is related to windspeed by a polynomial

$$u = 114.4069 + 25.7227\ C_t - 0.0043\ C_t^2 \qquad (3.7)$$

in which u is the windspeed in mm s^{-1} and C_t is the recorder counts per minute.

Correction factors for the different cup assemblies were obtained because of slight differences in their field performance. These were determined from periodic field intercomparisons where all anemometers were mounted on one level above the surface. Registered counts were multiplied by these factors prior to the application of equation 3.7.

4. Stomatal resistance measurements

Stomatal resistance measurements were made using a portable stomatal diffusion porometer similar to that described by Kanemasu et al. (1969) (Lambda Instruments Co.). The air in a chamber containing a hygroscopic sensor is dried to an initial low humidity level. The chamber is then clamped on a leaf. The diffusive resistance is evaluated

by recording the time for water vapour to diffuse from the leaf into the sensor chamber and vary the humidity over a known range. The relationship between elapsed time and diffusive resistance is linear.

The instrument was calibrated in a procedure similar to that outlined by Kanemasu et al. (1969) and the manufacturer. A plate supplied by the manufacturer contained pores which simulated five known stomatal resistances when placed over a saturated source. The sensor was calibrated for two humidity ranges since the unit had one for leaves with a low diffusive resistance as well as one for leaves of high resistance.

The calibration of the unit presented two difficulties. First, both the humidity sensing element and the rate of diffusion from a leaf are temperature dependent. Therefore it was necessary to calibrate the sensor over a range of temperatures. Following the manufacturer's guidelines, a correction factor, relating all sensor readings to a temperature of 298 K was established for data reduction purposes. This correction was found to hold for both sensor humidity ranges over the duration of the field program. A bead thermistor, built into the porometer sensing unit, was used for measuring leaf surface temperature.

Second, sensor response times at a given resistance for both sensor humidity ranges increased throughout the study. Similar features have been noted by Morrow and Slatyer (1971) and Gandar and Tanner (1976). This feature is attributed to water absorption by the sensing element and housing chamber and sensor deterioration from environmental contamination associated with prolonged field exposure. Prior anticipation of such possibilities lead to several sensor calibrations

throughout the course of the study so that corrections could be made.

Kanemasu et al. (1969), Morrow and Slatyer (1971) and the manufacturer stressed that during porometer storage, calibration and use certain procedures and precautions must be observed to obtain reliable results. These were followed during the field program.

Field measurements of stomatal resistance were made three times daily (morning, midday and late afternoon) when conditions permitted. The exact times of measurement varied due to decreasing daylength throughout the study. Adaxial and abaxial responses were monitored on a minimum sample of 10 leaves, and often (when time permitted) 20 leaves. From these measurements, harmonic adaxial and abaxial mean leaf resistances were computed for later analysis. Attempts were made to sample leaves representative of the full canopy. Sample leaves were tagged for ready identification in the field. This also aided in maintaining representative sequential measurements.

5. Crop parameter measurements

a. Crop description

The 2.6 hectare study plot was cultivated on June 5 (Day 156)[1] and fertilizer application was 168 kg ha^{-1} of 10-20-20 (N, P, K). The crop was planted on June 6 (Day 157) in rows oriented east-west. Row spacing was 0.53 m with a seed drop of 20 per metre of row. This resulted in a study plot density of 372,000 plants per hectare. The

1. For data display purposes, dates are expressed using Julian Day nomenclature. Appendix Ten provides a table for the conversion of date to Julian Day of the year.

depth of planting was 25 mm. The herbicide program employed pre-emergence application of Metribuzin (Sencor) with 0.42 kg active per hectare. Crop emergence occurred on June 10 (Day 161).

Crop development was terminated on September 22 (Day 265) with the occurance of heavy frost.

b. Crop height

Crop height was measured regularly throughout the field program using two approaches. The first was a component part of a routine destructive plant analysis program. Prior to removal of the plants from five randomly selected 1 m sections of crop row, the height of the individual plants was measured and the mean height assessed. The other approach involved in-situ non-destructive measurements taken periodically throughout the study. Again, mean values of these samples were taken. The change in crop height throughout the study period is shown in Figure 3.4.

c. Leaf area index

During a routine destructive plant analysis program carried on throughout the growing season, leaves from five randomly selected 1 m sections of crop row were separated from the plants. These were weighed, dried at 343 K for 3 days and then re-weighed. Prior to drying, a selected number of these samples were placed against a background of known area (0.25 m^2) and photographed. The negatives were analyzed after the experiment and the area of the leaves was determined. A relationship between leaf area (LA in m^2) and leaf dry weight (DW_L in g) (Figure 3.5) was evaluated:

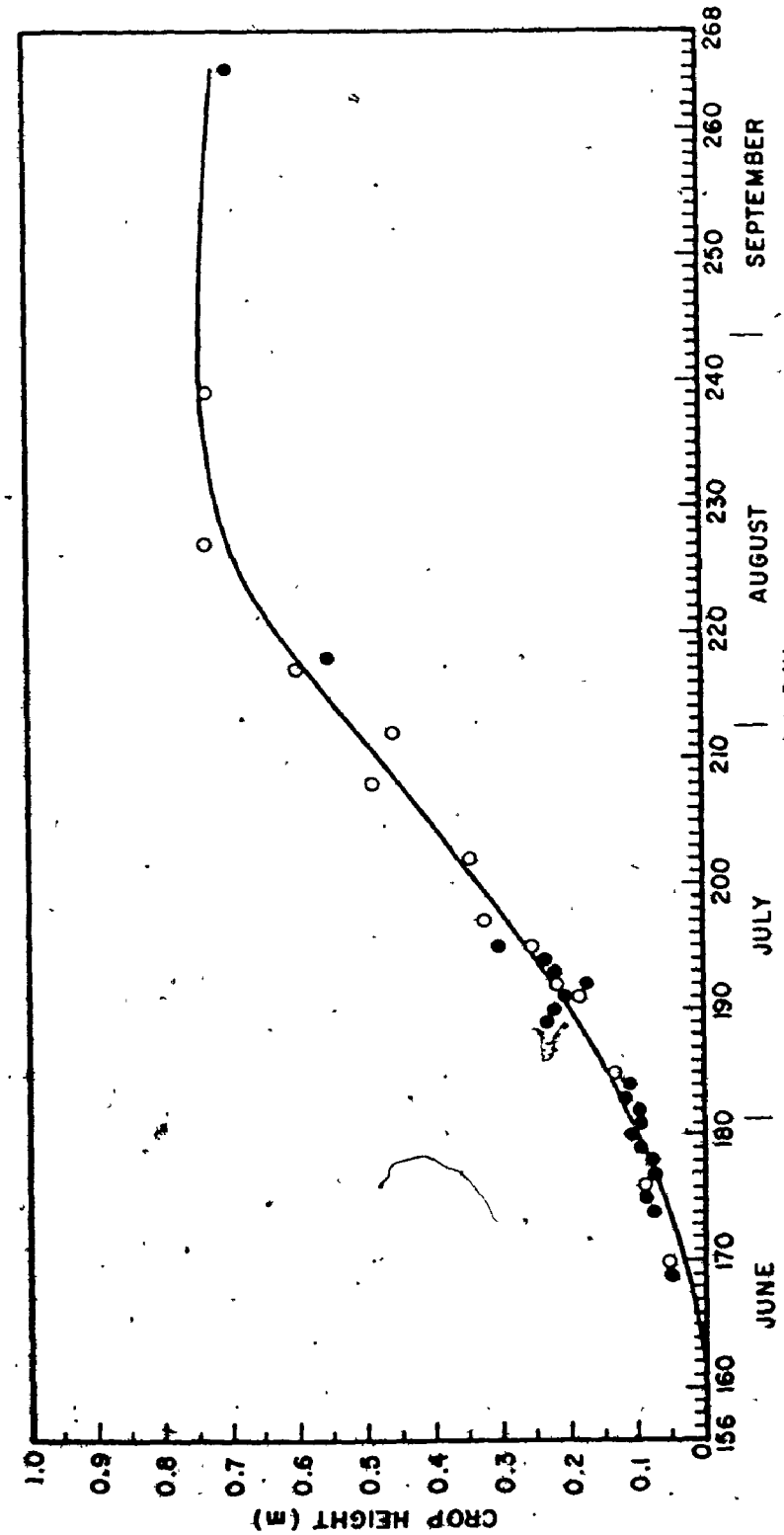

Figure 3.4. The progression of crop height during the growing season. Curve through data points fitted by hand. Data samples derived from non-destructive plant analysis are indicated with closed circles (●). Data samples derived from destructive plant analysis are indicated with open circles (○).

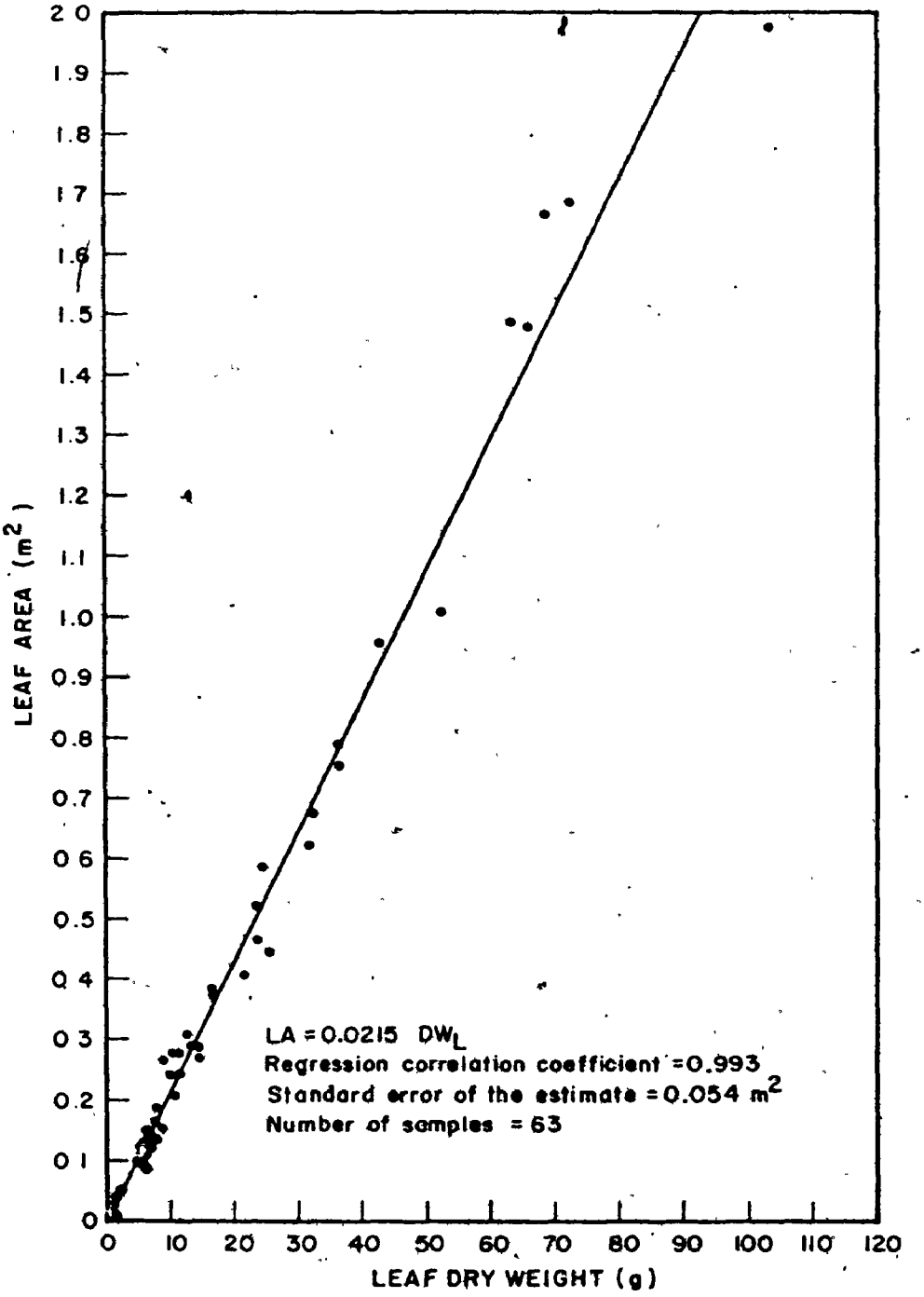

Figure 3.5. The relationship between leaf area and leaf dry weight.

$$LA = 0.0215\ DW_L \quad . \qquad (3.8)$$

Leaf area index throughout the season was then evaluated from leaf dry weight samples and known row spacing. The seasonal progression of leaf area index is presented in Figure 3.6.

d. Leaf temperature

Leaf temperature measurements commenced on July 2 (Day 188). They were measured directly by an array of ten #30 awg copper-constantan thermocouples arranged in series and referenced against an ice-point reference chamber. The ten sensor tips had an electrical insulating coating and were attached to the lower surfaces of representative leaves by adhesive tape. It was necessary to interpose a thin layer of adhesive tape between the thermocouple tip and the leaf to avoid direct contact and damage to the leaf tissue by the sensor. The sensor array was calibrated in a manner similar to that described for the temperature thermopile thermometers (Table 3.1).

6. Additional measurements

a. Global solar radiation flux density

Global solar radiation flux density was measured with an Eppley Precision Spectral Pyranometer Model 2 (Eppley Laboratory). This sensor has a 50-junction wirewound, plated (copper-constantan) thermopile enclosed in two concentric glass hemispheres. The receiver is mounted on an equatorial plane below the hemispheres and is coated with Parson's Optical Black. An internal temperature compensation circuit permits sensitivity to remain constant to within ± 0.5% over the ambient

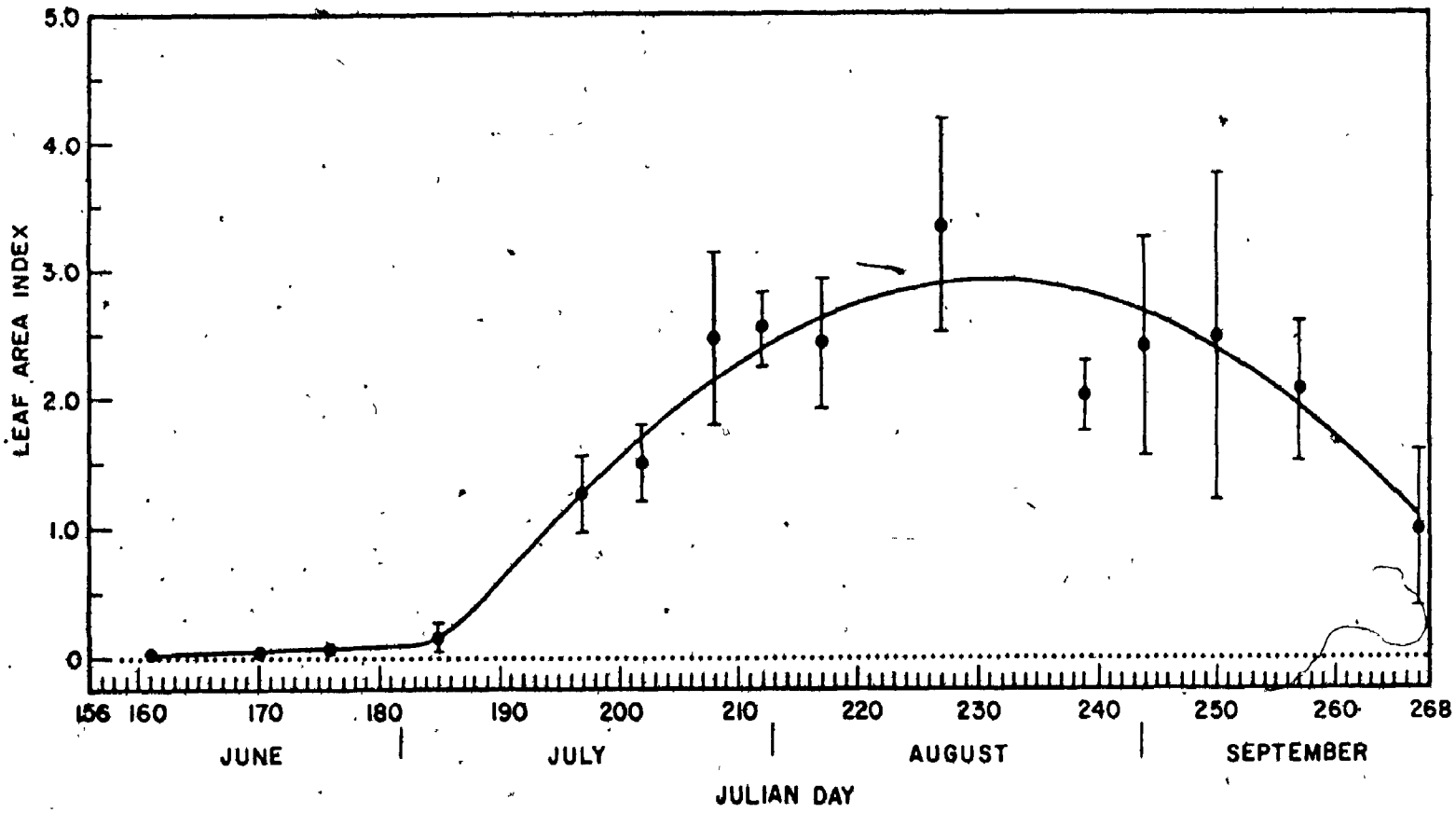

Figure 3.6. The progression of leaf area index during the growing season. Curve through data points fitted by hand. Bars denote ±1 standard deviation about the mean.

temperature range 253 to 313 K.

The pyranometer was mounted on a plate fixed atop a 3 m tower. This ensured that the sensor was free from obstructions above the plane of the sensing element.

The characteristics of the sensor and its calibration details are listed in Appendix Nine.

b. Supplemental measurements from the Atmospheric Environment Service

The Atmospheric Environment Service Simcoe First Class Station was located 250 m north-east of the instrument site. Supplemental measurements required within the study framework were obtained from this station. These included hourly barometric pressure, wind direction and precipitation measurements.

C. Recording and Data Reduction

All signals from the continuous operating instruments were passed through shielded multi-conductor cable to an air-conditioned field laboratory which housed the recording apparatus. The field laboratory was also equipped with a dehumidifying unit to aid in maintaining a controlled environment for this equipment. All signals were grounded to a copper rod inserted to a depth of approximately 3 m in the ground outside the laboratory.

During periods of electrical and thunderstorm activity, measurements were suspended. Care was taken to ensure electrical isolation of the data recording apparatus during these times.

1. Temperature and humidity

Signals from the dry-bulb and wet-bulb thermopile thermometers were monitored with a Solartron data logger (Model LM 1604 DC Digital Voltmeter with a 50 channel Low Level Scanner Type TS 50/3232) and recorded on magnetic tape at 200 bpi. Data from the field tapes were transferred to storage tapes for computer terminal storage. The accuracy of the data logging system was established to be ± 0.003 mV based on the manufacturer's specifications.

The hourly uncalibrated means of thermopile thermometer data were converted to temperature by application of the appropriate calibrations. These values were then converted to potential temperatures. Hourly means of dry-bulb and wet-bulb temperature, θ and θ_w, were used to compute vapour pressures:

$$e = e_s(\theta_w) - \gamma(\theta - \theta_w) \quad . \qquad (3.9)$$

Employing temperatures in degrees Celsius, $e_s(\theta_w)$ was computed following Dilley (1968)

$$e_s(\theta_w) = \alpha' \exp\left[\beta'\theta_w/(\phi'+\theta_w)\right] \qquad (3.10)$$

where $\alpha' = 610.78$, $\beta' = 17.209$ and $\phi' = 237.30$.

During the field experiment, problems with the wet-bulb feed system sometimes occurred. During the data reduction, any spurious wet-bulb data were discarded.

At the beginning of the study, measurements were recorded every

5 minutes from 0500 to 1900 EST. However as the daylight period decreased in length, shortening of this observation period resulted. Signals were monitored every 20 minutes when the 5 minute interval was not being used.

2. Net radiation and global solar radiation flux densities

The net pyrradiometer and pyranometer signals were recorded continuously on a recording potentiometer (Honeywell Electronik 194). The recorder precision was ± 0.25% of full range with a dead band error of ± 0.15% of full range. The data from the recorder charts were reduced by hand to yield hourly means.

3. Soil heat flux density

The signals from the soil heat flux transducers and the divergence thermopile were recorded on the data logger previously described. Mean uncalibrated hourly values from the soil heat flux transducers were obtained, after which calibration was applied. Hourly mean soil temperature in the 0 to 50 mm depth range was calculated and the difference from the previous hour's reading was obtained. This was used in conjunction with the volumetric soil moisture samples to evaluate the surface soil heat flux density.

4. Wind profile record

Cup revolutions were recorded on electromechanical counters which were read every hour. Data were transferred to computer cards for calibration and subsequent analysis. During periods of excessive rain, no profile measurements were made.

5. Soil moisture

The volumetric soil moisture measurements from the gravimetric and neutron moderation methods were combined to produce daily soil moisture profiles. The average morning gravimetric samples at 5 depths were combined with the average neutron moderation estimates at 11 depths. At the 0.25 m intersection, the values from the two methods were averaged. As a validity check on the consistency of the two techniques, the relationship between the two independent samples is presented in Figure 3.7. The good agreement exhibited between the methods provides confidence in both soil moisture sampling techniques.

From the volumetric soil moisture values at 15 depths, representative values for all 10 mm depth intervals between the surface and 1.75 m were established using a linear interpolation technique.

Soil moisture characteristic curves relating volumetric soil moisture to matric suction were experimentally determined by the University of Guelph's Department of Land Resource Science employing pressure-membrane apparatus (Wilson, 1971). Curves for the depths 0 to 0.25 m, 0.25 to 0.50 m and > 0.50 m were derived from representative soil samples taken from the experimental site. The curves for the three depth ranges are presented in Figure 3.8. These curves are used to convert volumetric soil moisture to matric suction. However when soil moisture levels fell below threshold volumetric soil moisture values equivalent to -1500 kPa, matric suction was arbitrarily set equal to -1500 kPa.

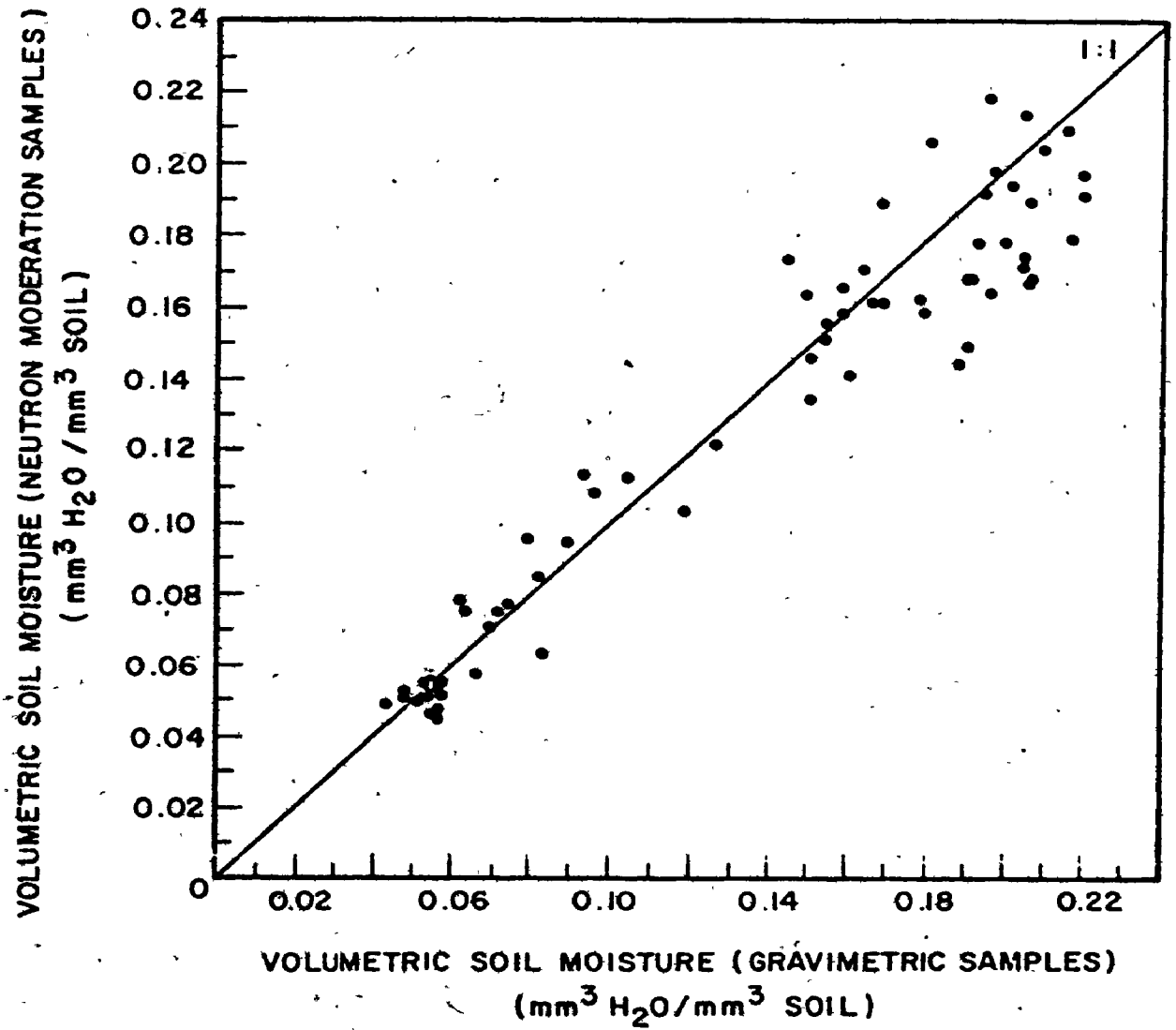

Figure 3.7. The relationship between gravimetric and neutron moderation volumetric soil moisture measurements. The data points displayed are average daily measurements at the 0.25 m depth. The sample size is 67.

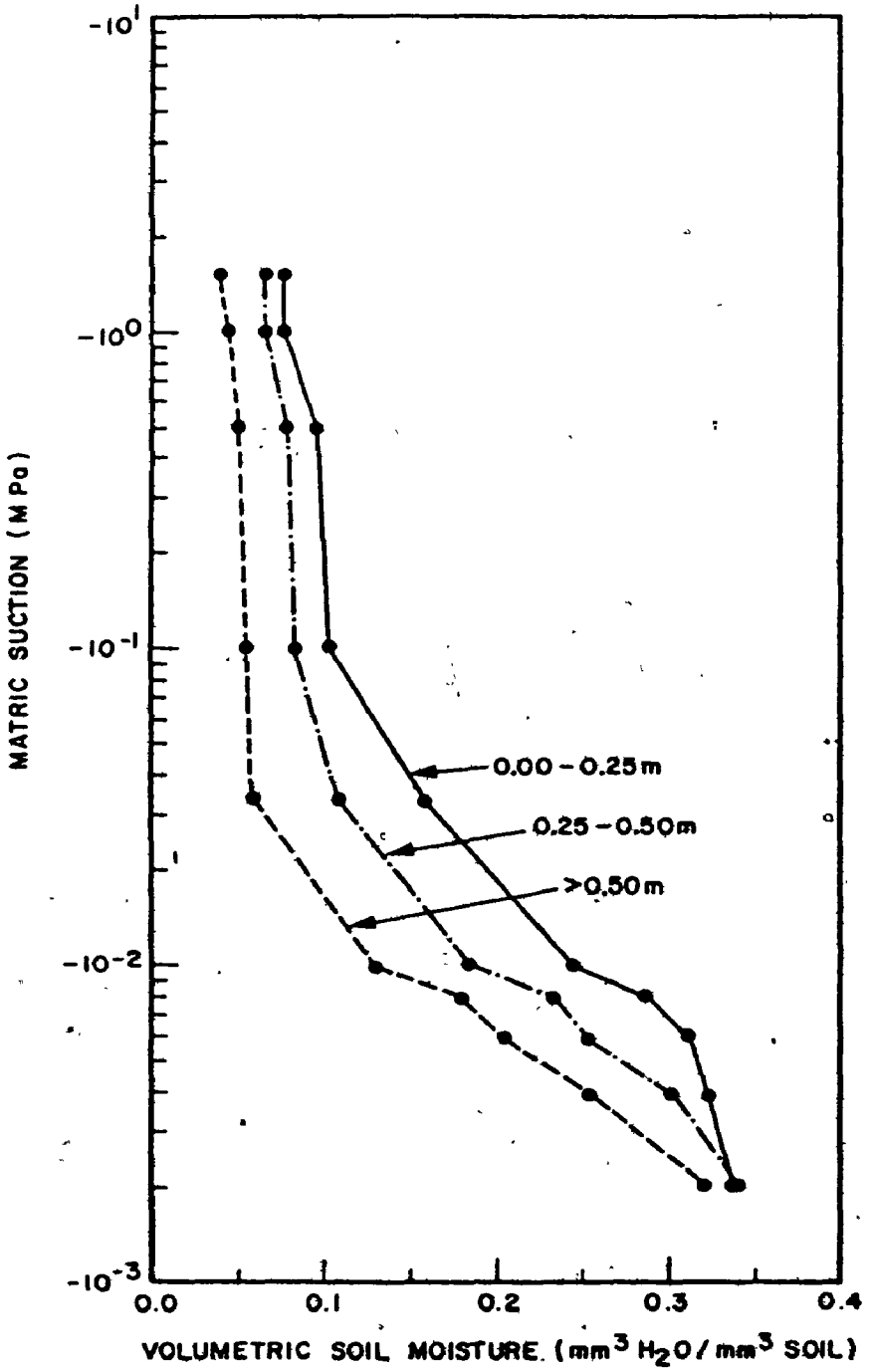

Figure 3.8. The moisture characteristic curves for three depths (0.00 - 0.25m, 0.25 - 0.50m and >0.50m) of Caledon sandy loam.

D. Error Analysis

The absolute and relative errors in temperature measurement were assessed and combined to determine errors in calculated vapour pressure. These in turn were combined with the errors in Q* and Q_G to estimate the errors in λQ_E.

The method of assessing errors follows Cook and Rabinowicz (1963), Fogel (1962), Fuchs and Tanner (1970) and Scarborough (1962). Any value Y can be expressed as a function of a set of measurements $x_1, x_2, \ldots x_n$ which have associated with them errors $\delta x_1, \delta x_2, \ldots \delta x_n$:

$$Y = f(x_1 \pm \delta x_1, x_2 \pm \delta x_2, \ldots x_n \pm \delta x_n) \quad . \tag{3.11}$$

The total error in Y, δY, is given by differentiating equation 3.11:

$$\delta Y = \frac{\partial Y}{\partial x_1}\delta x_1 + \frac{\partial Y}{\partial x_2}\delta x_2 + \ldots + \frac{\partial Y}{\partial x_n}\delta x_n \quad . \tag{3.12}$$

The probable absolute error in Y is smaller than δY and is found by taking the root-mean-square of equation 3.12:

$$\delta Y_{rms} = \left[\left(\frac{\partial Y}{\partial x_1}\delta x_1\right)^2 + \left(\frac{\partial Y}{\partial x_2}\delta x_2\right)^2 + \ldots + \left(\frac{\partial Y}{\partial x_n}\delta x_n\right)^2\right]^{\frac{1}{2}} \quad . \tag{3.13}$$

The relative error is evaluated as $\delta Y_{rms}/Y$.

Equations used in this error analysis and tabulated results are presented in Appendix Two.

1. Error in temperature and humidity measurements

The errors in dry-bulb and wet-bulb temperature were assessed from

the error in the calibration constant of a representative sensor and the resolution error in the data system. Errors due to radiative heating of sensor shields and incorrect water feeds could not be taken into account. Over the temperature range 273-303 K, the relative error in θ and θ_w is less than ± 0.01 % (Appendix Two). Errors in calculated values of $\Delta\theta$, e and Δe are shown in Appendix Two.

2. Error in net radiation and soil heat flux density measurements

The error in Q* was assessed from the resolution in the reading of the sensor output and the calibration error of the sensor. Appendix Two indicates a relative error of approximately ± 5% in Q*, with greater error for $Q^* < 200\ Wm^{-2}$.

In this experiment, an error of ± 5% was assigned to Q_G.

3. Error in latent heat flux density

Using the results in Appendix Two, the error present in the Bowen ratio method estimations of λQ_E was assessed. A sample tabulation is presented in Table 3.2. When humidity differences were large ($\Delta e > 25$ Pa), λQ_E is estimated with relative errors between ± 5% and ± 12%. At smaller Δe values, errors become very large. Hence, the difficulty of obtaining reliable values of λQ_E during dry conditions is apparent.

The results of the error analysis presented herein for λQ_E finds approximate agreement with Fritschen (1965), McCaughey and Davies (1975) and Sinclair et al. (1975).

TABLE 3.2. Errors in Latent Heat Flux Density

Q^*-Q_G [1] (Wm^{-2})	$\Delta\theta$ [2] (K)	Δe [3] (Pa)	λQ_E (Wm^{-2})	$\delta\lambda Q_{E_{rms}}$ (Wm^{-2})	$\frac{\delta\lambda Q_{E_{rms}}}{\lambda Q_E}$ (%)	Q^*-Q_G (Wm^{-2})	$\Delta\theta$ (K)	Δe (Pa)	λQ_E (Wm^{-2})	$\delta\lambda Q_{E_{rms}}$ (Wm^{-2})	$\frac{\delta\lambda Q_{E_{rms}}}{\lambda Q_E}$ (%)
0	0.00	1.0	0.0	6.3	-	250	0.00	1.0	250.0	445.8	178.3
		10.0	0.0	6.3	-			10.0	250.0	47.4	19.0
		25.0	0.0	6.3	-			25.0	250.0	24.1	9.6
		50.0	0.0	6.3	-			50.0	250.0	18.5	7.4
		100.0	0.0	6.3	-			100.0	250.0	16.8	6.7
	0.10	1.0	0.0	0.8	-		0.10	1.0	32.9	108.3	329.2
		10.0	0.0	3.8	-			10.0	150.6	29.5	19.6
		25.0	0.0	5.0	-			25.0	197.8	18.1	9.1
		50.0	0.0	5.6	-			50.0	220.8	16.0	7.2
		100.0	0.0	5.9	-			100.0	234.5	15.7	6.7
	0.25	1.0	0.0	0.4	-		0.25	1.0	14.3	50.9	356.6
		10.0	0.0	2.4	-			10.0	94.3	23.9	25.3
		25.0	0.0	3.8	-			25.0	150.6	14.8	9.8
		50.0	0.0	4.8	-			50.0	188.0	13.6	7.2
		100.0	0.0	5.4	-			100.0	214.6	14.3	6.7
	0.50	1.0	0.0	0.2	-		0.50	1.0	7.4	27.0	367.0
		10.0	0.0	1.5	-			10.0	58.1	17.4	30.0
		25.0	0.0	2.7	-			25.0	107.8	12.1	11.2
		50.0	0.0	3.8	-			50.0	150.6	11.2	7.4
		100.0	0.0	4.8	-			100.0	188.0	12.5	6.7
	1.00	1.0	0.0	0.1	-		1.00	1.0	3.7	13.9	372.4
		10.0	0.0	0.8	-			10.0	32.9	11.0	33.5
		25.0	0.0	1.7	-			25.0	68.7	8.8	12.9
		50.0	0.0	2.7	-			50.0	107.8	8.5	7.9
		100.0	0.0	3.8	-			100.0	150.6	10.1	6.7
100	0.00	1.0	100.0	178.4	178.4	500	0.00	1.0	500.0	891.5	178.3
		10.0	100.0	19.8	19.8			10.0	500.0	94.1	18.8
		25.0	100.0	11.2	11.2			25.0	500.0	46.9	9.4
		50.0	100.0	9.4	9.4			50.0	500.0	35.2	7.0
		100.0	100.0	8.9	8.9			100.0	500.0	31.7	6.3
	0.10	1.0	13.2	43.3	329.2		0.10	1.0	65.8	216.6	329.2
		10.0	60.2	12.3	20.4			10.0	301.2	58.6	19.4
		25.0	79.1	8.6	10.8			25.0	395.6	35.1	8.9
		50.0	88.3	8.2	9.3			50.0	441.7	30.5	6.9
		100.0	93.8	8.3	8.8			100.0	469.0	29.6	6.3
	0.25	1.0	5.7	20.4	356.7		0.25	1.0	28.6	101.9	356.6
		10.0	37.7	9.8	26.0			10.0	188.7	47.6	25.2
		25.0	60.2	6.9	11.4			25.0	301.2	28.8	9.6
		50.0	75.2	7.0	9.3			50.0	375.9	26.0	6.9
		100.0	85.8	7.6	8.8			100.0	429.2	27.0	6.3
	0.50	1.0	2.9	10.8	367.0		0.50	1.0	14.7	54.0	367.0
		10.0	23.3	7.1	30.6			10.0	116.3	34.8	29.9
		25.0	43.1	5.4	12.6			25.0	215.5	23.7	11.0
		50.0	60.2	5.7	9.4			50.0	301.2	21.4	7.1
		100.0	75.2	6.6	8.8			100.0	375.9	23.7	6.3
	1.00	1.0	1.5	5.6	372.5		1.00	1.0	7.5	27.8	372.4
		10.0	13.2	4.5	34.0			10.0	65.8	22.0	33.5
		25.0	27.5	3.9	14.1			25.0	137.4	17.4	12.7
		50.0	43.1	4.2	9.8			50.0	215.5	16.4	7.6
		100.0	60.2	5.3	8.9			100.0	301.2	19.1	6.4

1. Q_G was fixed at 15% of Q^*
2. $\delta\Delta\theta_{rms}$ was fixed at 0.027 K, representing $\delta\Delta\theta_{rms}$ at 293 K (refer to Appendix Two)
3. $\delta\Delta e_{rms}$ was fixed at 3.78 Pa, representing $\delta\Delta e_{rms}$ at e = 1500 Pa with D = 5.0 K (refer to Appendix Two)

CHAPTER FOUR

COMBINATION MODEL RESULTS

A. Aerodynamic Resistances to Momentum, Heat and Water Vapour Exchange

1. Surface roughness and zero plane displacement

Surface roughness and zero plane displacement parameters were calculated by an iterative procedure (Tanner, 1963) from wind profiles measured during neutral equilibrium. Values of the Richardson number were obtained for all height permutations of the four levels of measurement. Profiles with all R_i values $< |0.01|$ were selected as neutral. This criterion finds agreement with most that have been cited for neutral equilibrium.

Temporal changes in z_o and d are shown in Figures 4.1 and 4.2. Values of z_o increase throughout the growing season. Values of d increase until approximately Day 236 and then decrease. Stanhill (1969), Szeicz et al. (1969) and Tanner and Pelton (1960) have shown that both z_o and d correlate well with crop height. However, foliage density must also be important. The decrease in d is well correlated with canopy defoliation during the latter part of the growing season (Figure 3.6), while crop height remains almost constant (Figure 3.4). z_o however appears to be insensitive to defoliation. The correlation with crop height may have been sustained following defoliation by the observed stiffening of plant stems.

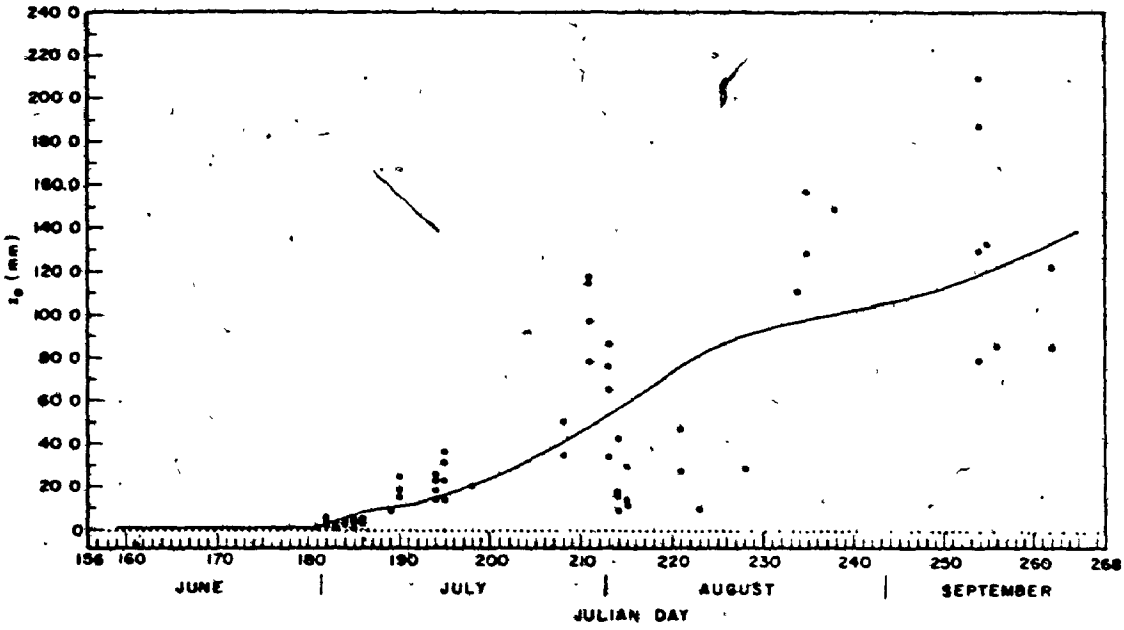

Figure 4.1. The progression of z_o throughout the growing season. The data points represent individual z_o values determined from hourly wind profiles during neutral equilibrium. The curve through the data points after Day 180 is given by $z_o = -27.49 + 281.47\ CH - 27.94\ LAI$. Prior to Day 180, $z_o = 1.0$ mm.

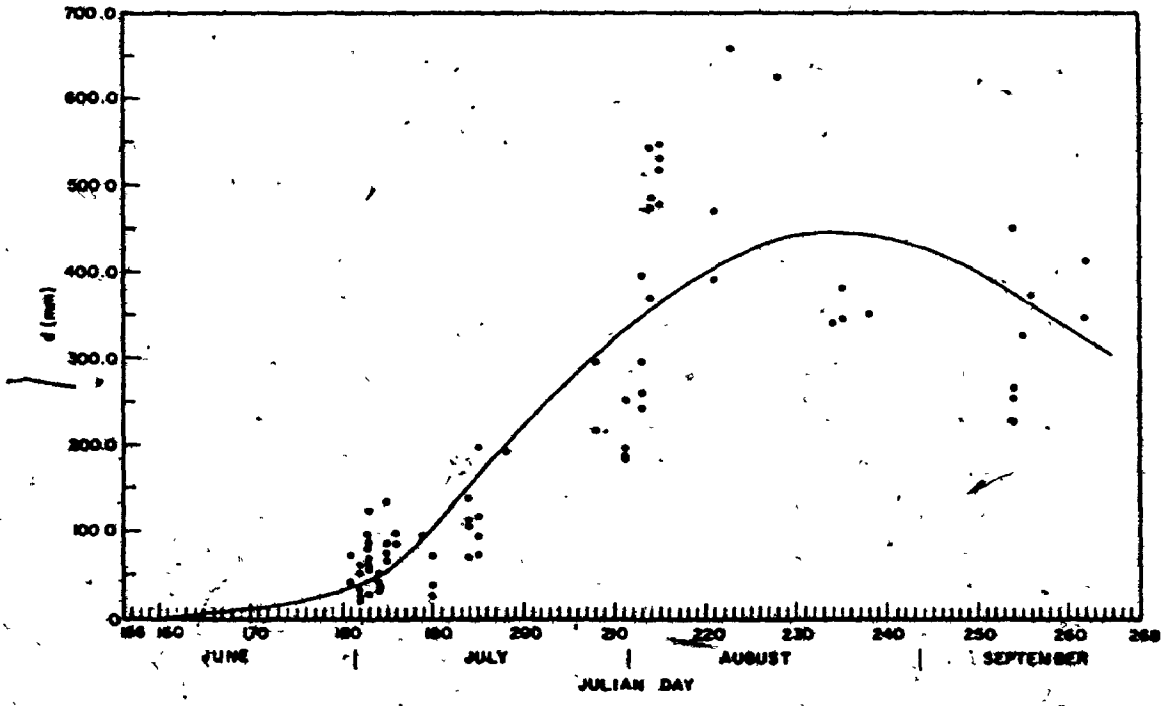

Figure 4.2. The progression of d throughout the growing season. The data points represent individual d values determined from hourly wind profiles during neutral equilibrium. The curve through the data points is given by $d = 0.83 + 245.73\ CH + 91.36\ LAI$.

As it was not possible to evaluate z_o and d each day, these parameters had to be estimated. Both z_o and d were statistically related to crop height (CH in m) and LAI:

$$z_o = -27.49 + 281.47\ CH - 27.94\ LAI \qquad (4.1)$$

and

$$d = 0.83 + 245.73\ CH + 91.36\ LAI \qquad (4.2)$$

Estimates of z_o and d from these expressions are shown in Figures 4.1 and 4.2. Prior to Day 180, when the crop was emerging, z_o was set equal to 1.0 mm.

The large scatter of observed values of z_o and d about model estimates (Figures 4.1 and 4.2) cannot be explained readily. No dependence on windspeed or direction was found. The scatter may well be a consequence of measurement errors.

Estimates of z_o and d from various regression models (Monteith, 1973; Stanhill, 1969; Szeicz et al., 1969; Tanner and Pelton, 1960) are compared with estimates from equations 4.1 and 4.2 (Figures 4.3 and 4.4). Also, z_o and d have been related to crop height by linear regression (Figures 4.3 and 4.4). These relations are

$$z_o = -20.78 + 163.71\ CH \qquad (4.3)$$

and

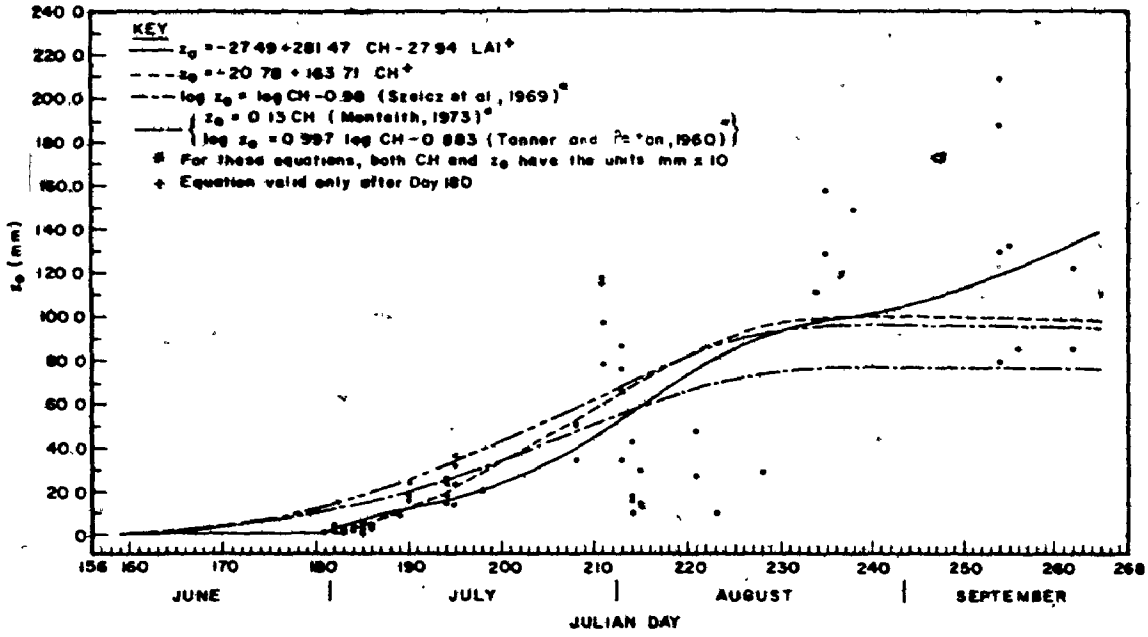

Figure 4.3. Comparison of z_o model estimates.

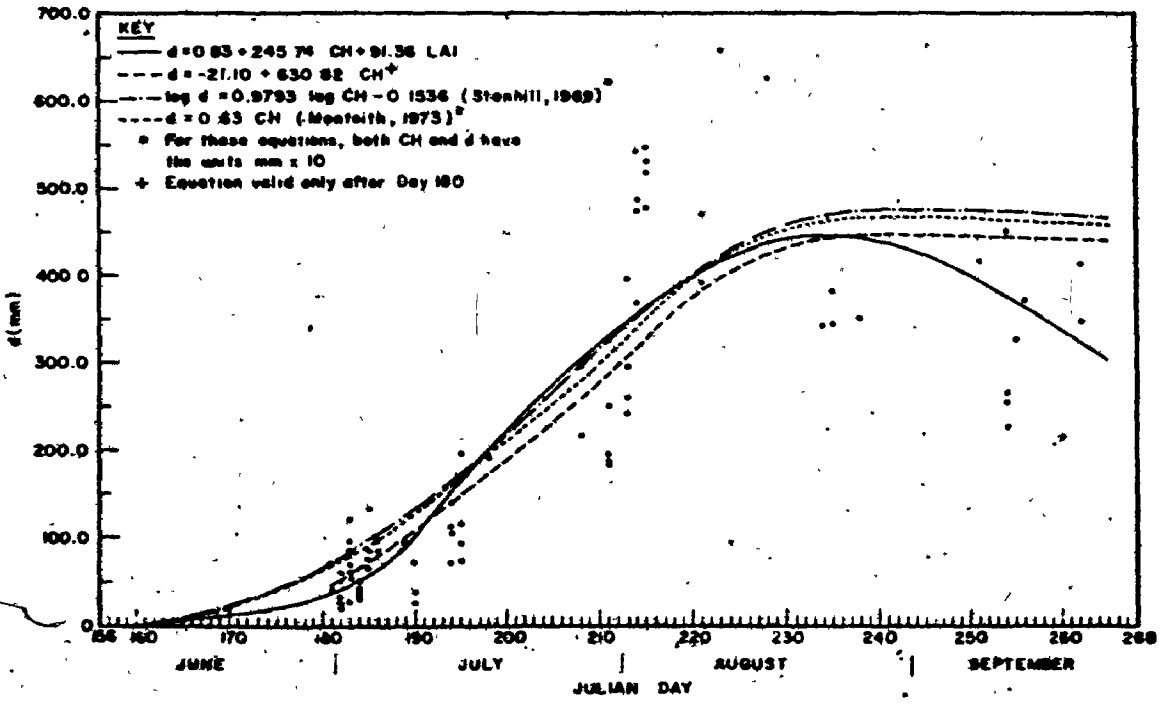

Figure 4.4. Comparison of d model estimates.

$$d = -21.10 + 630.82\ CH \quad . \qquad (4.4)$$

As one would expect, these fail to show the increase in z_o and decrease in d that continues after mid-August. Prior to this time, all models give similar results. It is worth noting that the Monteith and Tanner and Pelton models for z_o give results which are very similar to those from equation 4.3. Likewise, the Monteith and Stanhill expressions for d compare quite closely with equation 4.4.

2. The role of aerodynamic resistances in the combination model

The aerodynamic resistance for momentum exchange was calculated for each of the four measurement levels from equation 2.29 using daily values of z_o and d (equations 4.1 and 4.2). The aerodynamic resistance for heat and water vapour exchange was obtained from equation 2.37.

a. Sensitivity of aerodynamic resistances to z_o and d

Study of the sensitivity of aerodynamic resistances to z_o and d was prompted by the wide range in values for these parameters. Almost all of the field determinations of z_o and d are within ± 50% of the values estimated by equations 4.1 and 4.2 (Figures 4.5 and 4.6). Using the equation estimates of z_o and d, r_{aM}, r_b and r_{aVH} were evaluated, without stability correction, over the whole measurement period. For relative errors of 10%, 20% and 50% in z_o and d, the resulting errors (absolute and relative) in r_{aM}, r_b and r_{aVH} were calculated for four windspeeds. Details of this analysis are presented in Appendix Four. Results for 12 days evenly spaced throughout the study period are tabulated in Table 4.1. These data show that:

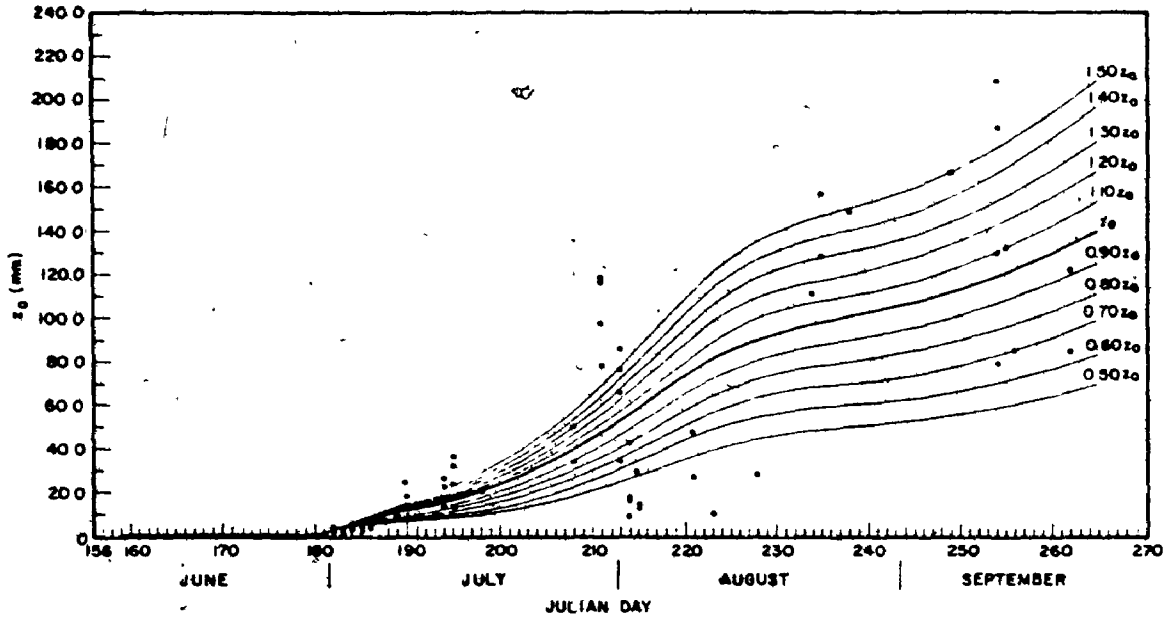

Figure 4.5. The progression of variable z_o throughout the growing season. Variation illustrated ranges from 50% to 150% of z_o computed from equation 4.1.

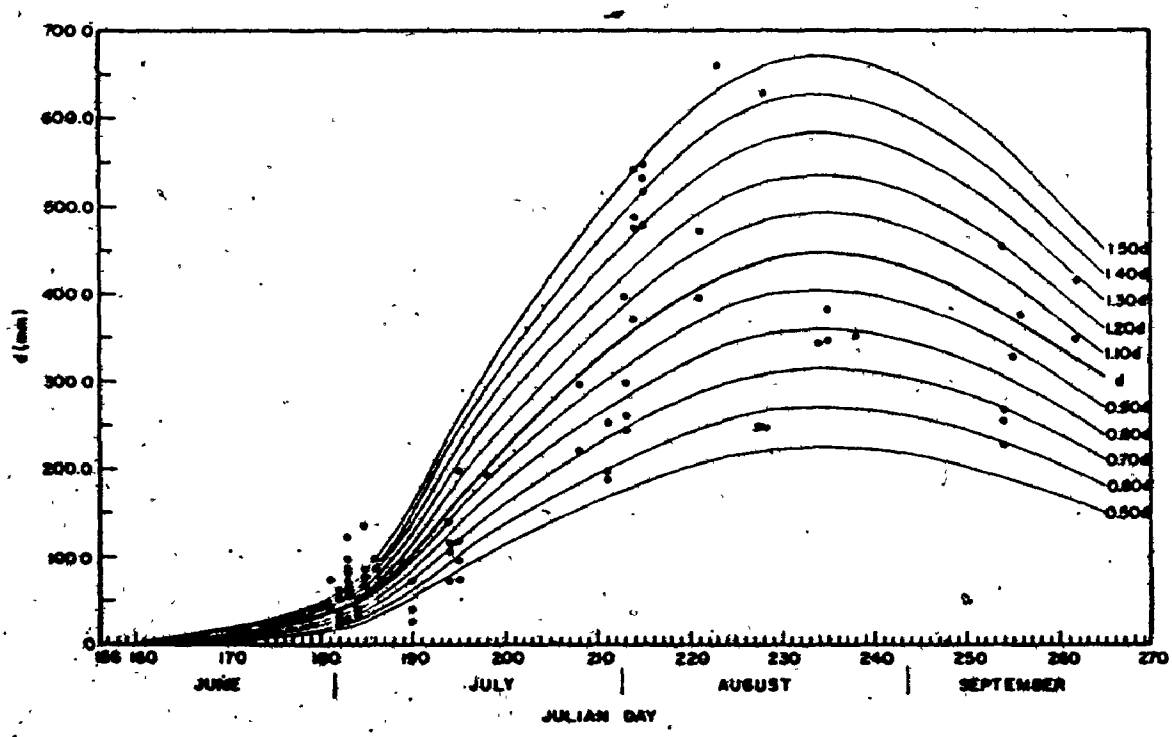

Figure 4.6. The progression of variable d throughout the growing season. Variation illustrated ranges from 50% to 150% of d computed from equation 4.2.

TABLE 4.1(a). Errors in Aerodynamic Resistance for Windspeed of 1.0 m s^{-1}

Reference height for wind velocity is 1.5 m

	z_o	d	r_{aN}	r_b	r_{aVH}	$\frac{\delta z_o}{z_o}$	δr_{aN}	$\frac{\delta r_{aN}}{r_{aN}}$	δr_b	$\frac{\delta r_b}{r_b}$	δr_{aVH}	$\frac{\delta r_{aVH}}{r_{aVH}}$	$\frac{\delta d}{d}$	δr_{aN}	$\frac{\delta r_{aN}}{r_{aN}}$	δr_b	$\frac{\delta r_b}{r_b}$	δr_{aVH}	$\frac{\delta r_{aVH}}{r_{aVH}}$
	(cm)	(cm)	($s m^{-1}$)			(%)	($s m^{-1}$)	(%)	($s m^{-1}$)	(%)	($s m^{-1}$)	(%)	(%)	($s m^{-1}$)	(%)	($s m^{-1}$)	(%)	($s m^{-1}$)	(%)
152	1.0	0.8	316.6	41.8	361.0	10.0	8.7	2.7	0.4	0.9	9.1	2.5	10.0	0.0	0.0	0.0	0.0	0.0	0.0
						20.0	17.4	5.5	0.8	1.9	18.2	5.0	20.0	0.0	0.0	0.0	0.0	0.0	0.0
						50.0	43.5	13.7	2.0	4.7	45.5	12.6	50.0	0.0	0.0	0.0	0.0	0.0	0.0
160	1.0	9.8	317.7	42.8	369.5	10.0	8.7	2.7	0.4	0.9	9.1	2.5	10.0	0.1	0.0	0.0	0.0	0.0	0.0
						20.0	17.4	5.5	0.8	1.9	18.2	5.0	20.0	0.1	0.0	0.0	0.0	0.1	0.0
						50.0	43.4	13.7	2.0	4.7	45.4	12.6	50.0	0.3	0.1	0.0	0.0	0.3	0.1
178	1.0	27.0	326.6	42.7	359.3	10.0	8.7	2.7	0.4	0.9	9.1	2.5	10.0	0.2	0.1	0.0	0.0	0.2	0.1
						20.0	17.4	5.5	0.8	1.9	18.2	5.1	20.0	0.5	0.1	0.0	0.0	0.5	0.1
						50.0	43.4	13.7	2.0	4.7	45.4	12.6	50.0	0.8	0.3	0.0	0.0	0.8	0.2
188	12.0	81.6	136.0	32.2	168.2	10.0	5.6	4.1	0.5	1.6	6.1	3.6	10.0	0.3	0.2	0.0	0.0	0.3	0.2
						20.0	11.3	8.3	0.9	2.8	12.2	7.2	20.0	0.7	0.5	0.1	0.3	0.9	0.5
						50.0	28.2	20.7	2.2	6.8	30.4	18.1	50.0	1.6	1.2	0.1	0.3	1.7	1.0
195	19.2	86.2	105.4	29.6	135.0	10.0	4.9	4.6	0.5	2.7	5.4	4.0	10.0	0.8	0.6	0.1	0.3	0.9	0.7
						20.0	9.7	9.2	0.9	3.0	10.6	7.9	20.0	1.6	1.5	0.2	0.7	1.8	1.3
						50.0	24.7	23.4	2.3	7.8	27.0	20.0	50.0	3.9	3.7	0.4	1.4	4.3	3.2
208	39.1	107.8	70.8	25.9	96.7	10.0	4.0	5.6	0.5	1.9	4.5	4.7	10.0	1.0	1.4	0.1	0.4	1.1	1.1
						20.0	8.0	11.3	1.0	3.9	9.0	9.3	20.0	2.1	3.0	0.3	1.2	2.4	2.5
						50.0	19.9	28.1	2.4	9.3	22.3	23.1	50.0	5.1	7.4	0.6	2.3	5.7	5.9
216	67.1	191.3	46.8	22.9	71.7	10.0	3.2	6.6	0.5	2.2	3.7	5.2	10.0	1.1	2.3	0.2	0.9	1.3	1.8
						20.0	6.4	13.1	1.0	4.4	7.4	10.3	20.0	2.3	4.7	0.4	1.7	2.7	3.8
						50.0	16.1	33.0	2.5	10.9	18.6	25.9	50.0	5.7	11.7	0.9	3.9	6.6	9.2
228	91.9	438.4	38.1	21.1	59.2	10.0	2.8	7.3	0.5	2.4	3.3	5.6	10.0	1.1	2.9	0.2	0.9	1.3	2.2
						20.0	5.4	14.2	1.0	4.7	6.4	10.8	20.0	2.3	6.0	0.4	1.9	2.7	4.6
						50.0	13.9	36.5	2.6	12.3	16.5	27.9	50.0	5.7	15.0	1.1	5.2	6.8	11.5
238	260.3	444.6	35.5	20.6	56.1	10.0	2.7	7.6	0.5	2.4	3.2	5.7	10.0	1.1	3.1	0.2	1.0	1.3	2.3
						20.0	5.3	14.9	1.0	4.9	6.3	11.2	20.0	2.2	6.2	0.4	1.9	2.6	4.6
						50.0	13.3	37.5	2.6	12.6	15.9	28.3	50.0	5.6	15.6	1.1	5.3	6.7	11.9
248	110.4	412.9	32.8	20.3	54.1	10.0	2.6	7.7	0.5	2.5	3.1	5.7	10.0	1.0	2.9	0.2	1.0	1.2	2.2
						20.0	5.2	15.4	1.0	4.9	6.2	11.5	20.0	2.0	5.9	0.4	2.0	2.4	4.4
						50.0	12.9	38.2	2.6	12.8	15.5	28.7	50.0	4.9	14.5	1.0	4.9	5.9	10.9
258	125.7	252.2	31.9	19.9	51.8	10.0	2.5	7.8	0.5	2.5	3.0	5.8	10.0	0.8	2.5	0.2	1.0	1.0	1.9
						20.0	5.0	15.7	1.0	5.0	6.0	11.6	20.0	1.5	4.7	0.3	1.5	1.8	3.5
						50.0	12.4	38.0	2.6	13.1	15.0	29.0	50.0	3.8	11.9	0.8	4.0	4.6	8.9
265	140.0	258.7	30.4	19.6	50.0	10.0	2.4	7.9	0.5	2.6	2.9	5.8	10.0	0.6	2.0	0.2	0.5	0.7	1.4
						20.0	4.8	15.8	1.0	5.1	5.8	11.6	20.0	1.2	3.9	0.3	1.5	1.5	3.0
						50.0	12.0	39.5	2.6	13.3	14.6	29.2	50.0	3.0	9.9	0.6	3.1	3.6	7.2

TABLE 4.1(b). Errors in Aerodynamic Resistance for Windspeed of 2.5 m s^{-1}

Reference height for wind velocity is 1.5 m

Station No.	z_o (mm)	d (m)	r_{aV}	r_b	r_{aVH} ($s\,m^{-1}$)	$\frac{\delta z_o}{z_o}$ (%)	δr_{aV} ($s\,m^{-1}$)	$\frac{\delta r_{aV}}{r_{aV}}$ (%)	δr_b ($s\,m^{-1}$)	$\frac{\delta r_b}{r_b}$ (%)	δr_{aVH} ($s\,m^{-1}$)	$\frac{\delta r_{aVH}}{r_{aVH}}$ (%)	$\frac{\delta d}{d}$ (%)	δr_{aV} ($s\,m^{-1}$)	$\frac{\delta r_{aV}}{r_{aV}}$ (%)	δr_b ($s\,m^{-1}$)	$\frac{\delta r_b}{r_b}$ (%)	δr_{aVH} ($s\,m^{-1}$)	$\frac{\delta r_{aVH}}{r_{aVH}}$ (%)
159	1.0	0.8	127.3	23.2	150.5	10.0	3.5	2.7	0.2	0.9	3.7	2.5	10.0	0.0	0.0	0.0	0.0	0.0	0.0
						20.0	7.0	5.5	0.4	1.7	7.4	4.9	20.0	0.0	0.0	0.0	0.0	0.0	0.0
						50.0	17.4	13.7	1.1	4.7	18.5	12.3	50.0	0.0	0.0	0.0	0.0	0.0	0.0
165	1.0	9.8	127.1	23.2	150.3	10.0	3.5	2.8	0.2	0.9	3.7	2.5	10.0	0.0	0.0	0.0	0.0	0.0	0.0
						20.0	7.0	5.5	0.4	1.7	7.4	4.9	20.0	0.1	0.1	0.0	0.0	0.1	0.1
						50.0	17.4	13.7	1.1	4.7	18.5	12.3	50.0	0.1	0.1	0.0	0.0	0.1	0.1
176	1.0	27.0	126.7	23.2	149.9	10.0	3.5	2.8	0.2	0.9	3.7	2.5	10.0	0.1	0.1	0.0	0.0	0.1	0.1
						20.0	6.9	5.4	0.4	1.7	7.3	4.9	20.0	0.1	0.1	0.0	0.0	0.1	0.1
						50.0	17.4	13.7	1.1	4.7	18.5	12.3	50.0	0.3	0.2	0.0	0.0	0.3	0.2
188	12.0	81.6	54.4	17.5	71.9	10.0	2.3	4.2	0.2	1.1	2.5	3.5	10.0	0.1	0.2	0.0	0.0	0.1	0.1
						20.0	4.5	8.3	0.5	2.9	5.0	7.0	20.0	0.3	0.6	0.0	0.0	0.3	0.4
						50.0	11.3	20.8	1.2	6.9	12.5	17.4	50.0	0.7	1.3	0.1	0.6	0.7	1.0
198	19.5	206.2	42.1	16.1	58.2	10.0	2.0	4.8	0.3	1.9	2.3	4.0	10.0	0.3	0.7	0.0	0.0	0.3	0.5
						20.0	4.0	9.5	0.5	3.1	4.5	7.7	20.0	0.6	1.4	0.1	0.5	0.7	1.2
						50.0	9.7	23.0	1.3	8.1	11.0	18.9	50.0	1.6	3.8	0.2	1.2	1.8	3.1
208	39.1	307.8	28.3	14.1	42.4	10.0	1.6	5.7	0.3	2.1	1.9	4.5	10.0	0.4	1.4	0.1	0.7	0.5	1.2
						20.0	3.2	11.3	0.5	3.5	3.7	8.8	20.0	0.8	2.8	0.1	0.7	0.9	2.1
						50.0	8.0	28.3	1.3	9.2	9.3	21.9	50.0	2.0	7.1	0.3	2.1	2.3	5.4
218	67.1	391.3	19.5	12.4	31.9	10.0	1.3	6.7	0.3	2.4	1.6	5.0	10.0	0.5	2.6	0.1	0.8	0.6	1.9
						20.0	2.6	13.3	0.6	4.8	3.2	11.0	20.0	0.9	4.6	0.2	1.6	1.2	3.8
						50.0	6.4	32.8	1.4	11.3	7.8	24.5	50.0	2.3	11.8	0.5	4.0	2.8	8.9
228	91.9	436.4	15.2	11.4	26.6	10.0	1.1	7.2	0.3	2.6	1.4	5.3	10.0	0.5	3.3	0.1	0.9	0.6	2.5
						20.0	2.2	14.5	0.6	5.3	2.8	10.5	20.0	0.9	5.9	0.2	1.8	1.1	4.1
						50.0	5.5	36.3	1.4	12.3	6.9	25.9	50.0	2.3	15.1	0.6	5.3	2.9	10.9
235	100.3	444.6	14.2	11.2	25.4	10.0	1.1	7.7	0.3	2.7	1.4	5.5	10.0	0.5	3.5	0.1	0.9	0.6	2.4
						20.0	2.1	14.8	0.6	5.4	2.7	10.6	20.0	0.9	6.3	0.2	1.8	1.1	4.3
						50.0	5.2	37.3	1.4	12.5	6.7	26.4	50.0	2.2	15.5	0.6	5.4	2.8	11.0
248	120.4	442.9	13.5	11.0	24.5	10.0	1.0	7.4	0.3	2.7	1.3	5.3	10.0	0.4	3.0	0.1	0.9	0.5	2.0
						20.0	2.1	15.6	0.6	5.5	2.7	11.0	20.0	0.8	5.9	0.2	1.8	1.0	4.1
						50.0	5.2	38.5	1.4	12.7	6.6	26.9	50.0	2.0	14.8	0.5	4.5	2.5	10.2
253	125.7	352.8	12.8	10.8	23.6	10.0	1.0	7.8	0.3	2.8	1.3	5.5	10.0	0.3	2.2	0.1	0.9	0.4	1.7
						20.0	2.0	15.6	0.6	5.6	2.6	11.0	20.0	0.6	4.7	0.2	1.9	0.8	3.4
						50.0	5.0	39.1	1.4	13.0	6.4	27.1	50.0	1.5	11.7	0.4	3.7	1.9	8.1
265	140.0	298.7	12.2	10.6	22.8	10.0	1.0	8.2	0.3	2.8	1.3	5.7	10.0	0.2	1.6	0.1	0.9	0.3	1.3
						20.0	1.9	15.6	0.6	5.7	2.5	11.0	20.0	0.5	4.1	0.1	0.9	0.6	2.6
						50.0	4.8	39.3	1.4	13.2	6.2	27.2	50.0	1.2	9.8	0.4	3.8	1.6	7.0

TABLE 4.1(c). Errors in Aerodynamic Resistance for Windspeed of 5.0 m s^{-1}

Peference height for wind velocity is 1.5 m

Day	z_o (cm)	d (cm)	r_{aM}	r_b	r_{aVH} ($s\,m^{-1}$)	$\frac{\delta z_o}{z_o}$ (%)	δr_{aM} ($s\,m^{-1}$)	$\frac{\delta r_{aM}}{r_{aM}}$ (%)	δr_b ($s\,m^{-1}$)	$\frac{\delta r_b}{r_b}$ (%)	δr_{aVH} ($s\,m^{-1}$)	$\frac{\delta r_{aVH}}{r_{aVH}}$ (%)	$\frac{\delta d}{d}$ (%)	δr_{aM} ($s\,m^{-1}$)	$\frac{\delta r_{aM}}{r_{aM}}$ (%)	δr_b ($s\,m^{-1}$)	$\frac{\delta r_b}{r_b}$ (%)	δr_{aVH} ($s\,m^{-1}$)	$\frac{\delta r_{aVH}}{r_{aVH}}$ (%)
159	1.0	0.0	63.6	14.6	78.2	10.0	1.7	2.7	0.1	0.7	1.8	2.3	10.0	0.0	0.0	0.0	0.0	0.0	0.0
						20.0	3.5	5.5	0.3	2.1	3.8	4.9	20.0	0.0	0.0	0.0	0.0	0.0	0.0
						50.0	8.7	13.7	0.7	4.8	9.4	12.0	50.0	0.1	0.2	0.0	0.0	0.1	0.2
163	1.0	9.0	63.5	14.6	78.1	10.0	1.7	2.7	0.1	0.7	1.8	2.3	10.0	0.0	0.0	0.0	0.0	0.0	0.0
						20.0	3.5	5.5	0.3	2.1	3.8	4.9	20.0	0.0	0.0	0.0	0.0	0.0	0.0
						50.0	8.7	13.7	0.7	4.8	9.4	12.0	50.0	0.1	0.2	0.0	0.0	0.1	0.2
178	1.0	27.0	63.3	14.6	77.9	10.0	1.7	2.7	0.1	0.7	1.8	2.3	10.0	0.0	0.0	0.0	0.0	0.0	0.0
						20.0	3.5	5.5	0.3	2.1	3.8	4.9	20.0	0.1	0.2	0.0	0.0	0.1	0.1
						50.0	8.7	13.7	0.7	4.5	9.4	12.1	50.0	0.2	0.3	0.0	0.0	0.2	0.3
188	12.0	61.6	27.2	11.0	38.2	10.0	1.1	4.0	0.2	1.8	1.3	3.4	10.0	0.1	0.4	0.0	0.0	0.1	0.3
						20.0	2.3	8.5	0.2	2.7	2.6	6.8	20.0	0.1	0.4	0.0	0.0	0.1	0.3
						50.0	5.6	20.6	0.5	7.3	6.4	16.6	50.0	0.3	1.1	0.0	0.0	0.3	0.8
198	19.5	206.2	21.1	10.1	31.2	10.0	1.0	4.7	0.2	2.0	1.2	3.9	10.0	0.2	0.9	0.0	0.0	0.0	0.0
						20.0	2.0	9.5	0.3	3.0	2.3	7.4	20.0	0.3	1.4	0.1	1.0	0.4	1.3
						50.0	4.9	23.2	0.8	7.9	5.7	18.3	50.0	0.8	3.8	0.1	1.0	0.9	3.0
208	39.1	307.8	14.2	8.9	23.1	10.0	0.8	5.6	0.2	2.2	1.0	4.3	10.0	0.2	1.4	0.0	0.0	0.2	0.9
						20.0	1.6	11.3	0.3	3.4	1.9	8.2	20.0	0.4	2.8	0.1	1.1	0.5	2.2
						50.0	4.0	28.2	0.8	9.0	4.8	20.8	50.0	1.0	7.0	0.2	2.2	1.2	5.2
218	67.1	391.3	9.8	7.8	17.6	10.0	0.8	6.1	0.2	2.6	0.8	4.5	10.0	0.2	2.0	0.1	1.3	0.5	2.7
						20.0	1.3	13.3	0.3	3.8	1.6	9.1	20.0	0.5	5.1	0.1	1.3	0.6	3.4
						50.0	3.2	32.7	0.9	11.5	4.1	23.3	50.0	1.1	11.2	0.3	3.8	1.4	8.0
228	91.9	436.4	7.6	7.2	14.8	10.0	0.8	7.9	0.2	2.8	0.8	5.4	10.0	0.2	2.6	0.1	1.4	0.3	2.0
						20.0	1.1	14.5	0.4	5.6	1.5	10.1	20.0	0.5	6.6	0.1	1.4	0.6	4.1
						50.0	2.8	36.8	0.9	12.5	3.7	25.0	50.0	1.1	14.5	0.4	5.6	1.5	10.1
238	100.3	444.6	7.1	7.0	14.1	10.0	0.8	7.0	0.2	2.9	0.7	5.0	10.0	0.2	2.6	0.1	1.4	0.3	2.1
						20.0	1.1	15.5	0.4	5.7	1.5	10.6	20.0	0.5	7.0	0.2	2.9	0.7	5.0
						50.0	2.7	38.0	0.9	12.9	3.6	25.5	50.0	1.1	15.5	0.4	5.7	1.5	10.6
248	109.4	432.9	6.8	6.9	13.7	10.0	0.8	7.4	0.2	2.9	0.7	5.1	10.0	0.2	2.9	0.1	1.4	0.3	2.2
						20.0	1.0	14.7	0.4	5.8	1.4	10.2	20.0	0.4	5.9	0.1	1.4	0.5	3.6
						50.0	2.6	38.2	0.8	13.0	3.5	25.5	50.0	1.0	14.7	0.3	4.3	1.3	9.5
258	125.7	352.2	6.4	6.8	13.2	10.0	0.8	7.8	0.2	2.9	0.7	5.3	10.0	0.2	3.1	0.1	1.5	0.3	2.3
						20.0	1.0	15.6	0.4	5.9	1.4	10.6	20.0	0.3	4.7	0.1	1.5	0.4	3.0
						50.0	2.5	39.1	0.9	13.2	3.4	25.8	50.0	0.8	12.5	0.3	4.4	1.1	8.3
265	140.0	298.7	6.1	6.7	12.8	10.0	0.5	8.2	0.2	3.0	0.7	5.5	10.0	0.1	1.6	0.0	0.0	0.1	0.8
						20.0	1.0	16.4	0.4	6.0	1.4	10.9	20.0	0.2	3.3	0.1	1.5	0.3	2.3
						50.0	2.4	39.3	0.9	13.4	3.3	25.8	50.0	0.6	9.6	0.2	3.0	0.8	6.3

TABLE 4.1(d). Errors in Aerodynamic Resistance for Windspeed of 10.0 m s^{-1}

Reference height for wind velocity is 1.5 m

Julian Day	z_o (cm)	d (cm)	r_{aM}	r_b	r_{aVH} (----- sm^{-1} -----)	$\frac{\delta z_o}{z_o}$ (%)	δr_{aM} (sm^{-1})	$\frac{\delta r_{aM}}{r_{aM}}$ (%)	δr_b (sm^{-1})	$\frac{\delta r_b}{r_b}$ (%)	δr_{aVH} (sm^{-1})	$\frac{\delta r_{aVH}}{r_{aVH}}$ (%)	$\frac{\delta d}{d}$ (%)	δr_{aM} (sm^{-1})	$\frac{\delta r_{aM}}{r_{aM}}$ (%)	δr_b (sm^{-1})	$\frac{\delta r_b}{r_b}$ (%)	δr_{aVH} (sm^{-1})	$\frac{\delta r_{aVH}}{r_{aVH}}$ (%)
159	1.0	9.8	31.8	9.2	41.0	10.0	0.9	2.8	0.1	1.1	1.0	2.4	10.0	0.0	0.0	0.0	0.0	0.0	0.0
						20.0	1.7	5.3	0.2	2.2	1.9	4.6	20.0	0.0	0.0	0.0	0.0	0.0	0.0
						50.0	4.4	13.8	0.4	4.3	4.8	11.7	50.0	0.0	0.0	0.0	0.0	0.0	0.0
168	1.0	9.8	31.8	9.2	41.0	10.0	0.9	2.8	0.1	1.1	1.0	2.4	10.0	0.0	0.0	0.0	0.0	0.0	0.0
						20.0	1.7	5.3	0.2	2.2	1.9	4.6	20.0	0.0	0.0	0.0	0.0	0.0	0.0
						50.0	4.3	13.6	0.4	4.3	4.7	11.5	50.0	0.0	0.0	0.0	0.0	0.0	0.0
178	1.0	27.0	31.7	9.2	40.9	10.0	0.9	2.8	0.1	1.1	1.0	2.4	10.0	0.0	0.0	0.0	0.0	0.0	0.0
						20.0	1.7	5.4	0.2	2.2	1.9	4.6	20.0	0.0	0.0	0.0	0.0	0.0	0.0
						50.0	4.3	13.6	0.4	4.3	4.7	11.5	50.0	0.1	0.3	0.0	0.0	0.1	0.2
188	12.0	81.6	13.6	6.9	20.5	10.0	0.6	4.4	0.1	1.4	0.7	3.4	10.0	0.0	0.0	0.0	0.0	0.0	0.0
						20.0	1.1	8.1	0.2	2.9	1.3	6.3	20.0	0.1	0.7	0.0	0.0	0.1	0.5
						50.0	2.8	20.6	0.5	7.2	3.3	16.1	50.0	0.2	1.5	0.0	0.0	0.2	1.0
198	19.5	205.2	10.5	6.4	16.9	10.0	0.5	4.8	0.1	1.6	0.6	3.6	10.0	0.1	1.0	0.0	0.0	0.1	0.6
						20.0	1.0	9.5	0.2	3.1	1.2	7.1	20.0	0.2	1.9	0.0	0.0	0.2	1.2
						50.0	2.5	23.8	0.5	7.8	3.0	17.8	50.0	0.4	3.8	0.1	1.6	0.5	3.0
208	39.1	307.8	7.1	5.6	12.7	10.0	0.4	5.6	0.1	1.8	0.5	3.9	10.0	0.1	1.4	0.0	0.0	0.1	0.8
						20.0	0.8	11.3	0.2	3.6	1.0	7.9	20.0	0.2	2.8	0.1	1.8	0.3	2.4
						50.0	2.0	28.2	0.5	8.9	2.5	19.7	50.0	0.5	7.0	0.1	1.8	0.6	4.7
218	67.1	392.3	4.9	4.9	9.8	10.0	0.3	6.1	0.1	2.0	0.4	4.1	10.0	0.1	2.0	0.0	0.0	0.1	1.0
						20.0	0.6	12.2	0.2	4.1	0.8	8.2	20.0	0.2	4.1	0.1	2.0	0.3	3.1
						50.0	1.6	30.7	0.5	10.2	2.1	21.4	50.0	0.6	12.2	0.2	4.1	0.8	8.0
228	91.9	432.4	3.8	4.5	8.3	10.0	0.3	7.9	0.1	2.2	0.4	4.8	10.0	0.1	2.6	0.1	2.2	0.2	2.4
						20.0	0.6	15.8	0.2	4.4	0.8	9.6	20.0	0.2	5.3	0.1	2.2	0.3	3.6
						50.0	1.4	36.8	0.6	13.3	2.0	24.1	50.0	0.6	15.8	0.2	4.4	0.8	9.5
238	103.8	444.6	3.6	4.4	8.0	10.0	0.3	8.3	0.1	2.3	0.4	5.0	10.0	0.1	2.8	0.1	2.3	0.2	2.5
						20.0	0.5	13.9	0.2	4.5	0.7	8.8	20.0	0.2	5.6	0.1	2.3	0.3	3.8
						50.0	1.3	35.1	0.6	13.6	1.9	23.8	50.0	0.6	16.7	0.2	4.5	0.8	10.0
248	115.4	422.9	3.4	4.4	7.8	10.0	0.3	8.8	0.1	2.3	0.4	5.1	10.0	0.1	2.9	0.0	0.0	0.1	1.5
						20.0	0.5	14.7	0.2	4.5	0.7	9.0	20.0	0.2	5.9	0.1	2.3	0.3	3.8
						50.0	1.3	38.2	0.6	13.6	1.8	24.4	50.0	0.5	14.7	0.2	4.5	0.7	9.0
258	125.7	352.2	3.2	4.3	7.5	10.0	0.3	9.4	0.1	2.3	0.4	5.3	10.0	0.1	3.1	0.0	0.0	0.1	1.1
						20.0	0.5	15.6	0.2	4.7	0.7	9.3	20.0	0.2	6.3	0.1	2.3	0.3	4.0
						50.0	1.2	37.5	0.6	14.0	1.8	24.0	50.0	0.4	12.5	0.2	4.7	0.6	8.0
265	140.0	298.7	3.0	4.2	7.2	10.0	0.2	6.6	0.1	2.4	0.3	4.2	10.0	0.1	3.3	0.0	0.0	0.1	1.4
						20.0	0.5	16.7	0.2	4.8	0.7	9.7	20.0	0.1	3.3	0.1	2.4	0.3	2.8
						50.0	1.2	40.0	0.6	14.3	1.8	25.0	50.0	0.3	10.0	0.1	2.4	0.4	5.6

(1) Errors in r_{aM} exceed those in r_b. Since absolute errors in r_{aVH} are the sum of those in r_{aM} and r_b, they are the largest.

(2) Errors in the resistances increase with errors in both z_o and d but are more sensitive to errors in z_o than in d.

(3) Errors in the resistances arising from errors in z_o increase throughout the study period and those arising from errors in d decrease towards the termination of the growing season.

(4) As the resistances r_{aM}, r_b and r_{aVH} decrease with increased windspeed, so do the errors arising from z_o and d.

As z_o and d are both evaluated from wind profiles, errors in these terms are unlikely to occur independently. Therefore, resistances, without stability correction, were evaluated for systematic errors in both z_o and d of ± 50%, ± 10% and 0%. This induced variability in r_{aVH} and its ratio to actual r_{aVH} (r_{aVH}'/r_{aVH}) is presented in Figure 4.7. The variation of r_{aVH} with time and windspeed is striking. The decrease in r_{aVH} as the surface becomes aerodynamically rougher and the windspeed increases is apparent. However, the variation of r_{aVH}'/r_{aVH} throughout the season is similar for all windspeeds.

The effect of r_{aVH} variability on λQ_E estimations is now considered. Employing the sensitivity analysis outlined in Appendix Five, for relative errors in r_{aVH} of 10%, 20% and 50%, the combination model (equation 2.20) is relatively insensitive to r_{aVH} error (Table 4.2).

Arising from the interaction between variables in the combination model, a definitive summary of the results in Table 4.2 is difficult. Hence, further analysis employing actual hourly data from the study was undertaken. From Figure 4.7, the range of variability in r_{aVH} due

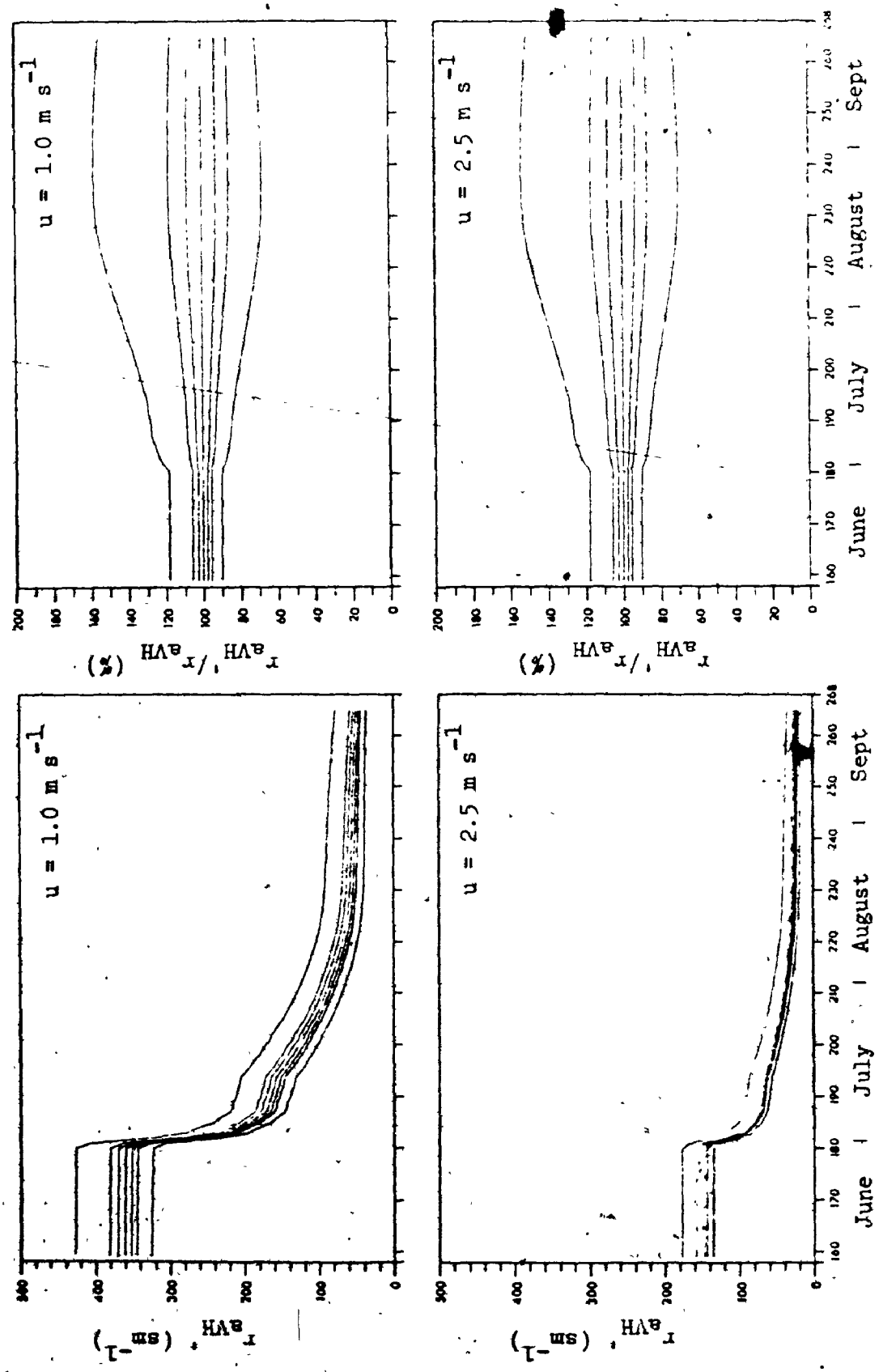

Figure 4.7. Influence of variable z_o and d on r_{aVH} for a range of windspeeds at a height of 1.5 m. In all figures, the group of curves, respectively from the uppermost to the lowest, represent r_{aVH}' computed for -50%, -20%, -10%, 0%, 10%, 20% and 50% variation in both z_o and d.

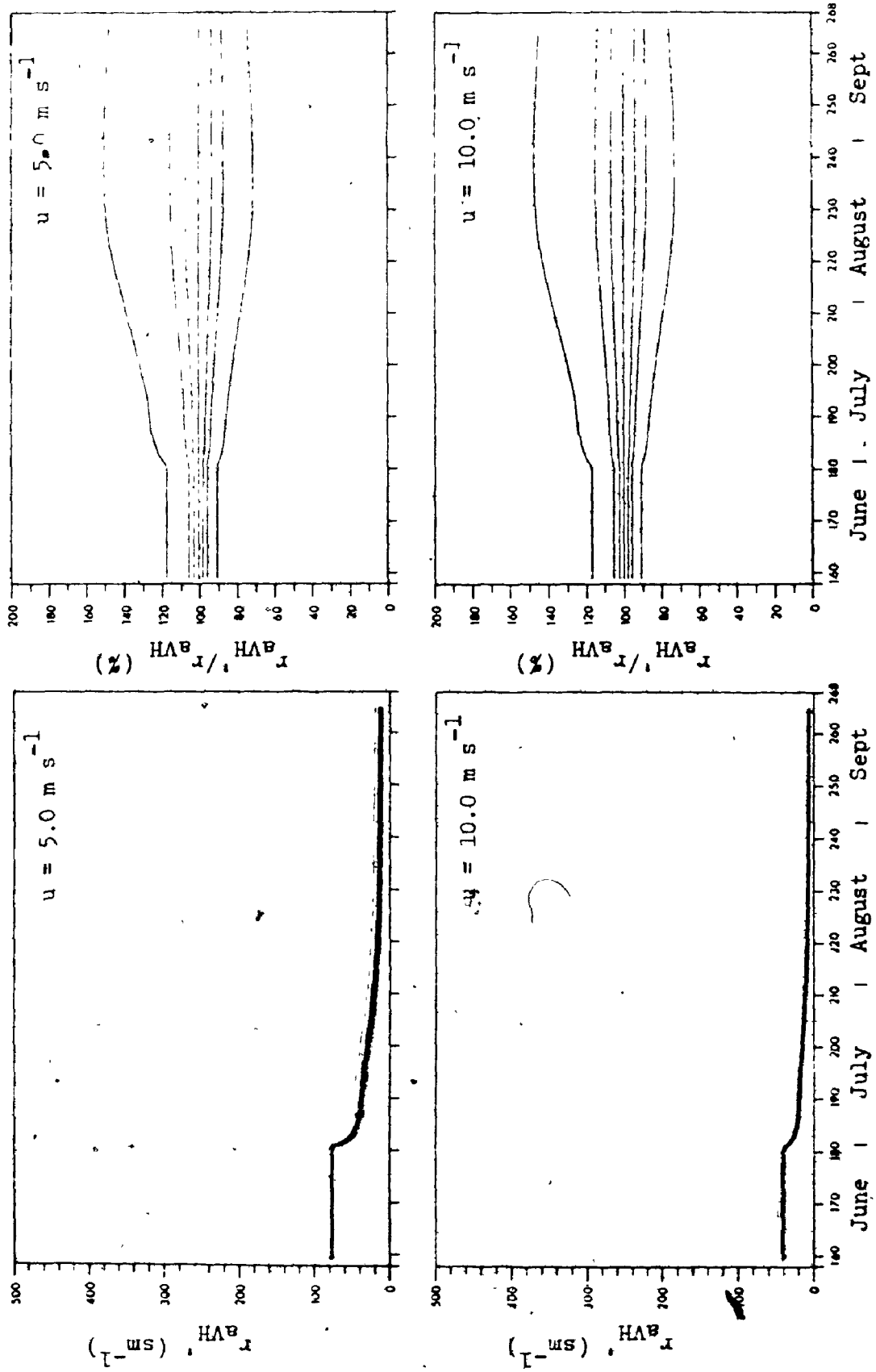

Figure 4.7 (cont'd.). Influence of variable z_o and d on r_{aVH} for a range of windspeeds at a height of 1.5 m.

TABLE 4.2. Sensitivity of Equation 2.20 to r_{aVH}

C^*-C_z (Ws^{-2})	r_{aVH} (sm^{-1})	r_{ST} (sm^{-1})	$e_s[\theta,z]-e(z)$ (Pa)	λE_z (Ws^{-2})	$\delta r_{aVH}/r_{aVH}$ = 10%		$\delta r_{aVH}/r_{aVH}$ = 20%		$\delta r_{aVH}/r_{aVH}$ = 50%	
					$\delta\lambda E_z$ (Ws^{-2})	$\delta\lambda E_z/\lambda E_z$ (%)	$\delta\lambda E_z$ (Ws^{-2})	$\delta\lambda E_z/\lambda E_z$ (%)	$\delta\lambda E_z$ (Ws^{-2})	$\delta\lambda E_z/\lambda E_z$ (%)
100	50	100	500	77.6	-.5	-.7	-1.1	-1.4	-2.7	-3.5
			1500	148.1	-4.9	-3.3	-9.8	-6.6	-24.4	-16.5
			2500	218.7	-9.2	-4.2	-18.4	-8.4	-46.1	-21.1
		200	500	56.0	.6	1.0	1.1	2.0	2.8	5.0
			1500	106.9	-1.7	-1.6	-3.4	-3.2	-8.5	-7.9
			2500	157.9	-4.0	-2.5	-7.9	-5.0	-19.8	-12.5
		500	500	50.5	.6	1.0	1.2	2.1	3.6	6.1
			1500	98.3	.3	.4	.5	.9	1.3	2.2
			2500	86.1	-.4	-.5	-.8	-1.0	-2.1	-2.4
	100	100	500	74.2	-.4	-.6	-.8	-1.1	-2.1	-2.8
			1500	117.9	-3.7	-3.2	-7.5	-6.4	-18.7	-15.9
			2500	161.6	-7.1	-4.4	-14.1	-8.8	-35.4	-21.9
		200	500	59.9	.5	.9	1.1	1.8	2.7	4.5
			1500	95.2	-1.6	-1.7	-3.3	-3.4	-8.1	-8.6
			2500	130.5	-3.8	-2.9	-7.6	-5.8	-19.0	-14.6
		500	500	55.0	.6	1.2	1.4	2.3	3.6	6.3
			1500	60.4	.3	.5	.7	1.1	1.6	2.7
			2500	82.7	-.5	-.7	-1.1	-1.3	-2.7	-3.3
	200	100	500	71.8	-.3	-.4	-.5	-.7	-1.3	-1.9
			1500	96.6	-2.4	-2.5	-4.8	-5.0	-12.1	-12.5
			2500	121.4	-4.6	-3.8	-9.1	-7.5	-22.8	-18.8
		200	500	63.3	.4	.7	.8	1.3	2.1	3.3
			1500	85.1	-1.2	-1.5	-2.5	-2.9	-6.2	-7.3
			2500	107.0	-2.9	-2.7	-5.8	-5.4	-14.6	-13.5
		500	500	56.6	1.2	2.1	2.5	5.3	6.2	13.3
			1500	67.7	.3	.5	.7	1.1	1.7	2.7
			2500	79.9	-.6	-.7	-1.1	-1.4	-2.8	-3.6
200	50	100	500	119.8	1.1	.9	2.2	1.8	5.4	4.5
			1500	150.4	-3.3	-1.7	-6.5	-3.4	-16.3	-8.6
			2500	268.9	-7.6	-2.9	-15.2	-5.8	-38.0	-14.6
		200	500	66.5	2.3	2.6	4.5	5.2	11.3	13.1
			1500	137.5	0.0	0.0	0.0	0.0	0.0	0.0
			2500	188.4	-2.3	-1.2	-4.5	-2.4	-11.3	-6.0
		500	500	47.2	2.2	4.6	4.4	9.3	10.9	23.2
			1500	75.0	1.5	2.0	3.0	4.0	7.6	10.1
			2500	102.8	.8	.8	1.7	1.6	4.2	4.1
	100	100	500	126.5	.8	.7	1.7	1.3	4.2	3.3
			1500	170.2	-2.5	-1.5	-5.0	-2.9	-12.5	-7.3
			2500	213.9	-5.8	-2.7	-11.6	-5.4	-29.1	-13.6
		200	500	102.2	2.2	2.1	4.3	4.2	10.8	10.6
			1500	137.5	0.0	0.0	0.0	0.0	0.0	0.0
			2500	172.7	-2.2	-1.3	-4.3	-2.5	-10.9	-6.3
		500	500	64.8	2.8	4.4	5.7	8.7	14.2	21.9
			1500	87.2	2.0	2.3	3.9	4.5	9.8	11.3
			2500	109.5	1.1	1.0	2.2	2.0	5.4	5.0
	200	100	500	135.3	.5	.4	1.1	.8	2.7	2.0
			1500	176.0	-1.6	-1.0	-3.2	-2.1	-8.0	-5.2
			2500	180.8	-3.6	-2.1	-7.5	-4.2	-18.8	-10.4
		200	500	115.0	1.7	1.4	3.3	2.9	8.3	7.2
			1500	137.5	0.0	0.0	0.0	0.0	0.0	0.0
			2500	159.3	-1.7	-1.0	-3.3	-2.1	-8.3	-5.2
		500	500	85.2	2.9	3.4	5.9	6.9	14.7	17.0
			1500	101.3	2.0	2.0	4.1	4.0	10.2	10.0
			2500	117.4	1.1	1.0	2.3	1.9	5.6	4.8

TABLE 4.2 (cont'd.). Sensitivity of Equation 2.20 to r_{aVH}

$\theta_0-\theta_g$ (rs^{-2})	r_{aVH} (sm^{-1})	r_{aT} (sm^{-1})	$\theta_0\left[\theta(z_r)-\theta(z)\right]$ (°a)	ΔQ_E (Wm^{-2})	$\delta r_{aVH}/r_{aVH}$ = 10%		$\delta r_{aVH}/r_{aVH}$ = 20%		$\delta r_{aVH}/r_{aVH}$ = 50%	
					$\delta\Delta Q_E$ (Wm^{-2})	$\delta\Delta Q_E/\Delta Q_E$ (%)	$\delta\Delta Q_E$ (Wm^{-2})	$\delta\Delta Q_E/\Delta Q_E$ (%)	$\delta\Delta Q_E$ (Wm^{-2})	$\delta\Delta Q_E/\Delta Q_E$ (%)
400	50	100	500	211.1	-.3	-.1	-.7	-.3	-1.7	-.8
			1500	274.0	0.0	0.0	0.0	0.0	0.0	0.0
			2500	315.5	-4.3	-1.3	-5.7	-2.5	-21.7	-6.3
		200	500	147.6	5.7	3.8	12.3	7.7	28.3	19.2
			1500	198.5	3.4	1.7	6.6	3.4	17.0	8.5
			2500	228.5	1.1	.5	2.3	.9	5.8	2.3
		500	500	80.6	4.7	5.9	9.4	11.7	23.5	29.3
			1500	138.3	4.0	2.7	8.1	7.5	20.2	18.6
			2500	167.1	3.4	2.5	6.7	4.9	16.3	12.4
	100	100	500	231.2	3.3	1.4	6.7	2.9	16.6	7.2
			1500	274.9	0.0	0.0	0.0	0.0	0.0	0.0
			2500	310.6	-3.3	-1.0	-6.7	-2.1	-16.6	-5.2
		200	500	186.7	5.4	2.9	10.8	5.8	27.1	14.5
			1500	226.0	3.3	1.5	6.6	2.9	16.3	7.3
			2500	257.3	1.1	.4	2.2	.9	5.4	2.1
		500	500	119.4	6.1	5.2	12.2	10.3	30.5	25.8
			1500	160.8	5.2	3.7	10.5	7.4	26.2	18.6
			2500	183.1	4.6	2.7	8.7	5.3	21.8	13.4
	200	100	500	253.1	2.1	.9	4.3	1.7	10.7	4.3
			1500	274.9	0.0	0.0	0.0	0.0	0.0	0.0
			2500	289.7	-2.1	-.7	-4.3	-1.4	-10.7	-3.6
		200	500	200.3	4.2	1.9	8.3	3.8	20.8	9.4
			1500	243.1	2.5	1.0	5.0	2.1	12.5	5.1
			2500	271.0	1.3	.5	2.7	1.0	6.1	2.3
		500	500	154.3	6.3	3.9	12.6	7.8	31.6	19.5
			1500	208.4	5.4	3.9	10.8	6.1	27.1	15.2
			2500	240.5	4.4	2.3	9.0	4.6	22.4	11.4
600	50	100	500	265.9	7.5	2.6	15.0	5.3	38.0	13.1
			1500	359.5	3.3	.9	6.5	1.8	16.3	4.5
			2500	410.0	-1.1	-.3	-2.2	-.5	-5.4	-1.3
		200	500	208.6	9.0	4.3	18.1	8.7	45.2	21.7
			1500	259.6	6.8	2.6	13.6	5.2	33.9	13.1
			2500	310.5	4.5	1.4	9.0	2.9	22.6	7.3
		500	500	113.8	7.2	6.4	14.5	12.7	36.2	31.8
			1500	161.6	6.6	4.6	13.1	9.3	32.8	23.2
			2500	169.3	5.9	3.5	11.8	7.0	29.4	17.4
	100	100	500	339.9	5.8	1.7	11.6	3.5	29.1	8.7
			1500	379.6	2.5	.7	5.0	1.3	12.5	3.3
			2500	403.3	-.8	-.2	-1.7	-.4	-4.2	-1.2
		200	500	271.3	8.7	3.2	17.4	6.4	43.5	16.0
			1500	306.6	6.5	2.1	13.0	4.2	32.5	10.6
			2500	317.4	4.1	1.3	8.7	2.5	21.7	6.8
		500	500	172.0	9.4	5.4	18.7	10.9	46.9	27.2
			1500	196.4	8.5	4.4	17.0	8.7	42.5	21.9
			2500	210.7	7.6	3.5	15.3	7.0	38.1	17.6
	200	100	500	359.0	3.6	1.0	7.5	2.0	18.8	5.1
			1500	393.8	1.6	.4	3.2	.8	8.0	2.0
			2500	414.5	-.5	-.1	-1.1	-.3	-2.7	-.6
		200	500	325.0	6.7	2.0	13.3	4.1	33.3	10.2
			1500	346.8	5.0	1.4	10.0	2.9	24.9	7.2
			2500	358.7	3.3	.9	6.6	1.8	16.6	4.5
		500	500	239.4	9.7	4.1	19.4	8.1	48.5	20.3
			1500	255.5	8.3	3.4	17.6	6.9	44.0	17.2
			2500	271.6	7.9	2.9	15.8	5.8	39.5	14.5

to errors in both z_o and d was determined. λQ_E was computed from equation 2.20 for values of 70%, 90%, 110% and 160% of actual r_{aVH}. These flux evaluations are compared with actual hourly λQ_E measurements (Bowen ratio method) in Figure 4.8. Values of r_{ST}, previously evaluated by residual, were employed. Model values agree well with Bowen ratio method determinations even with substantial errors (± 50%) in both z_o and d. Hence, estimates of z_o and d from the types of models presented in Figures 4.3 and 4.4 could be used in the combination model without incurring large errors.

b. Use of r_{aM} for evaluating λQ_E

In most previous work, r_{aM} has been used instead of r_{aVH} in estimating λQ_E by the combination model. Figure 4.9 shows that hourly r_{aVH} and r_{aM} are highly correlated, with the deviation from the 1:1 line being accounted for by the inclusion of r_b in r_{aVH}. If r_{aM} is used in place of r_{aVH} (Figure 4.10), λQ_E can still be calculated using equation 2.20 to an accuracy which is within ten percent of Bowen ratio method determinations in most cases. Since the evaluation of r_b requires no additional data input other than that required for r_{aM} calculation, the inclusion of r_b in r_{aVH} evaluation can be routine. The dependence on Thom's (1972) expression for r_b is acknowledged together with the necessity for further validation.

c. Dependency of r_{aVH} and λQ_E upon atmospheric stability

The dependency of r_{aVH} and λQ_E on stability correction is now considered. Figure 4.11 shows that r_{aVH} and r_{aVH} without stability correction are highly correlated, with only a few data points departing

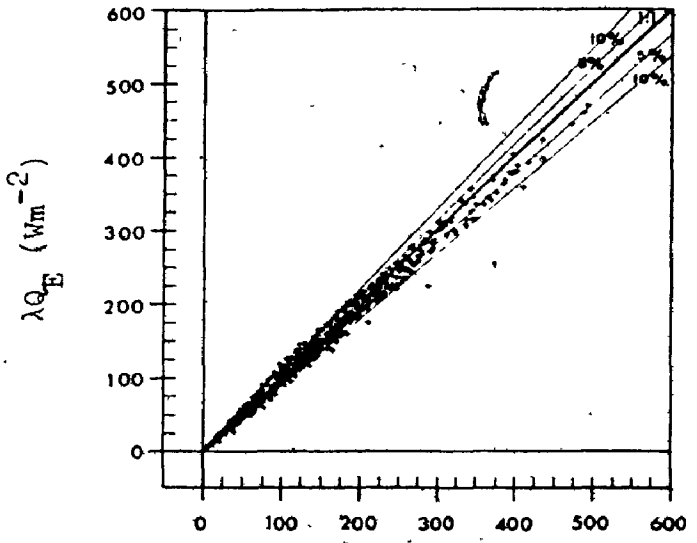

λQ_E (Wm^{-2}) with aerodynamic resistance input of 0.70 r_{aVH}

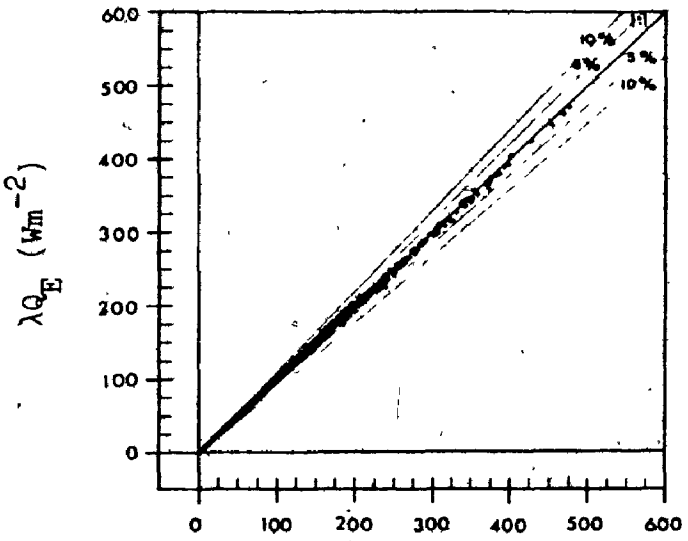

λQ_E (Wm^{-2}) with aerodynamic resistance input of 0.90 r_{aVH}

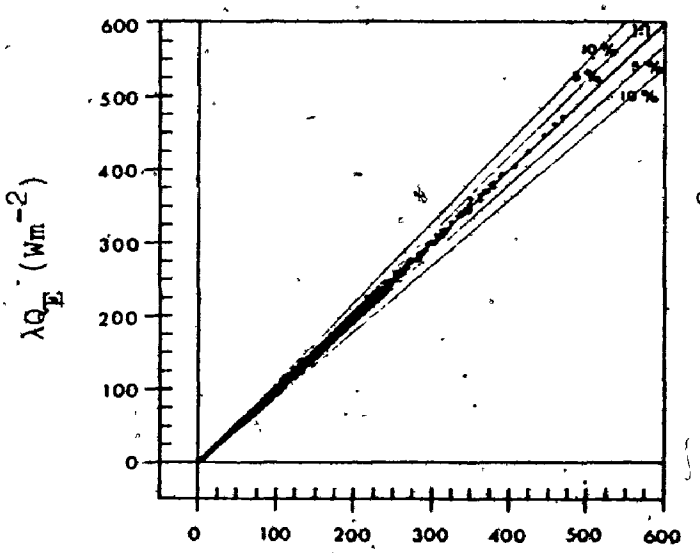

λQ_E (Wm^{-2}) with aerodynamic resistance input of 1.10 r_{aVH}

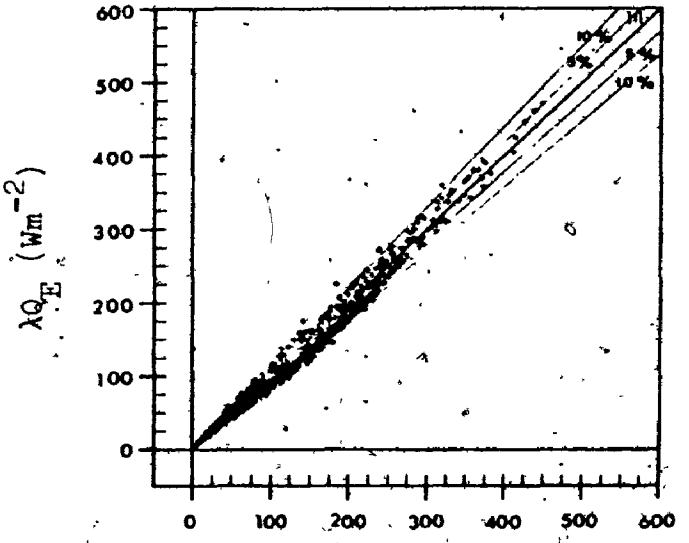

λQ_E (Wm^{-2}) with aerodynamic resistance input of 1.60 r_{aVH}

Figure 4.8. Hourly λQ_E estimates from equation 2.20 utilizing variable r_{aVH} input compared with hourly λQ_E measurements (Bowen ratio method). The number of hourly observations displayed is 895.

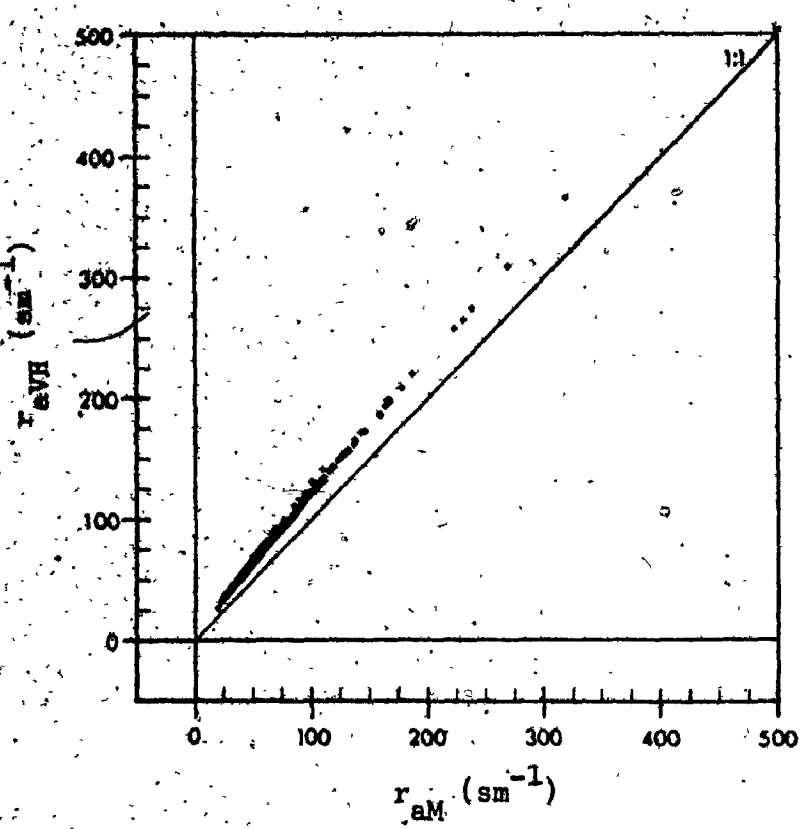

Figure 4.9. Comparison of hourly r_{aVH} and r_{aM}. The sample size is 895.

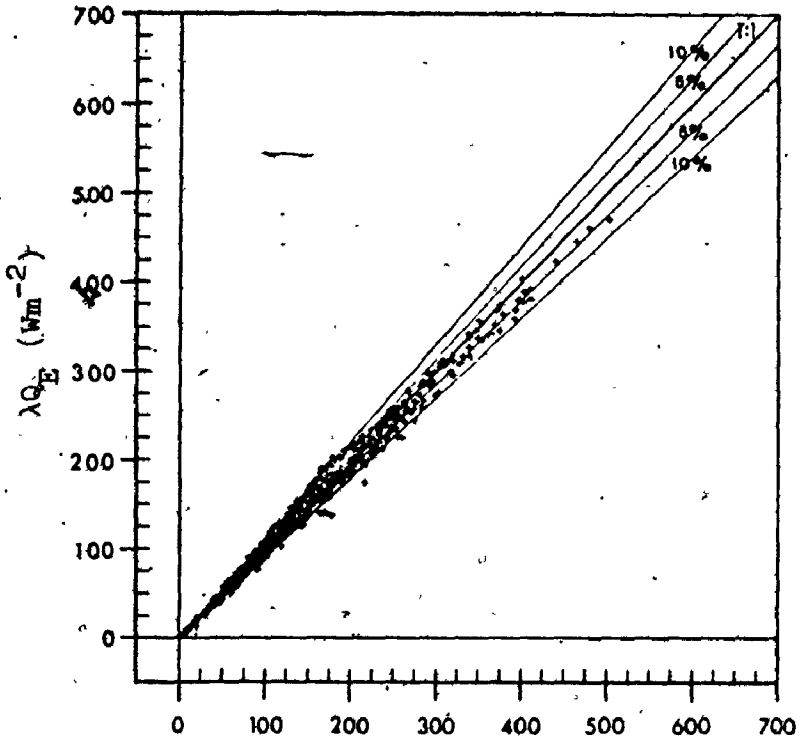

Figure 4.10. Hourly λQ_E estimates from equation 2.20 with r_{aM} used as aerodynamic resistance input compared with hourly λQ_E measurements (Bowen ratio method). The sample size is 895.

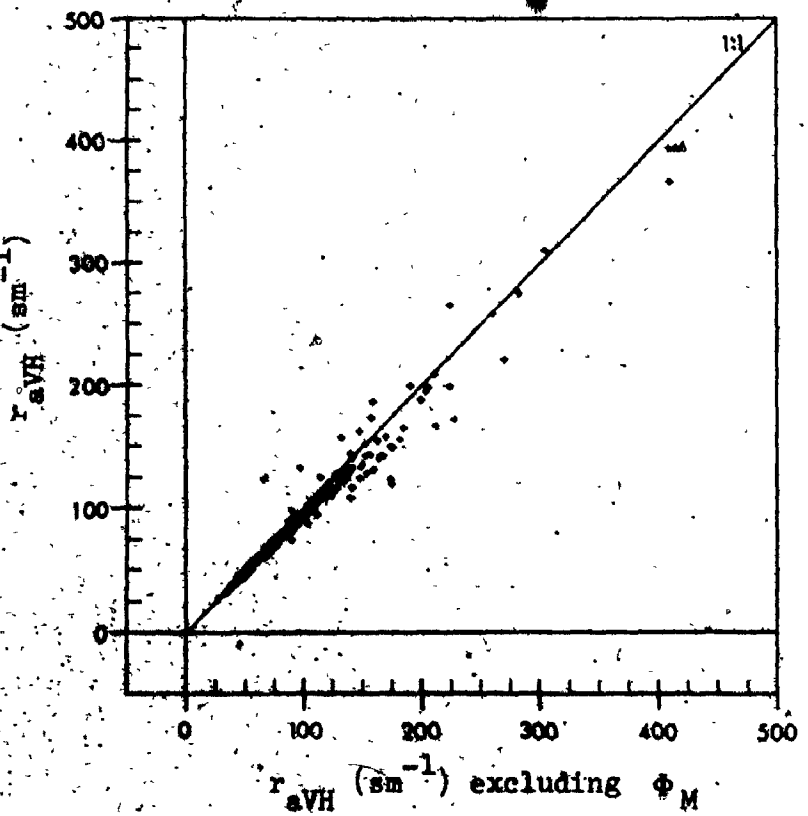

Figure 4.11. Comparison of hourly r_{aVH} and r_{aVH} with no stability factor included. The sample size is 895.

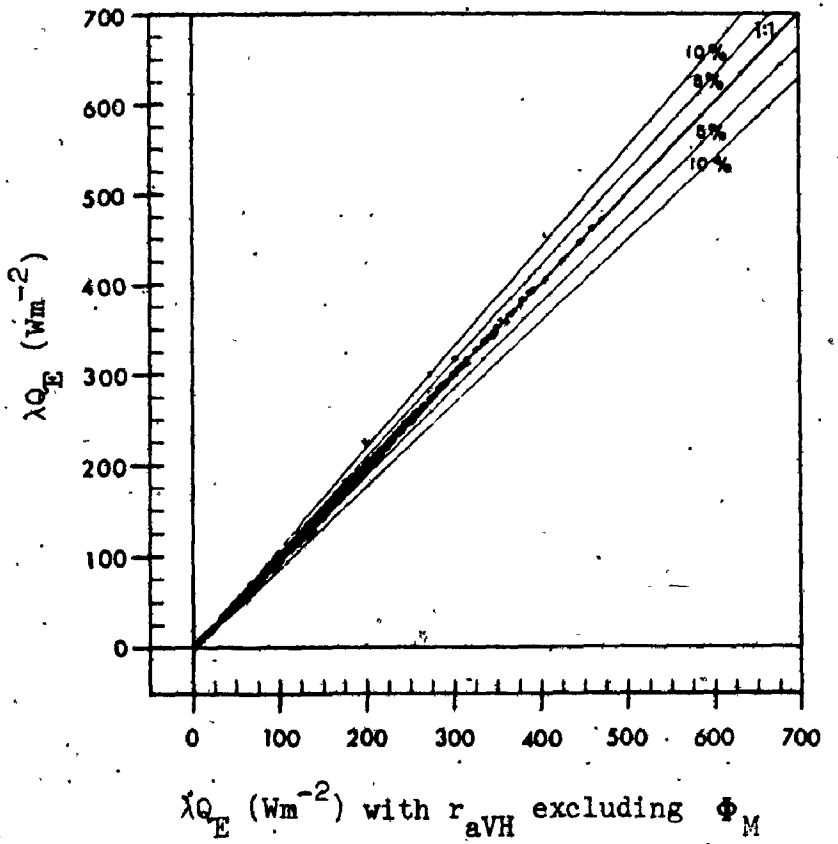

Figure 4.12. Hourly λQ_E estimates from equation 2.20 with r_{aVH} excluding a stability correction factor used as aerodynamic resistance input compared with hourly λQ_E measurements (Bowen ratio method). The sample size is 895.

significantly from the 1:1 line. Clearly Φ_M plays a rather insignificant role in aerodynamic resistance estimates. Hourly λQ_E evaluated from equation 2.20 with r_{aVH} replaced by r_{aVH} with stability correction excluded compares with hourly λQ_E measurements to within 5% in most cases (Figure 4.12).

This analysis shows that the inclusion of stability correction is unnecessary for most r_{aVH} determinations. Deacon and Swinbank (1958) and Swinbank (1964, 1968) argued that stability corrections are small enough to be neglected close to the ground since turbulence was controlled mainly by wind shear. Bradley (1972) showed experimentally that departures from neutral equilibrium are small below a height of 1 m. In the present study, the height of measurement was often within the first meter of the atmosphere, therefore, the small contribution of Φ_M is not unexpected. However, it should be stressed that stability correction can only be neglected if measurements are made sufficiently close to the surface. Then profile measurements of windspeed and temperature to evaluate stability are unnecessary. Hence, r_{aVH} can be evaluated from occasional wind profiles in neutral equilibrium to obtain z_o and d, or if reliable empirical estimates of z_o and d are available, windspeed measurements at one height. An example of the latter is presented in Figure 4.13. Using z_o and d from equations 4.1 and 4.2, r_{aM}, r_b and r_{aVH} excluding stability correction have been evaluated over a range of windspeeds for an arbitrary reference anemometer height of 1.5 m for the duration of the study period.

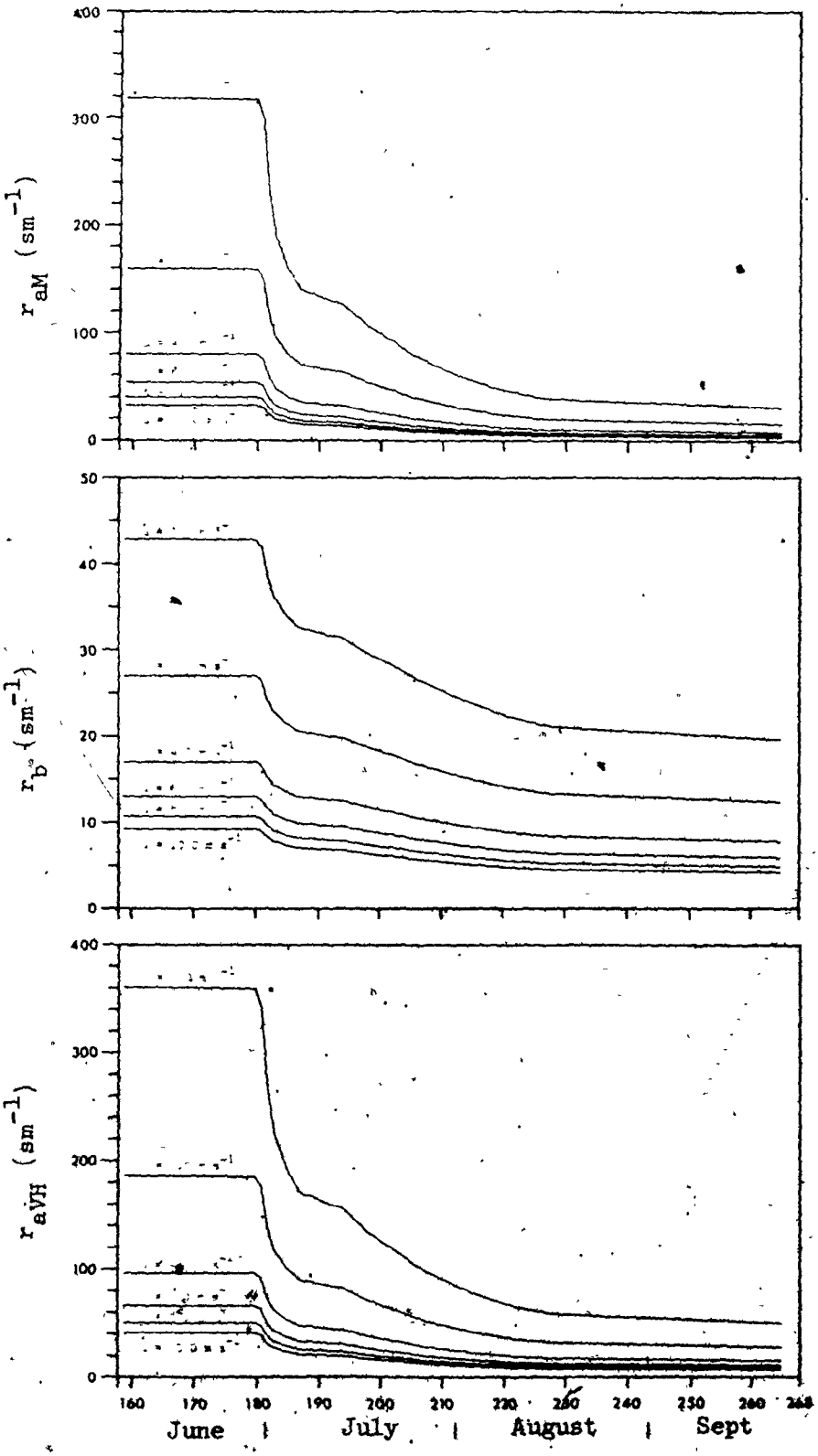

Figure 4.13. Variation of r_{aM}, r_b and r_{aVH} (with no stability correction factors included) throughout the study period for various

B. Bulk Stomatal Resistance

1. Evaluation of r_{ST} from leaf resistance measurements

Harmonic means of adaxial and abaxial leaf resistance, measured with a diffusion porometer, were evaluated three times daily (morning, midday and late afternoon) throughout the growing season (Figure 4.14). These were combined with LAI data (Figure 3.6) to estimate bulk stomatal resistance $r_{ST}(P)$ from equation 2.38. These data have been tabulated in Appendix Six.

The accuracy of $r_{ST}(P)$ evaluation is difficult to assess because the accuracy of LAI determinations and the representativeness of porometer estimates of leaf resistance cannot be specified. However, the sensitivity of $r_{ST}(P)$ to arbitrary relative errors in both LAI and leaf conductance $(\frac{1}{r_{AB}} + \frac{1}{r_{AD}})$ can be examined. Based on the error analysis outlined in Appendix Three, for a given relative error in either leaf conductance or LAI, the relative error in $r_{ST}(P)$ is equivalent in magnitude but of opposite size. These relative errors have been arbitrarily combined to evaluate probable relative errors in $r_{ST}(P)$ (Table 4.3). When relative errors for LAI and leaf conductance are of opposite sign, resultant error in $r_{ST}(P)$ is minimized. However, when these errors are of the same sign, relative errors for $r_{ST}(P)$ are large.

2. Micrometeorological estimates of r_{ST}

Two micrometeorological methods were used in the determination of r_{ST}. The first determines bulk stomatal resistance $r_{ST}(CM)$ by residual from the combination model (equation 2.20):

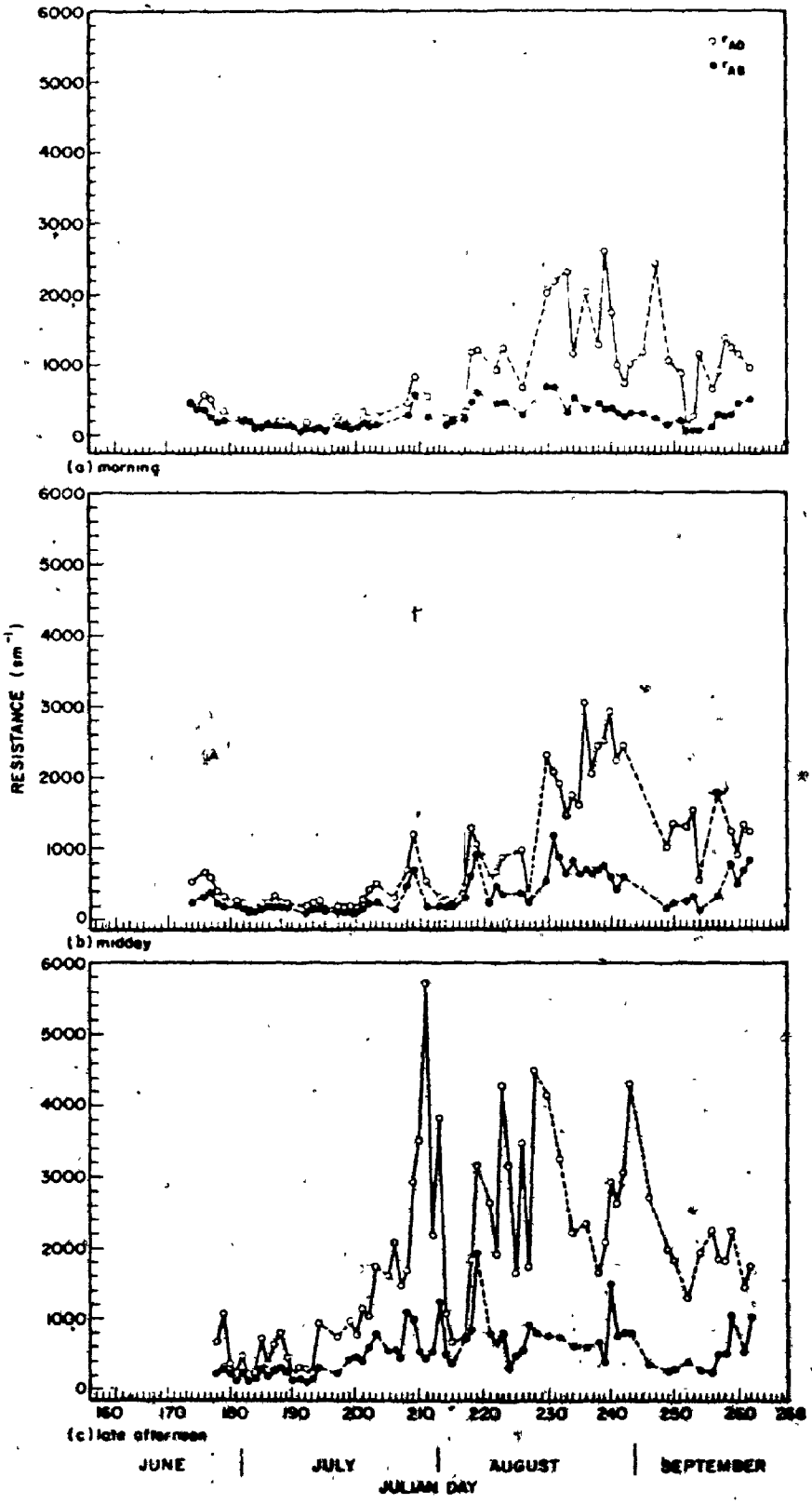

Figure 4.14. The variation of adaxial and abaxial leaf resistance throughout the growing season for morning, midday and late afternoon observations. Dashed lines are estimates when sequential data are missing.

TABLE 4.3. Sensitivity of $r_{ST}(P)$ to Errors in LAI and Leaf Conductance

$\delta\left[\frac{1}{r_{AD}}+\frac{1}{r_{AB}}\right]$ / $\left[\frac{1}{r_{AD}}+\frac{1}{r_{AB}}\right]$ (%)	$\delta r_{ST}(P)/r_{ST}(P)$ (%)						
	$\frac{\delta LAI}{LAI}$=-50%	$\frac{\delta LAI}{LAI}$=-20%	$\frac{\delta LAI}{LAI}$=-10%	$\frac{\delta LAI}{LAI}$=0%	$\frac{\delta LAI}{LAI}$=10%	$\frac{\delta LAI}{LAI}$=20%	$\frac{\delta LAI}{LAI}$=50%
-50	100	70	60	50	40	30	0
-20	70	40	30	20	10	0	-30
-10	60	30	20	10	0	-10	-40
0	50	20	10	0	-10	-20	-50
10	40	10	0	-10	-20	-30	-60
20	30	0	-10	-20	-30	-40	-70
50	0	-30	-40	-50	-60	-70	-100

$$r_{ST}(CM) = \frac{r_{aVH}\left[S(Q^*-Q_G-\lambda Q_E)-\gamma\lambda Q_E\right]+\rho Cp\left[e_s\left[\theta(z)\right]-e(z)\right]}{\gamma\lambda Q_E}. \quad (4.5)$$

In the second method, bulk stomatal resistance $r_{ST}(OLA)$ was determined from an Ohm's Law analogue. Combining equations 2.18 and 2.14 and approximating mean surface temperature $\theta(o)$ with leaf temperature $\theta(L)$:

$$\lambda Q_E = \frac{\rho Cp}{\gamma}\,\frac{\left[e_s\left[\theta(L)\right]-e(z)\right]}{r_{ST}+r_{aVH}}. \quad (4.6)$$

Hence:

$$r_{ST}(OLA) = \frac{\rho Cp}{\gamma}\,\frac{\left[e_s\left[\theta(L)\right]-e(z)\right]}{\lambda Q_E} - r_{aVH}. \quad (4.7)$$

Since $\theta(L)$ measurements commenced on July 7 (Day 188), $r_{ST}(OLA)$ could only be calculated beginning on this date.

Both expressions for r_{ST} were computed on an hourly basis using λQ_E determined from the Bowen ratio method (equation 2.11) and r_{aVH} from equation 2.29. Values of $r_{ST}(CM)$ and $r_{ST}(OLA)$ are plotted in Figure 4.15 for morning, midday and afternoon periods which coincide with r_L evaluations. At all times, the trends are similar but $r_{ST}(OLA)$ is consistently larger than $r_{ST}(CM)$. This can be attributed to two possible causes. First, there is possible consistent over-estimation of $\theta(o)$ by the leaf thermocouple array due to inadequate canopy sampling. Also, the array may have been subject to errors due to radiative heating. Second, in equation 4.5, S^* was evaluated at

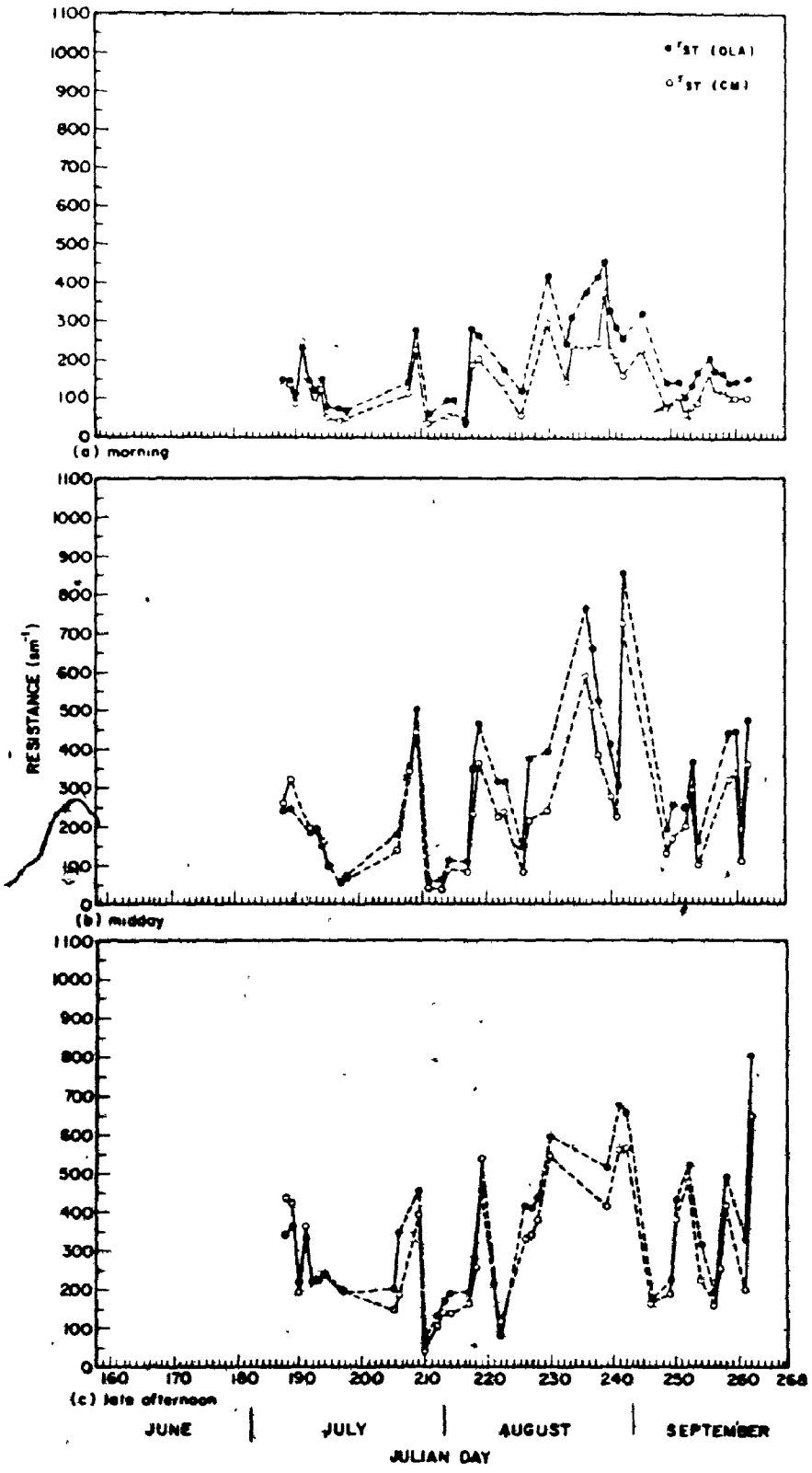

Figure 4.15. Comparison of r_{ST}(CM) and r_{ST}(OLA) throughout the growing season for morning, midday and late afternoon observations. Dashed lines are estimates when sequential data are

temperature $\theta(z)$ rather than at the mean of $\theta(z)$ and $\theta(o)$. This underestimation of S would result in reduced $r_{ST}(CM)$ values. The influence of this is anticipated to be small except in cases where $\theta(o) - \theta(z)$ was quite large.

An error analysis was undertaken to assess the probable absolute errors in both $r_{ST}(CM)$ and $r_{ST}(OLA)$. The analysis procedure is presented in Appendix Four, with the results tabulated, together with all of the bulk stomatal resistance data, in Appendix Six. For a given hour, $\delta r_{ST}(CM)_{rms}$ and $\delta r_{ST}(OLA)_{rms}$ are quite similar. However as expected, the range in relative errors $\delta r_{ST}(CM)_{rms}/r_{ST}(CM)$ and $\delta r_{ST}(OLA)_{rms}/r_{ST}(OLA)$ is quite large, reflecting the effects of instrumentation accuracy in widely variant environmental conditions. Acknowledging this, the differences found in Figure 4.15 are within the range of probable error in most cases.

3. Comparison of $r_{ST}(P)$ with $r_{ST}(CM)$ and $r_{ST}(OLA)$

In Figures 4.16 and 4.17, $r_{ST}(P)$ is compared with $r_{ST}(CM)$ and $r_{ST}(OLA)$ respectively for the three observational periods throughout the growing season. In both figures, several trends can be discerned. For all observation periods, until approximately Day 190, $r_{ST}(P)$ greatly exceeds both $r_{ST}(CM)$ and $r_{ST}(OLA)$ and agreement between the estimation procedures is poor. This arises because comparisons between equation 2.38 and equations 4.5 and 4.7 should not be made when LAI < 1 (LAI = 1 on Day 194 when crop height is 0.25 m). Comparisons are only valid when the surface energy balance is controlled by an extensive canopy with minimal influence from bare soil. During the early stages of the

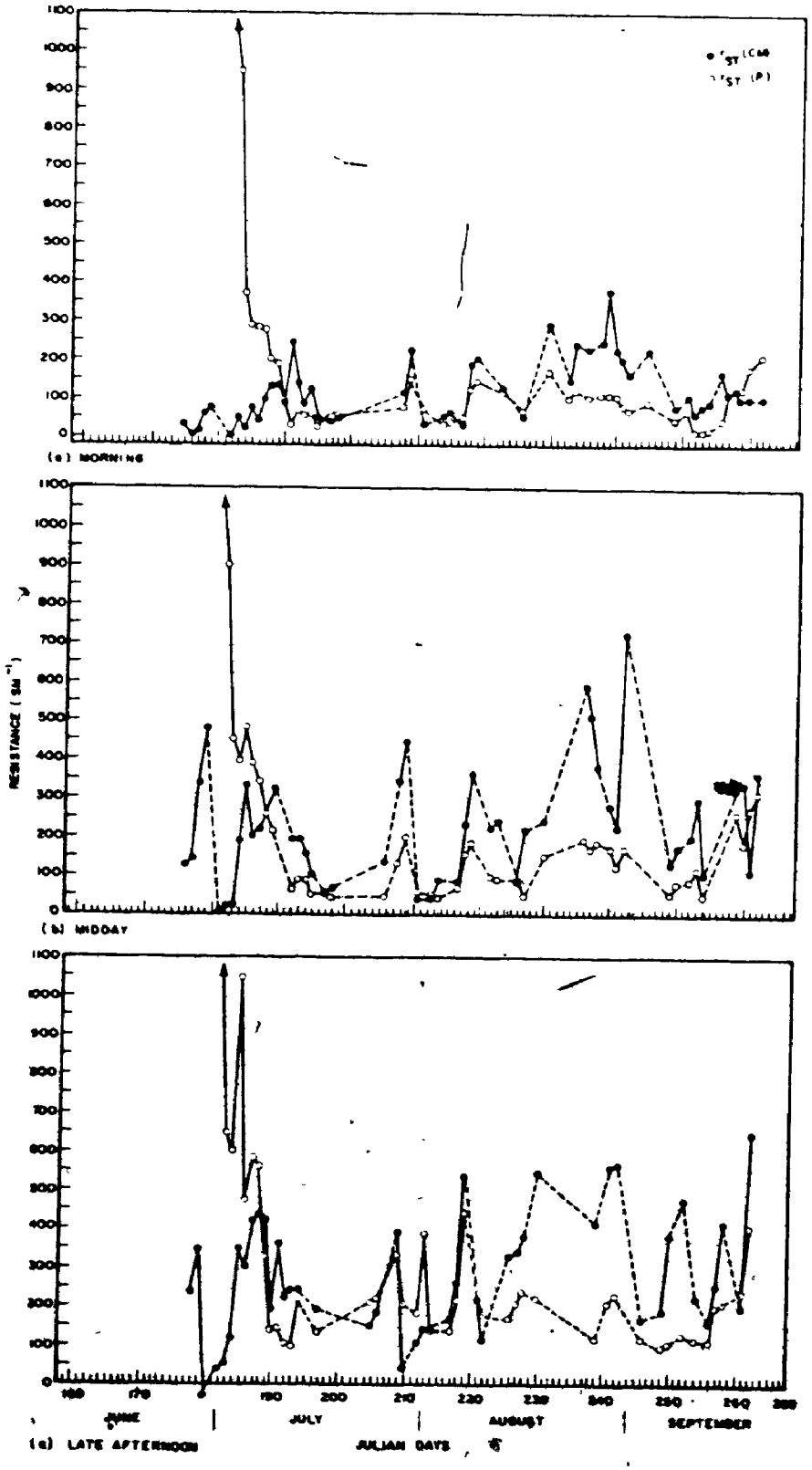

Figure 4.16. Comparison of $r_{ST}(P)$ and $r_{ST}(CM)$ throughout the growing season for morning, midday and late afternoon observations. Dashed lines are estimates when sequential data are

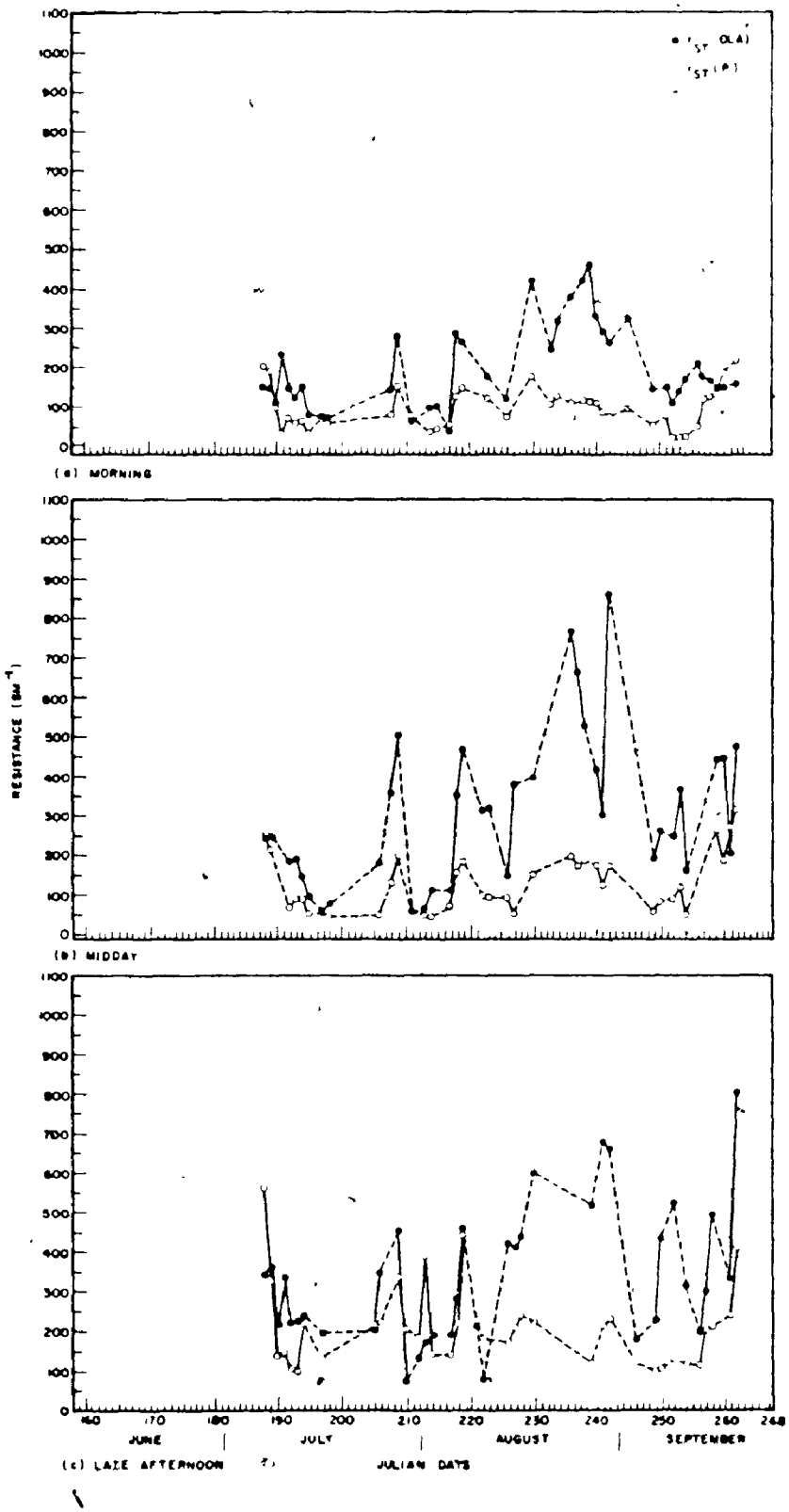

Figure 4.17. Comparison of $r_{ST}(P)$ and $r_{ST}(OLA)$ throughout the growing season for morning, midday and late afternoon observations. Dashed lines are estimates when sequential data are missing.

crop, the influence of the bare soil surface as a source of moisture efflux cannot be disregarded.

For the rest of the growing season, agreement between $r_{ST}(P)$ and both $r_{ST}(CM)$ and $r_{ST}(OLA)$ is better. Although the systematic differences between $r_{ST}(OLA)$ and $r_{ST}(CM)$ did not appear to be great (Figure 4.15), agreement between $r_{ST}(P)$ and $r_{ST}(CM)$ is much better than for $r_{ST}(OLA)$.

Excluding the early growing season data, the greatest discrepancies between $r_{ST}(P)$ and $r_{ST}(CM)$ appear after mid-August. Some suggestions for these differences can be made. The latter part of the study period was relatively dry with little soil moisture available to the crop (Figure 4.20). The previous λQ_E error analysis showed that energy flux density measurements are most subject to large error in such dry conditions. Hence, r_{ST} evaluations by residual will reflect this. The large probable absolute errors accompanying these larger $r_{ST}(CM)$ and $r_{ST}(OLA)$ observations bear this out (Appendix Six). Errors, not accounted for such as radiative heating of the temperature and humidity sensors and irregularities in wet-bulb feed systems are also pronounced during these conditions.

Due to the continued trend of $r_{ST}(CM) > r_{ST}(P)$, the accuracy of $r_{ST}(P)$ must also be considered. Errors in $r_{ST}(P)$ are difficult to assess but some suggestions about their influences can be made. During late July and the first half of August, agreement between $r_{ST}(P)$ and $r_{ST}(CM)$ is good. At this time, the canopy is still approaching maximum LAI. Once this is reached, sampling errors in the determination of r_L will be greatest unless r_L measurements are increased to compensate for

the larger leaf area. With limited observations (10 or 20 leaves), it is clear that systematic errors can easily arise. Since $r_{ST}(P)$ is less than $r_{ST}(CM)$ and $r_{ST}(OLA)$ for this period, a bias in leaf resistance sampling is possible, particularly if older, lower leaves in the canopy, which are not fully irradiated, are not adequately sampled. Monteith et al. (1965) have found that using total LAI was inappropriate when only upper canopy leaves were sampled. They defined an effective LAI to account for this. For their barley crop, all leaves were effective in transpiration until LAI reached half of the maximal value, after which an effective LAI of 0.5 LAI was employed. This technique has been applied by Szeicz et al. (1969) for a pine forest and Szeicz and Long (1969) for grass. However, this approach merely accounts for ineffective sampling of r_L. If an effective LAI of 0.5 LAI was used after mid-August, better agreement between $r_{ST}(P)$ and $r_{ST}(CM)$ could be obtained. The writer believes that this step cannot be justified in this investigation since the differences cannot be conclusively shown to result from bias in the sampling program.

From the foregoing, it is clear that a more detailed sampling program for r_L would be worthwhile. Methods of implementing this however are laborious. A layered canopy sampling program, similar to that applied in a Douglas fir forest by Tan and Black (1976), may be desirable, however its utility in a fast developing crop stand requires examination. The intensive labour requirements of increasing the number of measurements over a long study program and the problem of obtaining representative samples within a short period of steady state conditions must be acknowledged.

4. Estimates of λQ_E using $r_{ST}(P)$

Estimates of hourly λQ_E employing $r_{ST}(P)$ in the combination model (equation 2.20) and in an Ohm's Law analogue (equation 4.6) have been compared with hourly Bowen ratio method determinations (equation 2.11) of λQ_E for morning, midday and late afternoon periods throughout the growing season. The data used are tabulated in Appendix Seven. For the combination model (Figure 4.18), excluding the period of incomplete canopy (LAI < 1), the agreement is exceptionally good. Most of the estimates from the combination model are within the range of probable absolute errors in λQ_E evaluated from equation 2.11 (Appendix Seven). One discernable trend is present in the results; as $r_{ST}(P)$ is usually less than $r_{ST}(CM)$ once LAI > 1, λQ_E estimates from equation 2.20 exceed λQ_E from the Bowen ratio method.

In Figure 4.19, λQ_E estimates were derived from an Ohm's Law analogue (equation 4.6) using $r_{ST}(P)$. In these determinations, leaf temperature was determined, firstly, from the continuously monitored leaf thermocouple array, and, secondly, from the temperature readings made with the porometer's temperature sensor. For most observations, differences resulting from the two methods are not large. Both however lead to overestimates of λQ_E when compared with Bowen ratio method determinations. This contrasts with the very good agreement obtained with the combination model. This could be anticipated from the differences between $r_{ST}(OLA)$ and $r_{ST}(P)$. There is however a further reason. The sensitivity of equations 2.20 and 4.6 to r_{ST} has been summarized in Tables 4.4 and 4.5 based on the analysis outlined in Appendix Five. From this analysis, equation 2.20 is shown to be less

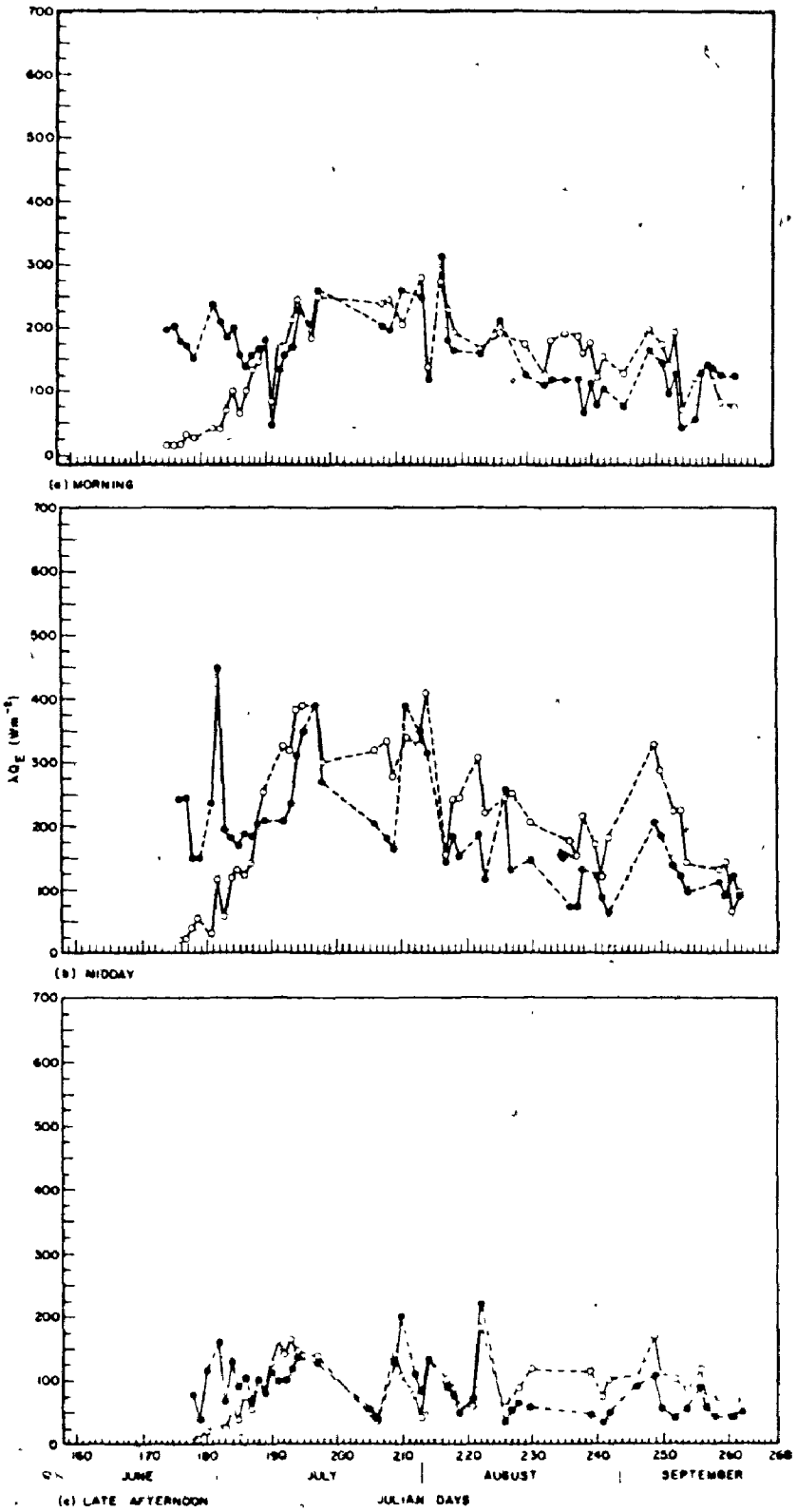

Figure 4.18. Hourly λQ_E estimates from equation 2.20 (○) employing $r_{ST}(P)$ compared with hourly λQ_E measurements (●) for morning midday and late afternoon periods. Dashed lines are estimates when sequential data are missing.

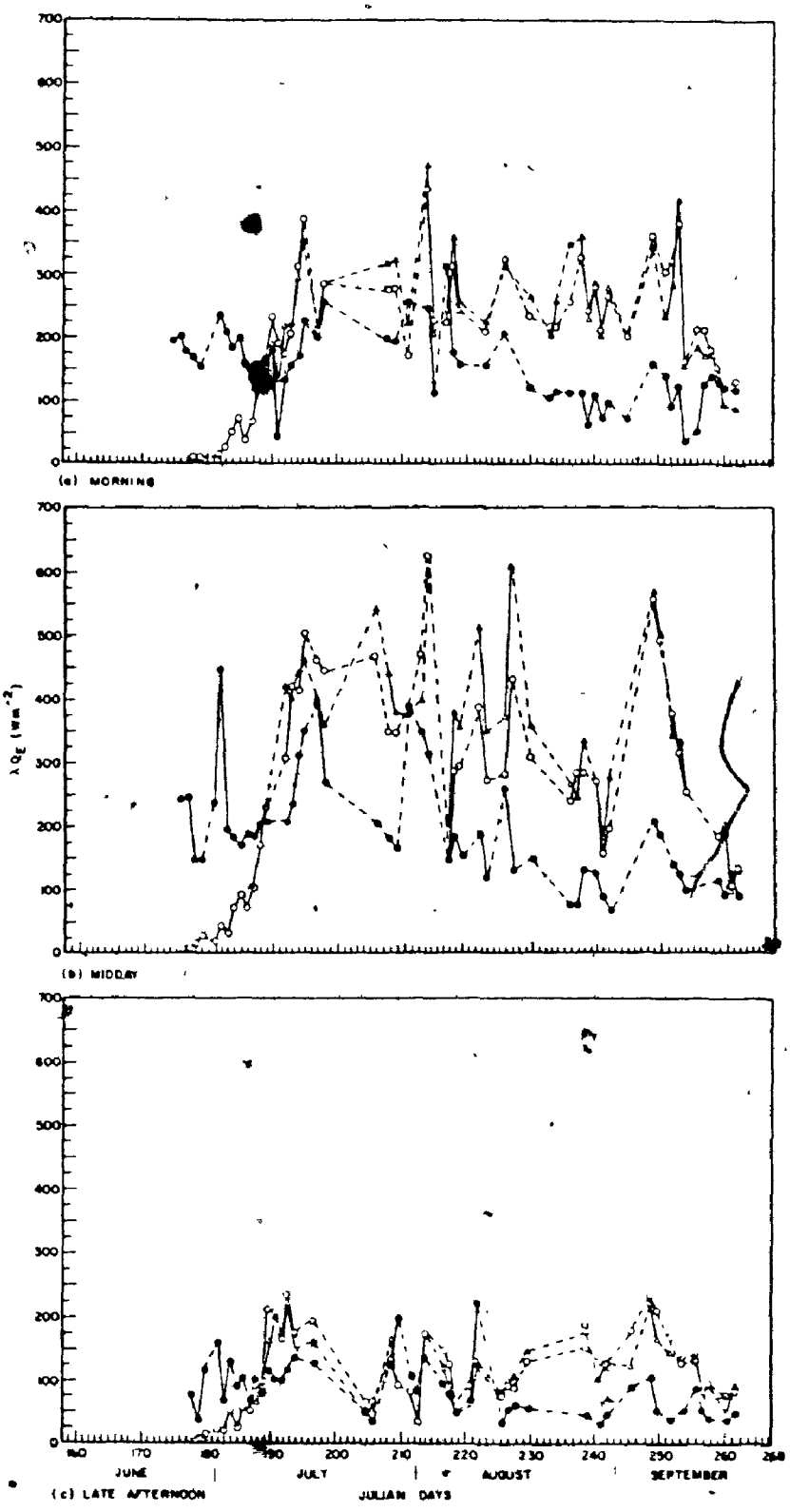

Figure 4.19. Hourly λQ_E estimates from equation 4.6 employing $r_{ST}(P)$ with $\theta(L)$ measured with a thermocouple array (Δ) and the porometer leaf temperature sensor (O) compared with hourly λQ_E measurements (●) for morning, midday and late afternoon periods. Dashed lines are estimates when sequential data are missing.

TABLE 4.4. Sensitivity of Equation 2.20 to r_{ST}

ζ^*-q_0 (Wm^{-2})	r_{ST} (sm^{-1})	r_{atm} (sm^{-1})	$e_c[\theta(z)]-e(z)$ (Pa)	λq_E (Wm^{-2})	$\delta r_{ST}/r_{ST}$ = 10%		$\delta r_{ST}/r_{ST}$ = 20%		$\delta r_{ST}/r_{ST}$ = 50%	
					$\delta\lambda q_E$ (Wm^{-2})	$\delta\lambda q_E/\lambda q_E$ (%)	$\delta\lambda q_E$ (Wm^{-2})	$\delta\lambda q_E/\lambda q_E$ (%)	$\delta\lambda q_E$ (Wm^{-2})	$\delta\lambda q_E/\lambda q_E$ (%)
100	100	50	500	77.4	-3.0	-3.8	-6.0	-7.7	-14.9	-19.2
			1500	148.1	-4.7	-3.6	-11.4	-7.7	-28.5	-19.2
			2500	218.7	-8.4	-3.8	-16.8	-7.7	-42.1	-19.2
		100	500	72.2	-1.5	-2.1	-3.5	-4.8	-8.6	-11.9
			1500	117.9	-2.6	-2.2	-5.6	-4.8	-13.9	-11.9
			2500	161.6	-3.8	-2.4	-7.7	-4.8	-19.2	-11.9
		200	500	71.8	-1.0	-1.4	-1.9	-2.7	-4.9	-6.8
			1500	86.6	-1.3	-1.5	-2.6	-2.7	-6.5	-6.8
			2500	121.4	-1.6	-1.3	-3.3	-2.7	-8.2	-6.8
	200	50	500	56.0	-3.1	-5.6	-6.2	-11.1	-15.6	-27.8
			1500	106.9	-5.9	-5.6	-11.8	-11.1	-29.7	-27.8
			2500	157.9	-8.0	-5.6	-17.6	-11.1	-43.9	-27.8
		100	500	59.9	-2.3	-3.8	-4.5	-7.7	-11.5	-19.2
			1500	95.2	-3.7	-3.8	-7.3	-7.7	-18.3	-19.2
			2500	133.5	-5.0	-3.8	-10.0	-7.7	-25.1	-19.2
		200	500	61.3	-1.5	-2.4	-3.0	-4.8	-7.5	-11.9
			1500	85.4	-2.0	-2.4	-4.1	-4.8	-10.1	-11.9
			2500	107.0	-2.5	-2.4	-5.1	-4.8	-12.7	-11.9
	500	50	500	50.5	-2.3	-7.6	-4.6	-15.2	-11.6	-37.9
			1500	50.3	-2.3	-7.6	-4.6	-15.2	-11.6	-37.9
			2500	86.1	-4.5	-7.6	-9.0	-15.2	-22.6	-37.9
		100	500	33.0	-1.3	-5.6	-2.6	-11.2	-6.5	-27.9
			1500	60.4	-2.7	-5.6	-5.4	-11.2	-13.4	-27.9
			2500	88.7	-4.0	-5.6	-8.1	-11.2	-20.2	-27.9
		200	500	46.6	-1.0	-2.4	-2.1	-4.8	-5.2	-11.9
			1500	62.7	-1.8	-2.4	-3.5	-4.8	-8.8	-11.9
			2500	79.2	-2.5	-2.4	-4.9	-4.8	-12.3	-11.9
200	100	50	500	119.6	-4.6	-3.8	-9.2	-7.7	-23.1	-19.2
			1500	193.4	-7.3	-3.8	-14.7	-7.7	-36.6	-19.2
			2500	260.9	-10.0	-3.8	-20.1	-7.7	-50.2	-19.2
		100	500	126.5	-3.0	-2.4	-6.0	-4.8	-15.1	-11.9
			1500	170.2	-4.1	-2.4	-8.1	-4.8	-20.3	-11.9
			2500	213.9	-5.2	-2.4	-10.2	-4.8	-25.5	-11.9
		200	500	131.3	-1.8	-1.4	-3.6	-2.7	-8.9	-6.8
			1500	156.0	-2.1	-1.4	-4.2	-2.7	-10.6	-6.8
			2500	180.8	-2.4	-1.4	-4.9	-2.7	-12.2	-6.8
	200	50	500	86.5	-3.8	-5.6	-6.5	-11.1	-16.0	-27.8
			1500	137.5	-7.6	-5.6	-15.3	-11.1	-38.2	-27.8
			2500	188.4	-10.5	-5.6	-20.9	-11.1	-52.4	-27.8
		100	500	107.2	-3.9	-3.8	-7.9	-7.7	-19.7	-19.2
			1500	137.5	-5.3	-3.8	-10.6	-7.7	-26.5	-19.2
			2500	172.7	-6.6	-3.8	-13.3	-7.7	-33.2	-19.2
		200	500	113.0	-2.6	-2.4	-5.5	-4.8	-13.8	-11.9
			1500	137.5	-3.3	-2.4	-6.6	-4.8	-16.4	-11.9
			2500	159.3	-3.8	-2.4	-7.6	-4.8	-19.0	-11.9
	500	50	500	67.2	-4.6	-6.8	-9.2	-13.2	-23.0	-33.0
			1500	75.0	-5.7	-7.6	-11.4	-15.2	-28.4	-37.9
			2500	103.8	-7.9	-7.6	-15.6	-15.2	-38.9	-37.9
		100	500	64.8	-4.0	-6.2	-7.9	-12.2	-19.8	-30.5
			1500	87.2	-5.3	-6.1	-10.6	-12.2	-26.6	-30.5
			2500	109.5	-6.7	-6.1	-13.4	-12.2	-33.4	-30.5
		200	500	68.2	-2.7	-4.0	-5.3	-7.8	-13.2	-19.3
			1500	80.3	-3.4	-4.2	-6.9	-8.5	-17.2	-21.2
			2500	92.4	-3.9	-4.2	-7.8	-8.5	-19.7	-21.2

TABLE 4.4 (cont'd). Sensitivity of Equation 2.20 to r_{ST}

$\theta^o-\theta_0$ (deg^{-2})	r_{ST} (sec^{-1})	$r_{s,TR}$ (sec^{-1})	$\theta_e[\theta(z)]-\theta(z)$ (^oK)	λC_z (wv^{-2})	$\delta r_{ST}/r_{ST}=1\%$		$\delta r_{ST}/r_{ST}=2\%$		$\delta r_{ST}/r_{ST}=5\%$	
					$\delta\lambda C_z$ (wv^{-2})	$\delta\lambda C_z/\lambda C_z$ (%)	$\delta\lambda C_z$ (wv^{-2})	$\delta\lambda C_z/\lambda C_z$ (%)	$\delta\lambda C_z$ (wv^{-2})	$\delta\lambda C_z/\lambda C_z$ (%)
400	100	50	500	291.4	-7.6	-2.6	-15.7	-5.4	-39.3	-13.5
			1500	274.0	-8.1	-3.0	-16.2	-5.9	-42.9	-15.7
			2500	345.5	-13.3	-3.8	-26.6	-7.7	-66.5	-19.2
		100	500	291.4	-7.5	-2.6	-14.0	-4.8	-27.5	-9.4
			1500	274.9	-6.6	-2.4	-13.1	-4.8	-32.8	-11.9
			2500	345.6	-7.6	-2.2	-15.2	-4.4	-38.0	-11.0
		200	500	291.1	-3.4	-1.2	-6.8	-2.3	-15.9	-5.5
			1500	274.9	-3.7	-1.4	-7.4	-2.7	-18.6	-6.8
			2500	268.7	-4.1	-1.4	-8.1	-2.7	-20.3	-6.8
	200	50	500	247.6	-4.2	-5.0	-10.4	-11.1	-11.0	-27.9
			1500	198.5	-11.0	-5.6	-22.1	-11.1	-55.2	-27.8
			2500	249.2	-13.0	-5.6	-27.7	-11.1	-69.3	-27.8
		100	500	246.7	-7.2	-3.8	-14.4	-7.7	-35.9	-19.2
			1500	199.0	-9.5	-3.8	-17.1	-7.7	-43.7	-19.2
			2500	251.3	-9.9	-3.8	-19.8	-7.7	-49.5	-19.2
		200	500	220.3	-5.2	-2.4	-10.5	-4.8	-26.2	-11.9
			1500	242.1	-5.8	-2.4	-11.5	-4.8	-28.8	-11.9
			2500	264.0	-6.3	-2.4	-12.6	-4.8	-31.5	-11.9
	500	50	500	140.5	-6.1	-7.6	-12.2	-15.2	-30.5	-37.9
			1500	104.3	-8.0	-7.6	-16.0	-15.2	-40.0	-37.9
			2500	136.1	-10.3	-7.6	-20.6	-15.2	-51.5	-37.9
		100	500	115.4	-7.2	-6.1	-14.4	-12.2	-36.1	-30.5
			1500	140.9	-8.6	-6.1	-17.2	-12.2	-43.0	-30.5
			2500	163.1	-10.0	-6.1	-19.9	-12.2	-49.8	-30.5
		200	500	162.3	-7.1	-4.4	-14.2	-8.8	-35.6	-21.9
			1500	178.1	-7.8	-4.4	-15.7	-8.8	-39.1	-21.9
			2500	194.4	-8.5	-4.4	-17.1	-8.8	-42.7	-21.9
600	100	50	500	288.9	-11.1	-3.8	-22.2	-7.7	-55.6	-19.2
			1500	359.5	-13.8	-3.8	-27.7	-7.7	-69.2	-19.2
			2500	433.0	-16.5	-3.8	-33.1	-7.7	-82.7	-19.2
		100	500	335.9	-8.0	-2.4	-16.0	-4.8	-40.0	-11.9
			1500	379.6	-9.0	-2.4	-18.1	-4.8	-45.2	-11.9
			2500	423.3	-10.1	-2.4	-20.2	-4.8	-50.4	-11.9
		200	500	325.5	-3.9	-1.2	-8.0	-2.7	-19.9	-6.8
			1500	393.5	-4.3	-1.4	-10.7	-2.7	-26.6	-6.8
			2500	418.5	-5.7	-1.4	-11.3	-2.7	-28.3	-6.8
	200	50	500	278.6	-11.0	-5.6	-22.2	-11.1	-58.0	-27.8
			1500	259.6	-11.4	-5.6	-28.9	-11.1	-72.1	-27.8
			2500	349.5	-17.3	-5.6	-34.5	-11.1	-86.3	-27.8
		100	500	271.3	-10.4	-3.8	-20.9	-7.7	-52.2	-19.2
			1500	306.0	-11.8	-3.8	-23.6	-7.7	-59.0	-19.2
			2500	341.0	-13.2	-3.8	-26.3	-7.7	-65.8	-19.2
		200	500	325.0	-3.7	-1.4	-8.5	-2.7	-21.7	-6.8
			1500	346.8	-8.3	-2.4	-16.5	-4.8	-41.3	-11.9
			2500	369.7	-8.8	-2.4	-17.6	-4.8	-43.9	-11.9
	500	50	500	113.8	-5.6	-7.6	-11.2	-15.2	-28.1	-37.9
			1500	104.3	-10.7	-7.6	-21.5	-15.2	-53.6	-37.9
			2500	99.1	-10.8	-7.6	-21.7	-15.2	-54.2	-37.9
		100	500	172.0	-11.5	-6.1	-22.0	-12.2	-55.5	-30.5
			1500	164.4	-11.9	-6.1	-23.7	-12.2	-59.3	-30.5
			2500	216.7	-13.2	-6.1	-26.4	-12.2	-66.1	-30.5
		200	500	203.4	-10.5	-4.4	-21.0	-8.8	-52.5	-21.9
			1500	255.5	-11.2	-4.4	-22.4	-8.8	-56.1	-21.9
			2500	271.6	-11.9	-4.4	-23.8	-8.8	-59.6	-21.9

TABLE 4.5. Sensitivity of Equation 4.6 to r_{ST}

r_{ST} (sec^{-1})	r_{a+H} (sec^{-1})	$\sigma_s[\theta(L)] - \sigma(z)$ (Pa)	λQ_E ($W m^{-2}$)	$\partial r_{ST}/r_{ST}$ = 10%		$\partial r_{ST}/r_{ST}$ = 20%		$\partial r_{ST}/r_{ST}$ = 50%	
				$\partial \lambda Q_E$ ($W m^{-2}$)	$\partial \lambda Q_E / \lambda Q_E$ (%)	$\partial \lambda Q_E$ ($W m^{-2}$)	$\partial \lambda Q_E / \lambda Q_E$ (%)	$\partial \lambda Q_E$ ($W m^{-2}$)	$\partial \lambda Q_E / \lambda Q_E$ (%)
100	50	500	91.4	-1.4	-1.7	-1.1	-3.3	-20.4	-33.3
		1500	183.3	-11.2	-6.7	-24.4	-13.3	-61.1	-33.3
		2500	305.6	-19.4	-6.7	-40.7	-13.3	-101.9	-33.3
		3500	427.8	-28.5	-6.7	-57.0	-13.3	-142.6	-33.3
	100	500	58.8	-3.9	-5.0	-4.6	-10.0	-11.9	-20.0
		1500	237.5	-16.9	-5.0	-33.8	-10.0	-84.6	-25.0
		2500	429.2	-31.5	-5.0	-28.9	-10.0	-97.3	-25.0
		3500	620.8	-46.6	-5.0	-32.1	-10.0	-80.2	-25.0
	200	500	30.6	-1.0	-3.3	-2.0	-6.7	-5.1	-16.7
		1500	91.7	-3.1	-3.3	-6.1	-6.7	-15.3	-16.7
		2500	152.8	-5.1	-3.3	-10.2	-6.7	-25.5	-16.7
		3500	213.9	-7.1	-3.3	-14.3	-6.7	-35.6	-16.7
200	50	500	96.7	-11.9	-8.0	-5.9	-16.0	-14.7	-40.0
		1500	110.0	-26.6	-8.0	-17.6	-16.0	-44.0	-40.0
		2500	183.3	-41.7	-8.0	-29.3	-16.0	-77.3	-40.0
		3500	256.7	-20.5	-8.0	-41.1	-16.0	-102.7	-40.0
	100	500	30.6	-2.0	-6.7	-4.1	-13.3	-10.2	-33.3
		1500	91.7	-6.1	-6.7	-12.2	-13.3	-30.6	-33.3
		2500	152.8	-10.2	-6.7	-20.4	-13.3	-50.9	-33.3
		3500	213.9	-14.3	-6.7	-28.5	-13.3	-71.3	-33.3
	200	500	15.9	-1.1	-5.0	-2.3	-10.0	-5.7	-25.0
		1500	68.8	-4.4	-5.0	-8.9	-10.0	-22.2	-25.0
		2500	121.6	-7.7	-5.0	-11.5	-10.0	-28.8	-25.0
		3500	174.4	-11.0	-5.0	-16.0	-10.0	-40.1	-25.0
500	50	500	46.7	-2.5	-9.1	-3.0	-18.2	-7.6	-45.5
		1500	50.0	-4.6	-9.1	-9.1	-18.2	-22.7	-45.5
		2500	83.3	-7.6	-9.1	-15.2	-18.2	-37.9	-45.5
		3500	116.7	-10.6	-9.1	-21.2	-18.2	-53.0	-45.5
	100	500	23.3	-1.5	-6.7	-2.5	-10.7	-6.4	-27.7
		1500	45.8	-3.8	-8.3	-7.6	-16.7	-19.1	-41.7
		2500	76.4	-6.4	-8.3	-12.7	-16.7	-31.8	-41.7
		3500	106.9	-8.9	-8.3	-17.8	-16.7	-44.6	-41.7
	200	500	15.1	-.9	-7.1	-1.9	-14.3	-4.7	-35.7
		1500	39.3	-2.3	-7.1	-5.6	-14.3	-14.0	-35.7
		2500	65.5	-4.7	-7.1	-9.4	-14.3	-23.4	-35.7
		3500	91.7	-6.5	-7.1	-13.1	-14.3	-32.7	-35.7

sensitive than equation 4.6 to relative errors in r_{ST}. Hence, the trend in Figure 4.19 results partly from underestimation of $r_{ST}(OLA)$ by $r_{ST}(P)$ but also from the greater sensitivity of equation 4.6 to errors in r_{ST}.

From the data presented herein, the use of equation 2.20 is preferred over the use of equation 4.6. Although equation 2.20 requires surface net available energy, it does not require $\theta(L)$. Equation 2.20, from previous analysis, is relatively insensitive to r_{aVH} error. As the sensitivity of equation 4.6 to relative error is equal for r_{ST} and r_{aVH}, the further superiority of the combination model is apparent.

5. Relationship of leaf and bulk stomatal resistances to environmental parameters

In this section, the relationship of r_L and r_{ST} to environmental parameters will be examined. As shown previously, the combination model provides reliable hourly estimates of λQ_E if r_{ST} can be specified. Focus will now centre on relationships of r_{ST} and r_L with environmental parameters, with the goal of estimating r_{ST} independent of porometer measurements and knowledge of the evapotranspiration regime.

a. Precipitation, volumetric soil moisture and matric suction

Figure 4.20 shows volumetric soil moisture and matric suction averages for the upper four 0.25 m soil layers throughout the growing season. Soil moisture values were determined from morning gravimetric analysis and neutron moderation estimates. Daily precipitation totals are shown for reference.

The limitation of the pressure plate technique for evaluating

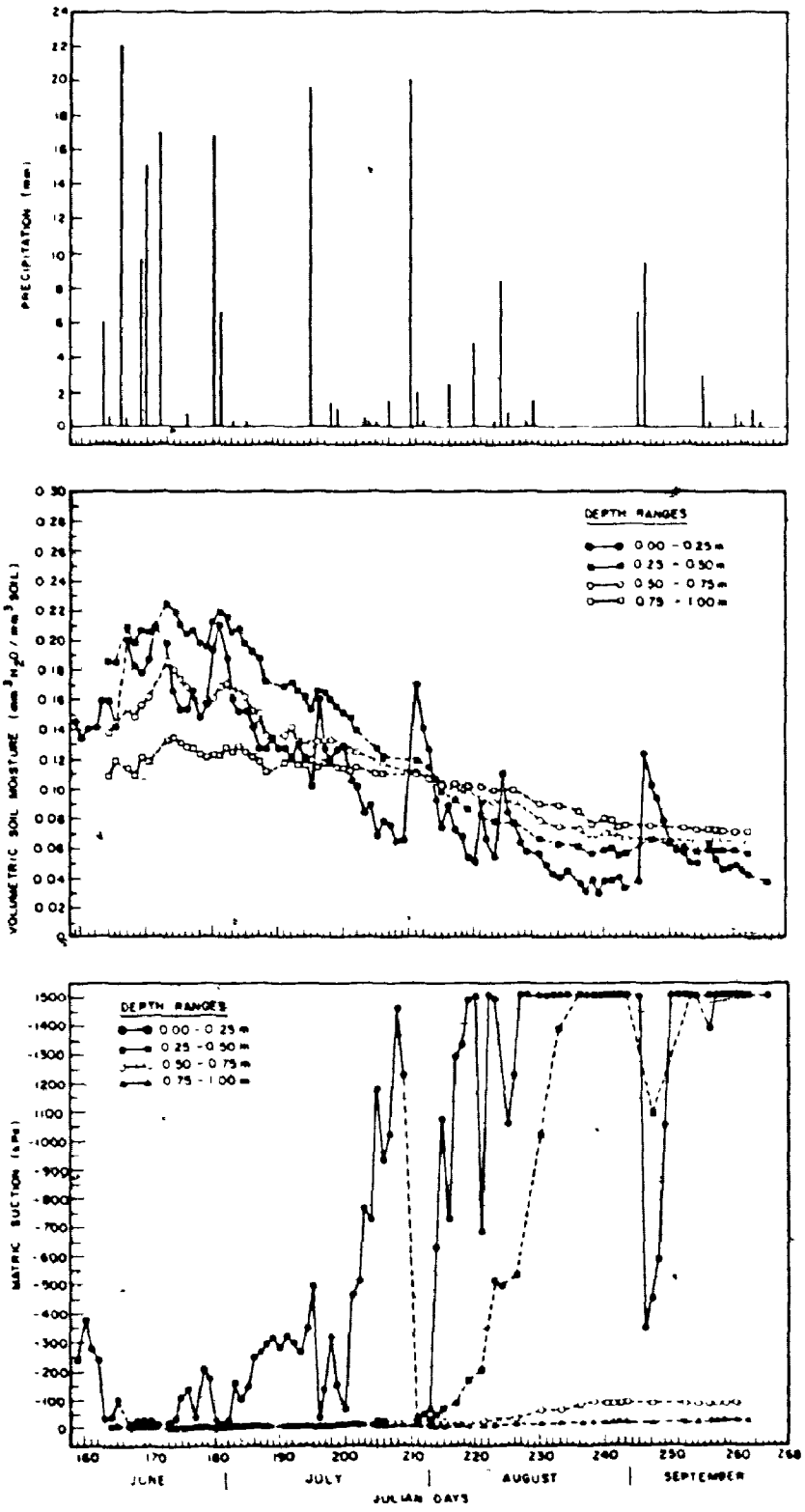

Figure 4.20. The course of precipitation, volumetric soil moisture and matric suction throughout the growing season. Dashed lines are estimates when sequential data are missing.

matric suction is apparent (the arbitrary setting of matric suction equal to -1500 kPa when values fell below this threshold level) as very small values of matric suction dominate the seasonal trends. Because of this limitation, emphasis has been placed upon volumetric soil moisture in this investigation.

Although moisture availability in the rooting zone should be considered for any analysis, this zone was difficult to assess with confidence due to rapidly changing rooting depth and densities and difficulty in root observation and extraction. Volumetric soil moisture for four depth ranges (0.00-0.25 m, 0.00-0.50 m, 0.00-0.75 m and 0.00-1.00 m) were originally considered representative of the rooting depth. Moisture values for the upper 0.25 m layer are used throughout the analysis however, since (1) other layers shared trends similar to it, and (2) morning gravimetric samples, taken almost daily, supplemented the less frequent neutron probe measurements, to provide the greatest continuity of observations for this layer.

b. Relationship between leaf resistance and global solar radiation

Figure 4.21 shows a plot of r_L against global solar radiation K↓ measured above the canopy at times when LAI > 1 and the volumetric soil moisture ≥ 0.12 mm^3 H_2O/mm^3 soil (a matric suction of approximately -70 kPa). Under this condition of ample soil moisture, the minimum leaf resistance is approximately 25-50 s m^{-1}. Leaf resistance begins to increase sharply at approximately 200 Wm^{-2} but the trend below this irradiance level is poorly defined. The scatter of points is not unduly large given the difficulty of defining non-limiting water conditions

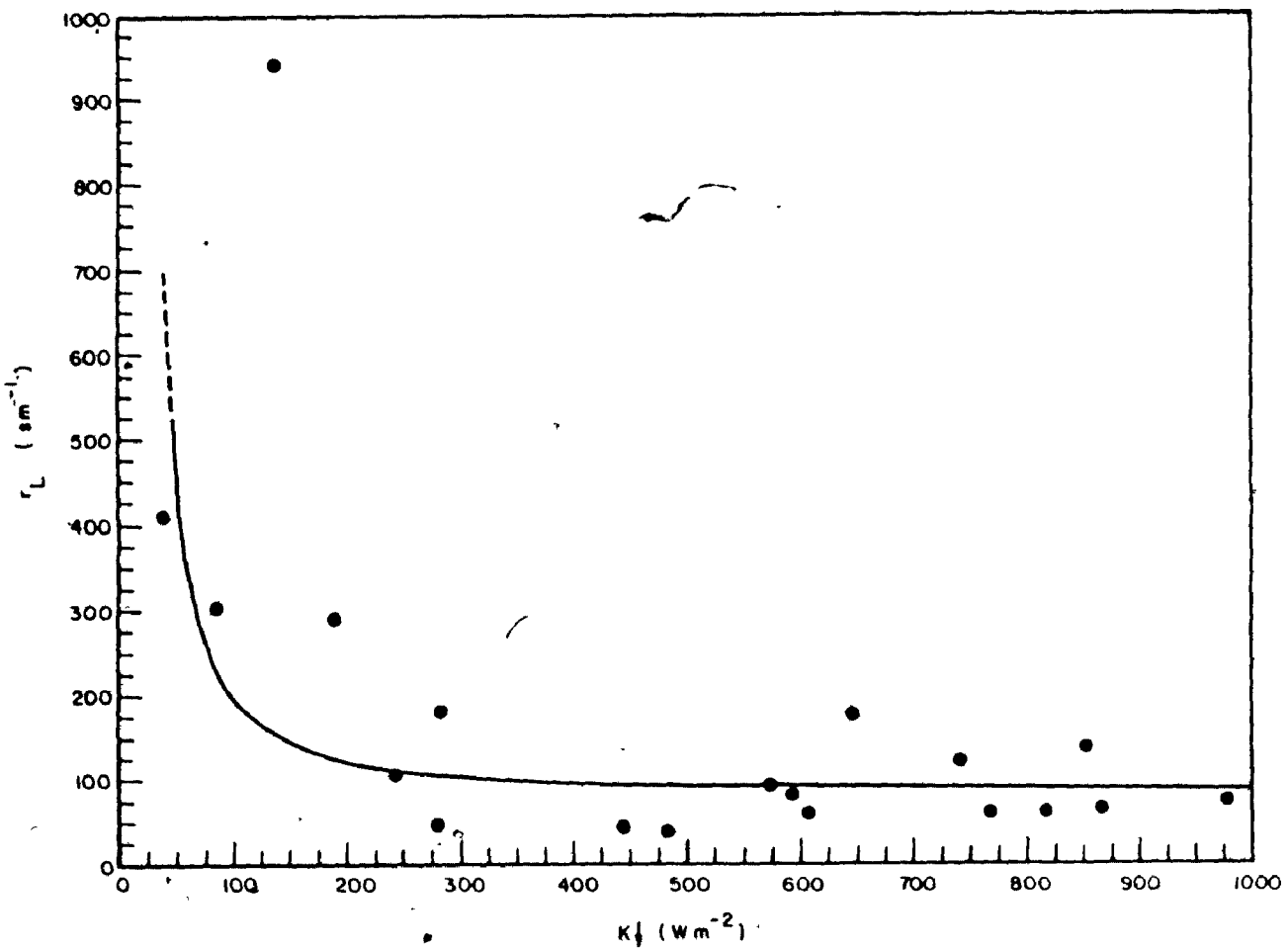

Figure 4.21. Relationship between global solar radiation and leaf resistance when soil moisture is non-limiting. Curve through the 19 data points is given by

$$r_L = 78.32\ e^{(88.96/K\downarrow)}$$

(particularly when late afternoon observations are employed) and the feature that r_L is a composite of adaxial and abaxial measurements representative of the full canopy.

c. r_L and r_{ST} relationships with soil moisture and vapour pressure deficit

Figure 4.22 illustrates the progression of bulk stomatal resistance and vapour pressure deficit during a nine-day, drying cycle period. On Day 210, precipitation (20 mm) replenished previous soil moisture losses. For Days 211 through 213, $r_{ST}(CM)$ is almost constant throughout the day, rarely exceeding 50 s m^{-1} except towards the end of the daylight period. It is worth noting that although moisture is non-limiting, $r_{ST}(CM) > 0$. Towards the end of the period, in response to reduced soil moisture availability (volumetric soil moisture had decreased from 0.169 mm^3 H_2O/mm^3 soil on Day 211 to 0.067 mm^3 H_2O/mm^3 soil on Day 218), an increase of $r_{ST}(CM)$, correlated with vapour pressure deficit trends, is apparent. This is well illustrated for Day 219.

Brady et al. (1975), for soybeans, and Szeicz and Long (1969), for grass-clover, have related r_L to soil water potential and r_{ST} to soil water deficit respectively. Tan and Black (1976) have shown that the scatter found in such relationships may be attributable to a secondary relationship with the atmospheric vapour pressure deficit. They defined relationships between r_L for Douglas fir and soil water potential for several ranges of vapour pressure deficit. A similar relationship is suggested in Figure 4.22 since $r_{ST}(CM)$ response to $\left[e_s\left[\theta(z)\right] - e(z)\right]$ is discernable when soil moisture becomes limiting.

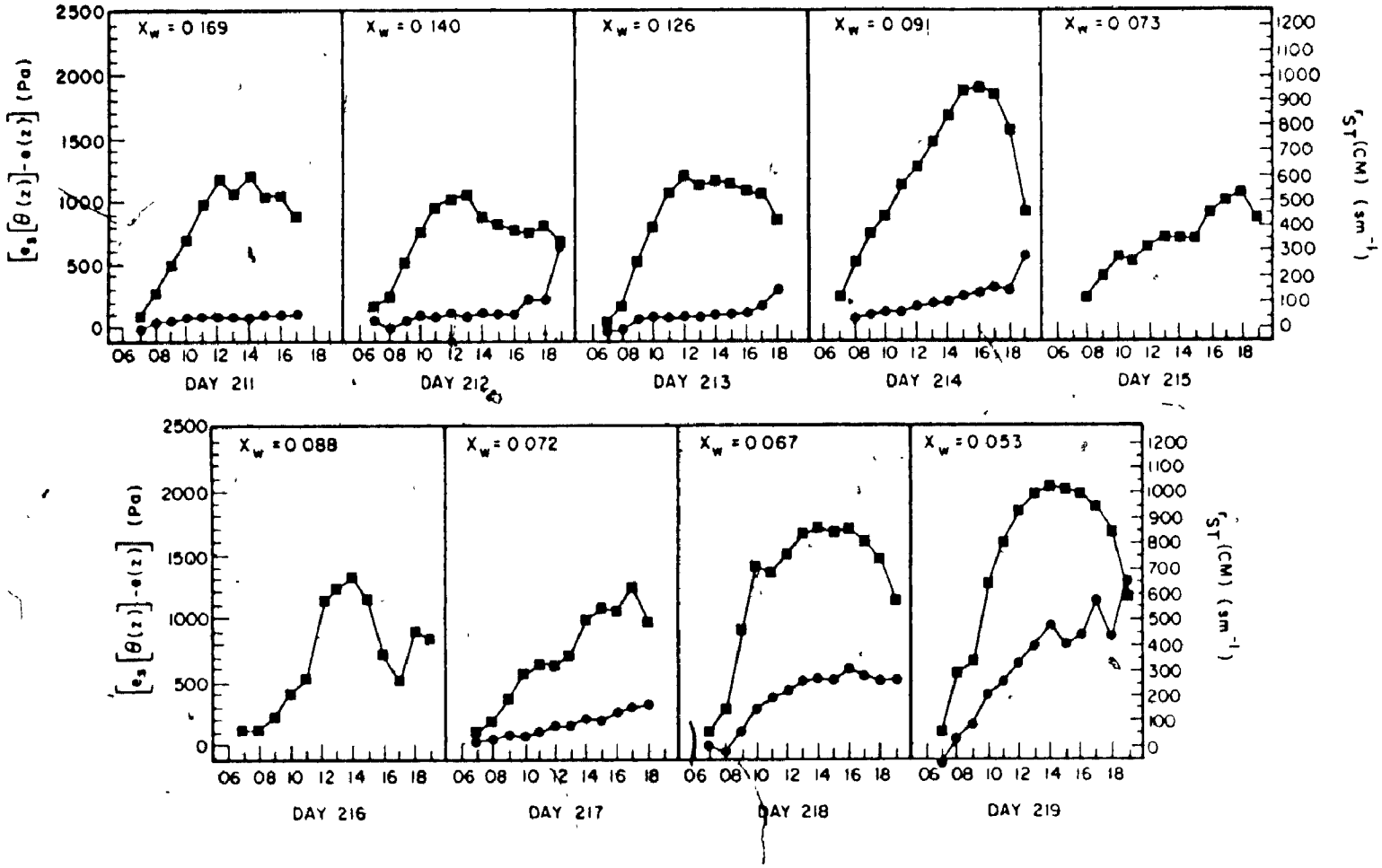

Figure 4.22. The progression of bulk stomatal resistance (●) and vapour pressure deficit (■) during a nine day drying cycle. Volumetric soil moisture X_w (mm^3 H_2O/mm^3 soil) for depth 0.00 - 0.25 m is denoted for each day.

The relationship between measured values of r_L during the drying cycle and volumetric soil moisture for six ranges of vapour pressure deficit is illustrated in Figure 4.23. Late afternoon 0.00-0.25 m gravimetric measurements were used in plotting late afternoon r_L data. An increase in r_L with decreasing soil moisture is suggested but a pattern for the vapour pressure deficit ranges is difficult to discern.

In Figure 4.24, a similar presentation is made for $r_{ST}(CM)$. With decreasing soil moisture, $r_{ST}(CM)$ increases. However, accompanying this is a large increase in scatter about the general trend. In this scatter, a poorly defined pattern for vapour pressure deficit ranges is discernable. With increased vapour pressure deficit at a fixed volumetric soil moisture, $r_{ST}(CM)$ values are generally larger. However, the relationship exhibited is not definitive.

All leaf stomatal resistance data on days where LAI > 1 have been pooled for morning, midday and late afternoon periods in Figure 4.25 to examine the relationship between r_L and volumetric soil moisture. Late afternoon gravimetric samples are used for afternoon r_L data plotting. With the larger data sample, a more well defined relationship with soil moisture is apparent. However, the scatter is considerable, even when vapour pressure deficit ranges are considered. It can be seen that a larger vapour pressure deficit correlates with larger r_L at a fixed soil moisture. The distribution presented for midday data agrees well with that presented by Brady et al. for soybeans. Since they present no other data, further comparison is not possible.

When comparison is made between the three observation periods, the distributions are different even if vapour pressure deficit influence

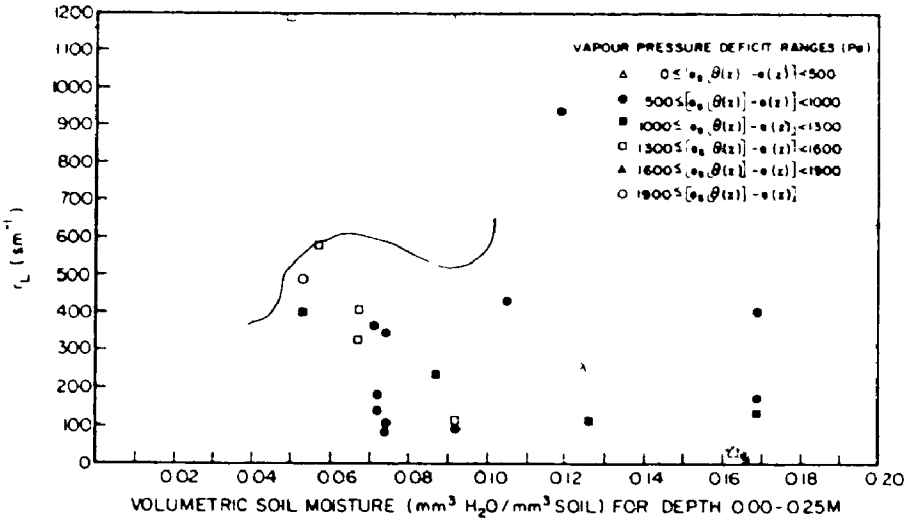

Figure 4.23. Relationship between leaf resistance and volumetric soil moisture for six ranges of vapour pressure deficit.

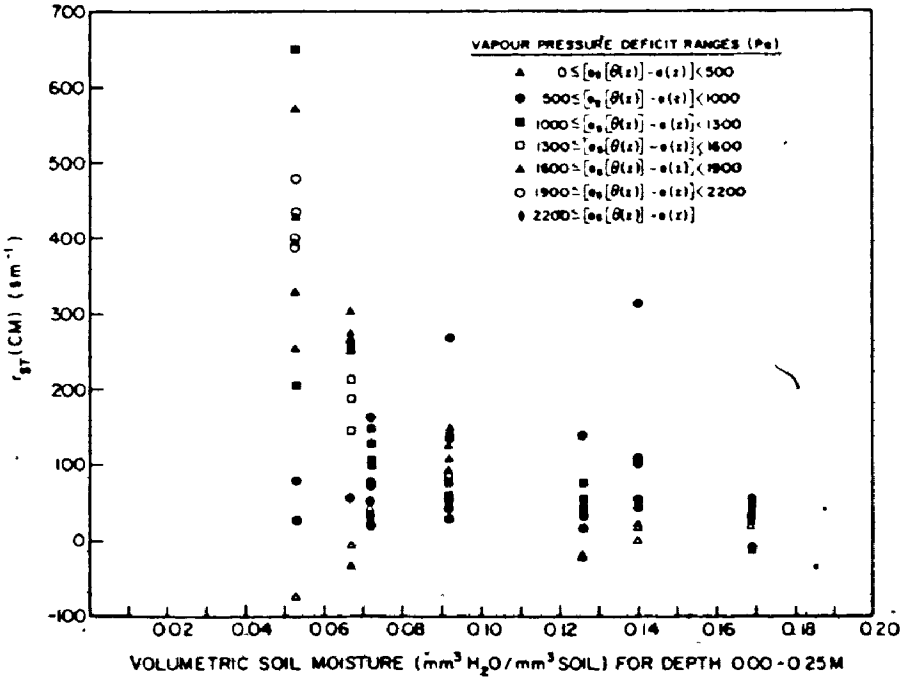

Figure 4.24. Relationship between bulk stomatal resistance and volumetric soil moisture for seven ranges of vapour pressure deficit.

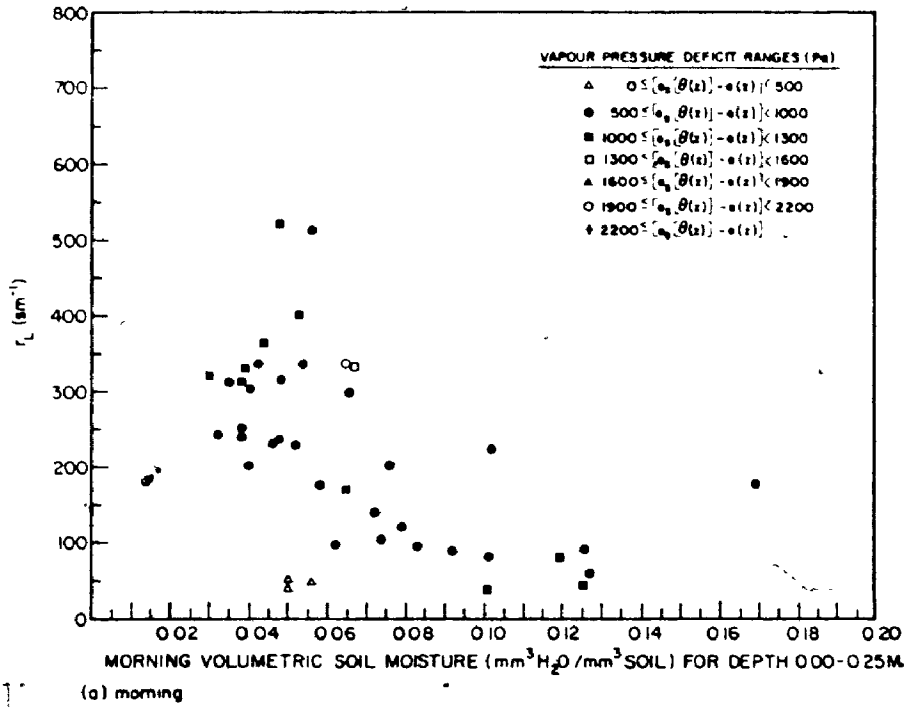

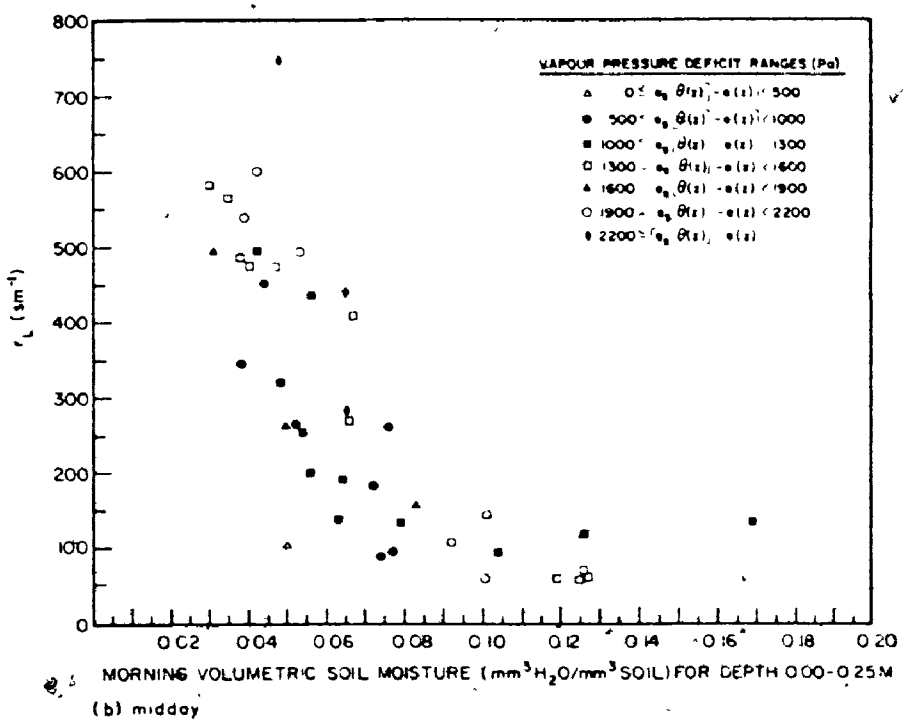

Figure 4.25. Relationship between leaf resistance and volumetric soil moisture for seven ranges of vapour pressure deficit for morning, midday and afternoon observations.

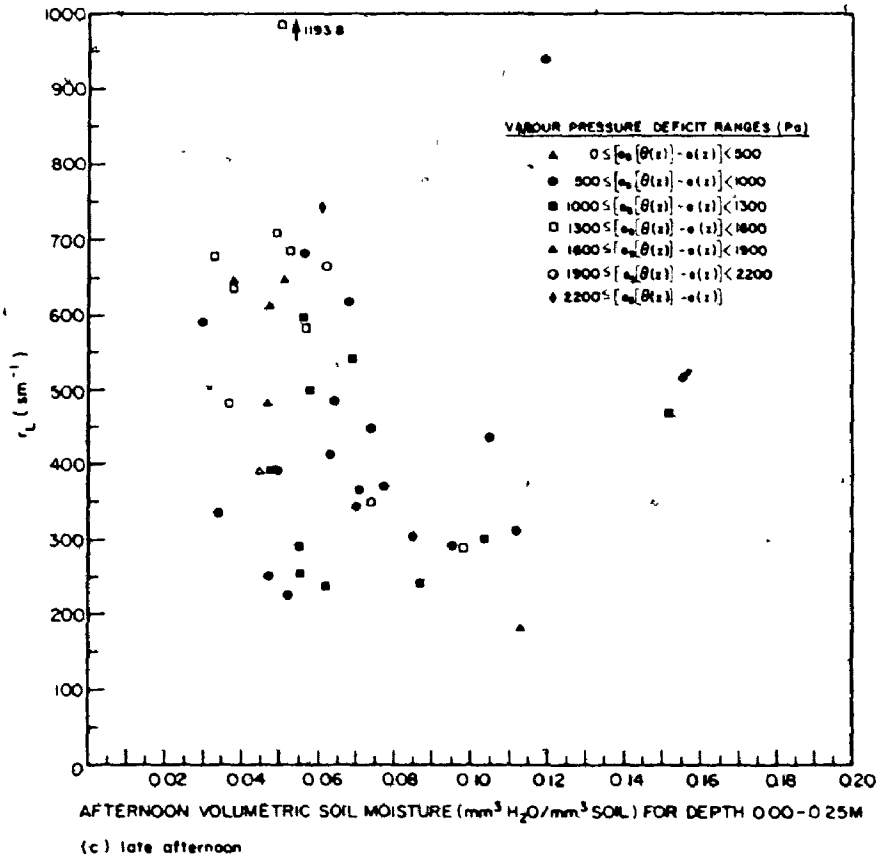

Figure 4.25 (cont'd.). Relationship between leaf resistance and volumetric soil moisture, for seven ranges of vapour pressure deficit for morning, midday and afternoon observations.

is acknowledged. Particularly for the late afternoon observations, r_L increase at a given soil moisture level is evident. The possible influence of other environmental parameters is suggested. The effects of irradiance on stomatal behaviour was investigated using the approach of Szeicz et al. (1973). r_L was normalized by leaf conductance in non-limiting water conditions (Figure 4.21). Analysis of soil moisture and vapour pressure deficit influence was then examined. The results were inconclusive and produced no additional insight. Internal plant water status was not assessed in this investigation. It is suggested that this must be known on a short time basis (hourly for example) before a more detailed interpretation of Figure 4.25 can be made.

From this investigation, it is evident that the response of r_L and hence r_{ST} to environmental conditions is not simple. Resistance variability, even over short periods, illustrates that a more detailed understanding of stomatal behaviour in field environments is required. For the conditions present during this study, the ability to account for internal plant water status is required before r_{ST} estimation procedures can be routinely employed in hourly evapotranspiration calculations using the combination model.

CHAPTER FIVE

DAYTIME EVAPOTRANSPIRATION RESULTS

In this chapter, the results from daytime evapotranspiration analysis are presented. As an introduction to this, the course of energy balance components during a drying cycle is examined.

A. Energy Balance Components During a Drying Cycle

Daily values of energy balance components during a ten day (July 30 through August 08) drying cycle are shown in Figure 5.1. Daily precipitation, volumetric soil moisture and evapotranspiration are listed in Table 5.1. On July 29 (Day 210) 20 mm of precipitation fell, replenishing previous soil moisture losses. On the ensuing three days, most of the net available energy was utilized in evapotranspiration. Estimates of potential evapotranspiration from the Priestley and Taylor (1972) model compared very well with λQ_E on an hourly basis for these days. On a daytime basis, α' is 1.22, 1.30 and 1.26, values which compare well with the average value of 1.26 found by Priestley and Taylor and previous findings at Simcoe (Davies and Allen, 1973). Light precipitation on Days 211 and 212 served to increase available soil moisture and aided in the maintenance of potential daily rates. On the fourth and fifth days of the cycle, soil moisture fell below 0.12 mm^3 H_2O/mm^3 soil. On these days, λQ_{ES} approximates λQ_E closely on an hourly basis. Daytime α' values are 1.07 and 1.05. Rainfall (2.5 mm) on the

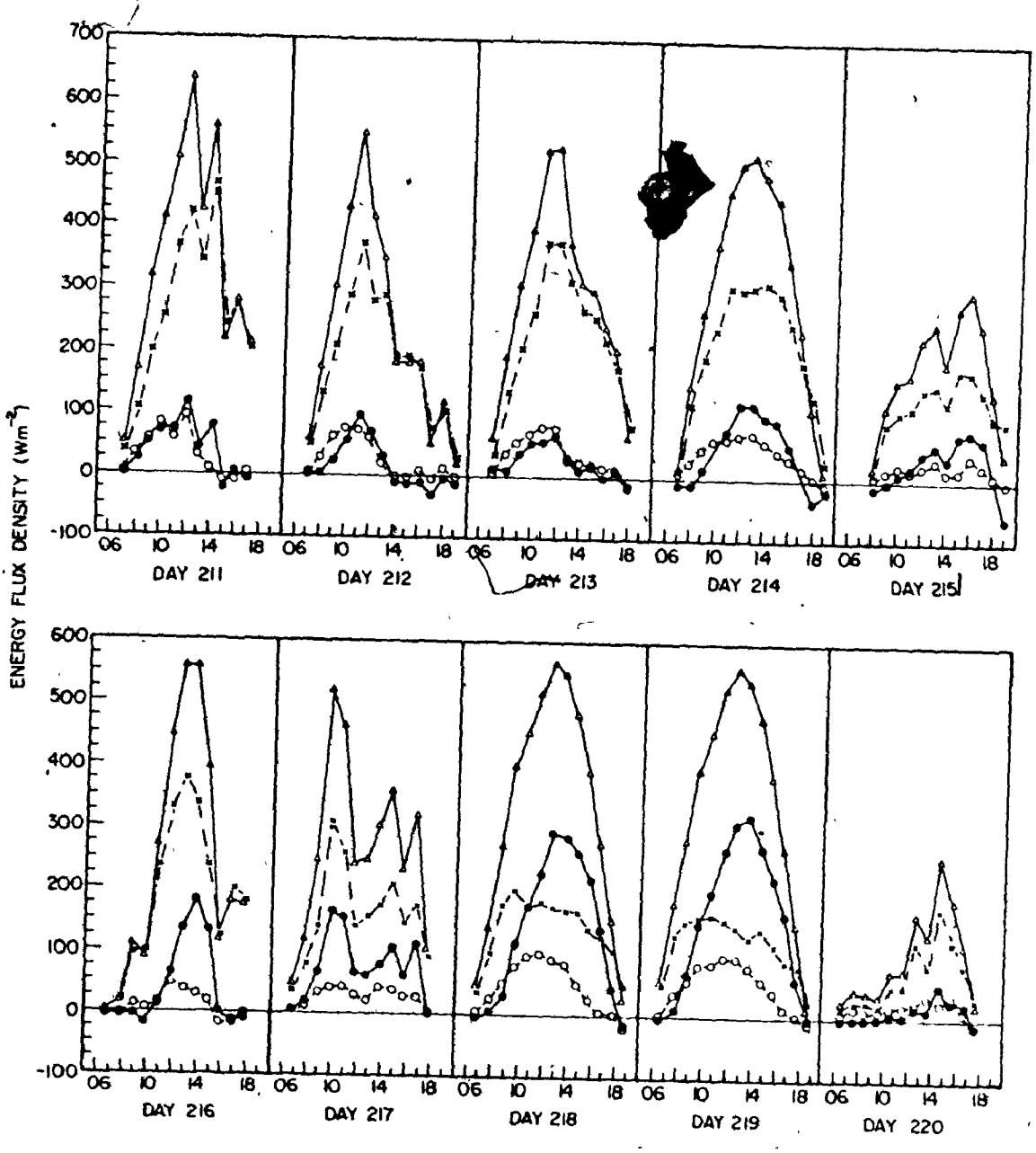

Figure 5.1. The course of energy balance components during a drying cycle. Symbolism employed: Q^* (Δ), λQ_E (x), Q_H (●) and Q_G (O).

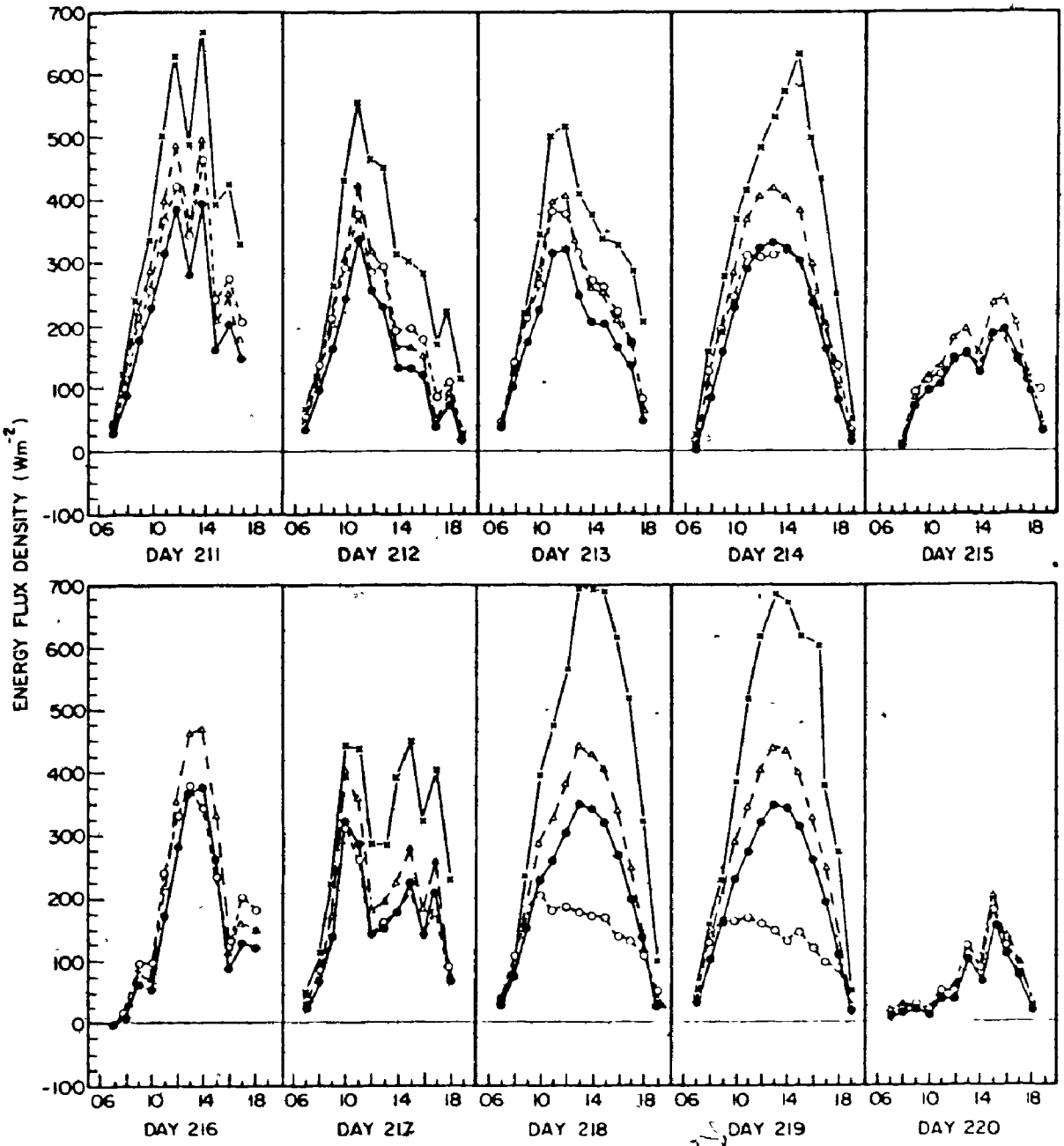

Figure 5.1 (cont'd.). The course of energy balance components during a drying cycle. Symbolism employed: λQ_{PE} from equation 2.39 (*), λQ_{PE} from equation 2.40 (Δ), λQ_E (O) and λQ_{ES} (●).

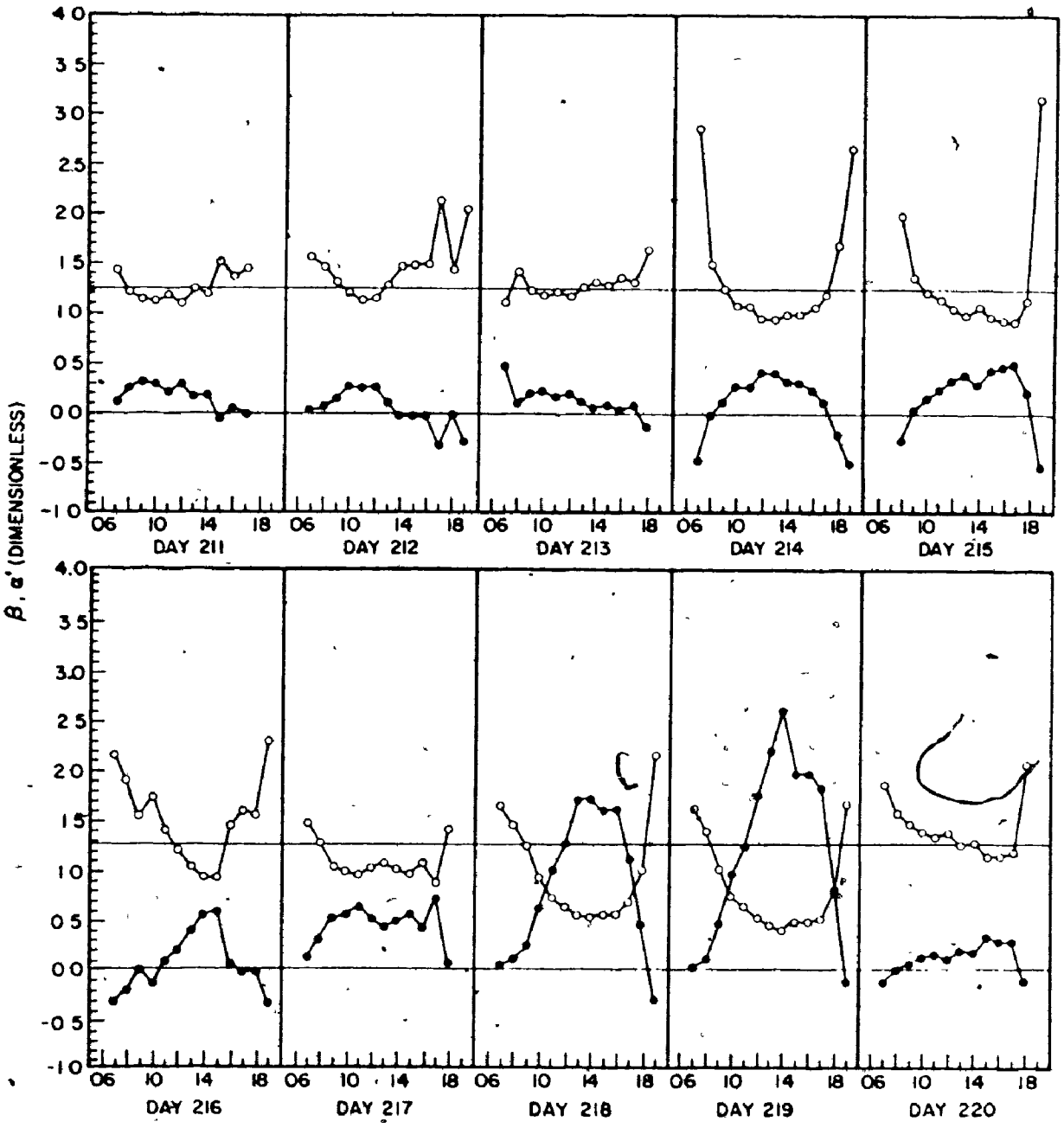

Figure 5.1 (cont'd.). The course of energy balance components during a drying cycle. Symbolism employed: α' (○) and β (●).

TABLE 5.1. Precipitation, Soil Moisture and Evapotranspiration Drying Cycle Data

Julian Day	Date	Precipitation (24 Hour Total) (mm)	Morning Volumetric Soil Moisture for Depth 0.00 - 0.25 m ($mm^3 H_2O/mm^3$ soil)	λQ_E	λQ_{ES}	λQ_{PE} (eq'n. 2.40)	λQ_{PE} (eq'n. 2.39)	α'
				(-------- MJ m^{-2} day^{-1} --------)[1]				
210	July 29	20.1	M	M	M	M	M	M
211	July 30	2.0	0.169	10.461	8.583	10.815	14.977	1.22
212	July 31	0.3	0.140	8.502	6.536	8.236	13.014	1.30
213	August 01		0.126	9.745	7.719	9.726	13.259	1.26
214	August 02		0.092	9.731	9.080	11.441	17.451	1.07
215	August 03		0.074	5.057	4.812	6.063	M	1.05
216	August 04	2.5	0.088	8.105	6.956	8.765	M	1.17
217	August 05		0.072	6.849	6.932	8.734	12.980	0.99
218	August 06		0.067	6.263	9.311	11.732	19.227	0.67
219	August 07		0.053	5.315	9.492	11.960	18.509	0.56
220	August 08	4.8	M	2.879	2.352	2.963	M	1.22

M denotes missing data

1. Daytime totals were calculated for the period 0700-1800 EST for all days except July 30 where the period 0700-1700 EST was used.

sixth day did not restore soil moisture to a level that would maintain potential evapotranspiration rates, consequently daytime evapotranspiration was between λQ_{ES} and λQ_{PE} with $\alpha' = 1.17$. Response to the additional moisture however is clear. On the next day, λQ_{ES} is again a good approximation of both hourly and daytime λQ_E. Further soil moisture depletion on the eighth and ninth days results in decreased λQ_E and a sharp increase in Q_H. Precipitation (4.8 mm) on the last day returns evapotranspiration to the potential rate ($\alpha' = 1.22$).

The results of this drying cycle show that on a daytime basis, the Priestley and Taylor potential evapotranspiration model with $\alpha' = 1.26$ performs well when moisture is not limiting. On an hourly basis however, α' varies widely but consistently. In the morning, it usually exceeds 1.26, decreases as λQ_E increases towards noon and increases again with reduced λQ_E in the afternoon.

The estimation of hourly and daytime λQ_{PE} from the combination model in which r_{ST} has been set equal to 0 (equation 2.39) is seen to provide overestimations. This arises for two reasons. First, the assumption that $r_{ST} = 0$ in non-limiting moisture conditions is invalid. As previously illustrated in Figure 4.22, $r_{ST} > 0$ during such conditions. Second, the increase in inflated values of λQ_{PE} throughout the progression of the drying cycle as compared to Priestley and Taylor model estimates arise from the influence of increasing vapour pressure deficits during moisture limiting conditions.

Daytime evapotranspiration is strongly linked with available soil moisture (Figure 5.2). The relationship is similar in form to that displayed by Priestley and Taylor (1972) and Davies and Allen (1973).

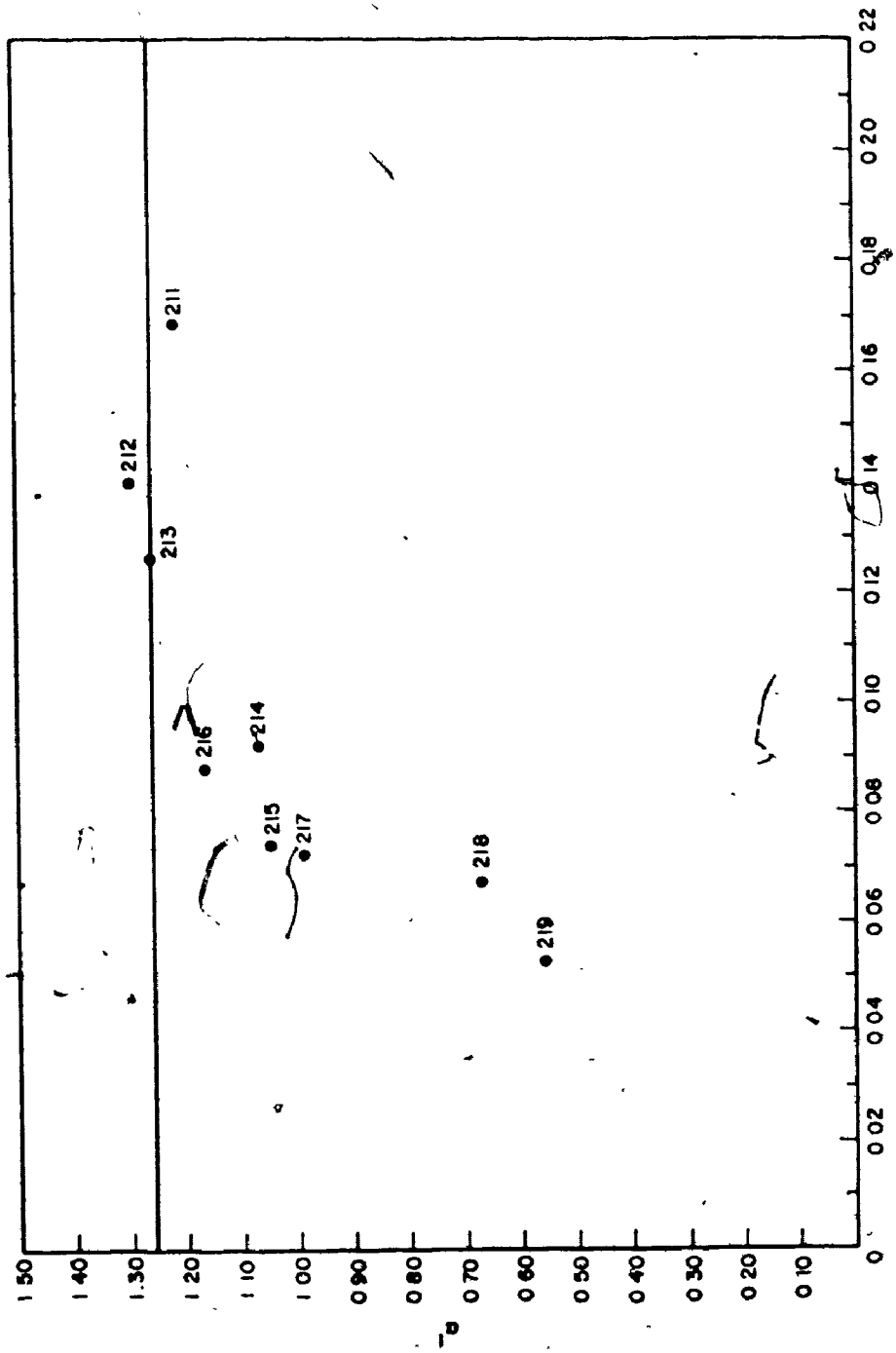

Figure 5.2. Variation of daytime α' with soil moisture during a ten day drying cycle (Days 211 - 220).

The upper evapotranspiration limit, denoted by the largest α' values, is attained when soil moisture exceeds 0.12 mm^3 H_2O/mm^3 soil. Below this threshold, α' is linearly related to soil moisture. As this scheme has merit in λQ_E estimation, attention will be given to the full growing season data set and the study of evaporative response to soil moisture availability.

B. Variation of Daytime α' with Soil Moisture

The variation of daytime α' with morning volumetric soil moisture for the layer 0.00 - 0.25 m is presented in Figure 5.3. Daytime α' was evaluated from daytime totals of λQ_E and λQ_{ES}. Daytime evapotranspiration totals were accumulated over a standardized period, 0700 to 1800 EST (Appendix Eight), with a few exceptions. Days with missing hourly observations or soil moisture data were eliminated. Days with unrepresentative soil moisture data were also discarded. This usually coincided with soil moisture readings taken before rainfall, hence they were unrepresentative of soil moisture availability for that day.

When all data are considered, the scatter is considerable with definitive trends difficult to discern. A distinct trend emerges if days with LAI > 1 are considered. The results displayed are similar in form to those displayed by Priestley and Taylor (1972) and Davies and Allen (1973). The upper evapotranspiration level, denoted by the largest α' values, is attained when volumetric soil moisture exceeds approximately 0.12 mm^3 H_2O/mm^3 soil. Above this level, values are constant and this data agree well with $\alpha' = 1.26$ for potential conditions as proposed by Priestley and Taylor (1972). However, the very limited data set for

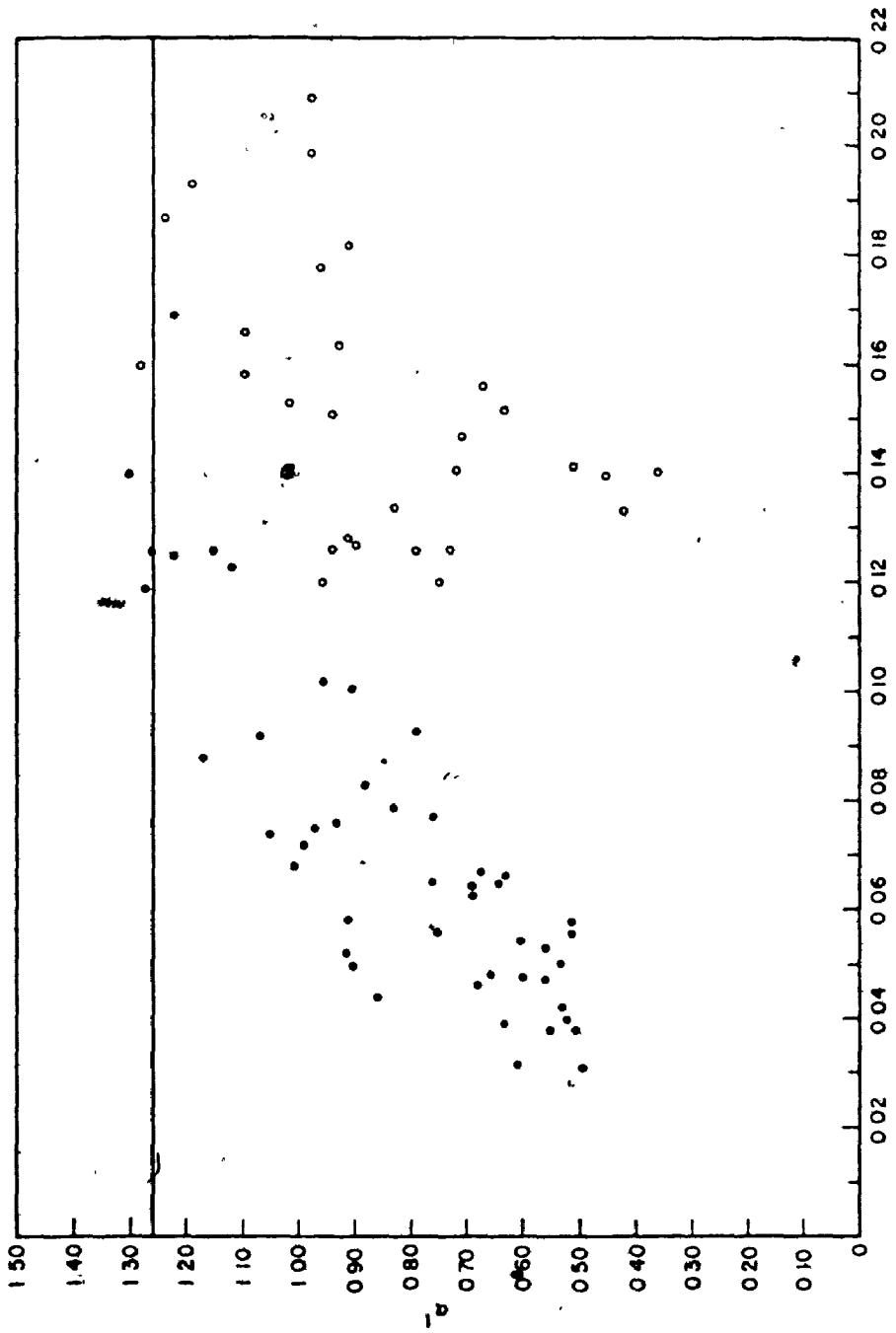

Figure 5.3. Variation of daytime α' with soil moisture for 28 days with LAI ≤ 1 (○) and 47 days with LAI > 1 (●).

potential conditions must be acknowledged. When soil moisture drops below the level where potential evapotranspiration rates can be maintained, evaporative response is linearly related to soil moisture availability. If estimates of λQ_E are required on a daytime basis, the relationship presented in Figure 5.3 could be utilized in a manner similar to that proposed by Davies and Allen (1973).

A number of researchers (Denmead and McIlroy, 1970; Davies, 1972; Stewart and Rouse, 1976(a); Rouse and Stewart, 1972; Wilson and Rouse, 1972) have found that λQ_{ES} provides a good estimation of λQ_E for a wide variety of surfaces. As λQ_{ES} corresponds to $\alpha' = 1.0$, Figure 5.3 shows that this is a transitory stage in evapotranspiration response to decreasing soil moisture availability. Hence, widespread applicability of λQ_{ES} to these data is not found. In comparison with other work, several points can be noted. The results of Stewart and Rouse (1976(a)) and Rouse and Stewart (1972) are for a lichen mat. This surface is unique in that, although surface soil moisture levels were found to be high, the non-transpiring, aerodynamically smooth lichen vegetation strongly inhibited the flux of moisture into the atmosphere. Hence, evapotranspiration was less than potential and the agreement with λQ_{ES} appears to be coincidental with this unique surface characteristic. From Figure 5.3, it is clear that for a first approximation of λQ_E, λQ_{ES} could be employed due to its approximate midrange position on the α' - soil moisture depletion curve. Davies (1972), Denmead and McIlroy (1970) and Wilson and Rouse (1972) found that the equilibrium model performed satisfactorily in moderately dry conditions. This would be in agreement with the relationship displayed in Figure 5.3. Any

interpretation regarding general widespread use of λQ_{ES} is invalid due to the restricted data base employed in these investigations.

For cases when LAI $\leq$ 1, the scatter of data points is large. Again a maximal α' appears to be approximately 1.26 but volumetric soil moisture limitations appear inconsequential. Two suggestions to account for this can be presented. The first is that daily totals of λQ_E accumulated from hourly Bowen ratio method measurements may be theoretically invalid. This is attributable to the incomplete crop canopy and its potential influence in the creation of significant sensible and latent heat flux density divergence. The second is due to the ineffectiveness of volumetric soil moisture for the depth 0.00-0.25 m to adequately represent moisture availability to the plants during early canopy development stages. During this phase, the surface is not dominated by a plant canopy but rather by individual plants located on a bare soil surface. Hence, soil moisture data must reflect the rapidly changing root distribution and complex water extraction patterns. If the soil moisture sample interval depth is reduced from 0.00-0.25 m to 0.00-0.10 m, the data points are shifted towards the distribution for days where LAI > 1, but the wide scatter remains. Clearly, simple soil moisture observations are inadequate in such complex cases. Until the sampling and theoretical difficulties are overcome, generalized schemes such as relating daytime α' to soil moisture will be impractical for incomplete canopy conditions.

CHAPTER SIX

CONCLUSIONS

This thesis was directed towards the study of atmospheric and surface control on hourly and daytime evapotranspiration. The combination model variant proposed by Monteith (1965) with amendment by Thom (1972) was used in the analysis of hourly relationships. Daytime evapotranspiration totals normalized by equilibrium evapotranspiration was the basis for daytime analysis.

From the study of atmospheric and surface control on hourly evapotranspiration, three important results can be summarized:

(1) The combination model variant of Monteith was found to be insensitive to errors in the aerodynamic resistance to water vapour exchange. r_{aVH} itself was found to be insensitive to stability correction. Hence, r_{aVH} could be evaluated with confidence using simple estimations of z_o and d and single level windspeed measurements.

(2) Bulk stomatal resistances were evaluated throughout the duration of the growing season by residual from the combination model and an Ohm's Law analogue. When compared with estimates derived from leaf stomatal resistance and leaf area index measurements, $r_{ST}(CM)$ compared well once canopy development was sufficient to dominate surface energetics. Employing $r_{ST}(P)$ in the combination model provided

λQ_E estimates which agreed well with Bowen ratio method determinations. Hence, with reliable independent estimates of r_{ST}, hourly evapotranspiration can be evaluated with confidence.

(3) The validity of estimations of r_{ST} derived from leaf resistance and leaf area index measurements for use in the combination model has been documented. However, general applicability rests in the prediction of leaf resistance response to environmental parameters. Leaf resistance was found to be related to global solar radiation during non-limiting moisture conditions. Increased leaf resistance during decreasing soil moisture availability was also observed. However, the influence of other factors was in evidence and definitive predictive procedures could not be developed. The procedures used by Brady et al. (1975), Szeicz et al. (1973) and Tan and Black (1976) in relating stomatal resistance to environmental influence were of limited application.

Daytime evapotranspiration totals normalized by equilibrium evapotranspiration were strongly linked with available soil moisture after leaf area index exceeded 1. With volumetric soil moisture above approximately 0.12 mm^3 H_2O/mm^3 soil, maximum values of normalized evapotranspiration were constant. Confirmation of the Priestley and Taylor model was found, with $\alpha' = 1.26$. When soil moisture drops below this threshold level, evaporative response is linearly related to soil moisture availability. This relationship could be employed in estimating daytime water loss from the cropped surface.

Prior to canopy dominance of surface energetics, the relationship between α' and soil moisture is poorly defined. Theoretical limitations to the accurate assessment of λQ_E and the inability to accurately account for the rooting density and soil moisture extraction patterns using simple gravimetric sampling schemes is acknowledged.

APPENDIX ONE

NOTATION

UPPER CASE ROMAN

B'	constant in equation 3.10, equal to 17.269	dimensionless
C	soil heat capacity	$J\ m^{-3}\ K^{-1}$
CH	crop height	m
C_a	heat capacity of air	$J\ m^{-3}\ K^{-1}$
C_m	heat capacity of mineral matter	$J\ m^{-3}\ K^{-1}$
C_o	heat capacity of organic matter	$J\ m^{-3}\ K^{-1}$
Cp	specific heat at constant pressure	$J\ kg^{-1}\ K^{-1}$
C_v	specific heat of vegetal matter	$J\ kg^{-1}\ K^{-1}$
C_w	heat capacity of water	$J\ m^{-3}\ K^{-1}$
D	wet-bulb depression	K
DW_L	leaf dry weight	g
F	property flux density	
K_H	eddy diffusivity for heat exchange	$m^2\ s^{-1}$
K_M	eddy diffusivity for momentum exchange	$m^2\ s^{-1}$
K_W	eddy diffusivity for water vapour exchange	$m^2\ s^{-1}$
K↓	global solar radiation flux density	Wm^{-2}
LA	leaf area	m^2
LAI	leaf area index	dimensionless
P	atmospheric pressure	Pa
Q_E	evapotranspiration rate	$kg\ m^{-2}\ S^{-1}$

Q_G	soil heat flux density	Wm^{-2}; MJm^{-2} day^{-1}
Q_{G_z}	soil heat flux density at depth z	Wm^{-2}; MJm^{-2} day^{-1}
Q_H	sensible heat flux density	Wm^{-2}; MJm^{-2} day^{-1}
Q_P	energy flux density stored by net photosynthesis	Wm^{-2}; MJm^{-2} day^{-1}
Q_S	energy flux density from net storage of sensible and latent heat in the air	Wm^{-2}; MJm^{-2} day^{-1}
Q_{SH}	energy flux density from net storage of sensible heat in the air	Wm^{-2}; MJm^{-2} day^{-1}
Q_{SV}	energy flux density from net storage of latent heat in the air	Wm^{-2}; MJm^{-2} day^{-1}
Q_V	energy flux density from net heat storage in phytomass	Wm^{-2}; MJm^{-2} day^{-1}
Q^*	net radiation flux density	Wm^{-2}; MJm^{-2} day^{-1}
R_i	gradient Richardson number	dimensionless
S	slope of the saturation vapour pressure-temperature curve	$Pa\ K^{-1}$
T	arbitrary temperature	K
X	volume fraction of soil, subscripts a, m, o and w denote air, mineral matter, organic matter and water	m^3/m^3 soil
Y	dependent variable	

LOWER CASE ROMAN

a'	constant in equation 3.10, equal to 610.78	dimensionless
a_n	polynomial regression coefficient, order denoted by numerical subscript	dimensionless
c	calibration constant	
c_t	anemometer cup revolutions	rpm
d	zero plane displacement	m

$divQ_H$	horizontal divergence of sensible heat flux density	Wm^{-2}; MJm^{-2} day^{-1}
$div\lambda Q_E$	horizontal divergence of latent heat flux density	Wm^{-2}; MJm^{-2} day^{-1}
e	vapour pressure	Pa
e_i	vapour pressure at stomatal wall	Pa
e_0	vapour pressure at leaf surface	Pa
$\bar{e}$	average vapour pressure from soil surface to height z_R	Pa
e(0)	surface vapour pressure	Pa
e(z)	vapour pressure at height z	Pa
$e_s(\theta_i)$	saturation vapour pressure at stomatal wall temperature	Pa
$e_s(\theta_0)$	saturation vapour pressure at leaf surface temperature	Pa
$e_s[\theta(0)]$	saturation vapour pressure at surface temperature	Pa
$e_s[\theta(z)]$	saturation vapour pressure at height z temperature	Pa
g	gravitational acceleration	$m\ s^{-2}$
k	von Karman's constant, equal to 0.41	dimensionless
m	electromotive force	mV
m_s	soil solids mass	g
m_v	vegetation mass	g
m_w	soil water mass	g
r_{AB}	abaxial leaf resistance	$s\ m^{-1}$
r_{AD}	adaxial leaf resistance	$s\ m^{-1}$
r_{aH}	aerodynamic resistance for heat exchange	$s\ m^{-1}$
r_{aM}	aerodynamic resistance for momentum exchange	$s\ m^{-1}$

r_{aV}	aerodynamic resistance for water vapour exchange	$s\ m^{-1}$
r_{aVH}	aerodynamic resistance for heat and water vapour exchange	$s\ m^{-1}$
$r_{aVH'}$	r_{aVH} with variable z_o and d input	$s\ m^{-1}$
r_b	aerodynamic resistance due to the absence of bluff-body influences	$s\ m^{-1}$
r_f	aerodynamic resistance for property flux density F exchange	$s\ m^{-1}$
r_L	leaf resistance	$s\ m^{-1}$
r_s	stomatal resistance	$s\ m^{-1}$
r_{ST}	bulk stomatal resistance	$s\ m^{-1}$
$r_{ST}^{(CM)}$	bulk stomatal resistance evaluated from equation 4.5	$s\ m^{-1}$
$r_{ST}^{(OLA)}$	bulk stomatal resistance evaluated from equation 4.7	$s\ m^{-1}$
$r_{ST}^{(P)}$	bulk stomatal resistance evaluated from equation 2.38	$s\ m^{-1}$
rms	subscript denoting root-mean-square	
t	time	s
u	windspeed	$m\ s^{-1}$
u(z)	windspeed at height z	$m\ s^{-1}$
$\bar{u}$	average windspeed from soil surface to height z_R	$m\ s^{-1}$
u*	friction velocity	$m\ s^{-1}$
x_n	independent variable	
x(m)	mean surface concentration	
x(z)	concentration at height z	
z	height above the surface	m
z_o	surface roughness parameter	m
z_R	reference height	m

UPPER CASE GREEK

θ	potential air temperature	K
θ_i	temperature of stomatal wall	K
θ_0	temperature at leaf surface	K
θ_v	vegetation temperature	K
θ_{v*}	virtual potential temperature	K
θ_w	potential wet-bulb temperature	K
$\overline{\theta}$	average air temperature from soil surface to height z	K
$\overline{\theta}_{o-z}$	mean soil temperature between surface and depth z	K
$\theta(L)$	leaf temperature	K
$\theta(0)$	surface temperature	K
$\theta(z)$	potential air temperature at height z	K
$\theta_w(z)$	potential wet-bulb temperature at height z	K
Φ_M	height integrated stability correction for momentum	dimensionless

LOWER CASE GREEK

α	constant in equation 2.40, equal to 1.26	dimensionless
α'	ratio of actual to equilibrium evapotranspiration	dimensionless
β	Bowen ratio	dimensionless
γ	psychrometric constant	Pa K^{-1}
ϵ	ratio of molecular weight of water to mean molecular weight of dry air	dimensionless
λ	latent heat of vapourization of liquid water	J kg^{-1}
λQ_E	latent heat flux density	Wm^{-2}; MJm^{-2} day^{-1}

λQ_{ES}	equilibrium latent heat flux density	Wm^{-2}; MJm^{-2} day^{-1}
λQ_{PE}	potential latent heat flux density	Wm^{-2}; MJm^{-2} day^{-1}
ρ	density of air	$kg\ m^{-3}$
ρ_s	bulk density of soil	$kg\ m^{-3}$
ρ_v	density of vegetation	$kg\ m^{-3}$
τ	momentum flux density	Pa
ϕ_M	stability correction for momentum exchange	dimensionless
ϕ'	constant in equation 3.10, equal to 237.30	dimensionless
χ	horizontal distance	m

APPENDIX TWO

ENERGY BALANCE ERROR ANALYSIS

Any value Y can be expressed as a function of a set of measurements X_1, X_2, ..., X_n which have associated with them errors δX_1, δX_2, ..., δX_n:

$$Y = f(X_1 \pm \delta X_1, X_2 \pm \delta X_2, \ldots, X_n \pm \delta X_n) . \qquad (A2.1)$$

The probable absolute error in Y is given by

$$\delta Y_{rms} = \left[\left(\frac{\partial Y}{\partial X_1} \delta X_1\right)^2 + \left(\frac{\partial Y}{\partial X_2} \delta X_2\right)^2 + \ldots + \left(\frac{\partial Y}{\partial X_n} \delta X_n\right)^2 \right]^{\frac{1}{2}} . \qquad (A2.2)$$

The relative error is defined by $\delta Y_{rms}/Y$ and is expressed as a percentage.

A. Temperature

The reduction equation for both dry-bulb and wet-bulb temperature data is

$$T = cm \qquad (A2.3)$$

where T is temperature (representing θ or θ_w), c is the calibration constant and m is the electromotive output from the recording apparatus. Since both sources of error in equation A2.3 are independent and random:

$$\delta T_{rms} = \left[\left(\frac{\partial T}{\partial m}\,\delta m\right)^2 + \left(\frac{\partial T}{\partial c}\,\delta c\right)^2\right]^{\frac{1}{2}}$$

$$= \left[(c\delta m)^2 + (m\delta c)^2\right]^{\frac{1}{2}} . \qquad (A2.4)$$

From the error in the calibration constant of a representative sensor (±0.00277 K mV^{-1} for sensor 05 in Table 3.3) and the resolution error in the data system (±0.003 mV), errors present in θ and θ_w were assessed (Table A2.1). Over the temperature range 273-308 K, the relative error is less than ±0.01%.

B. Temperature Difference

Dry and wet-bulb temperature differences were evaluated from

$$\Delta T = T_{z_1} - T_{z_2} \qquad (A2.5)$$

where the subscripts z_1 and z_2 denote heights 1 and 2 respectively. Therefore:

$$\delta\Delta T_{rms} = \left[\left(\frac{\partial \Delta T}{\partial T_{z_1}}\,\delta T_{z_1}\right)^2 + \left(\frac{\partial \Delta T}{\partial T_{z_2}}\,\delta T_{z_2}\right)^2\right]^{\frac{1}{2}}$$

$$= \left[2(\delta T_{rms})^2\right]^{\frac{1}{2}} . \qquad (A2.6)$$

Absolute and relative errors in $\Delta\theta$ and $\Delta\theta_w$ for finite differences of 0 to 2 K at 283, 293 and 303 K are presented in Table A2.2.

TABLE A2.1. Errors in Temperature

$T^{1.}$ (K)	δT_{rms} (K)	$\delta T_{rms}/T$ (%)
273	0.016	0.006
278	0.016	0.006
283	0.017	0.006
288	0.018	0.006
293	0.019	0.006
298	0.021	0.007
303	0.023	0.008
308	0.025	0.008

1. T represents θ or θ_w

TABLE A2.2. Errors in Temperature Differences

	T = 283 K		T = 293 K		T = 303 K	
$\Delta T^{1.}$ (K)	$\delta\Delta T_{rms}$ (K)	$\delta\Delta T_{rms}/\Delta T$ (%)	$\delta\Delta T_{rms}$ (K)	$\delta\Delta T_{rms}/\Delta T$ (%)	$\delta\Delta T_{rms}$ (K)	$\delta\Delta T_{rms}/\Delta T$ (%)
0.0	0.024	-	0.027	-	0.033	-
0.2	0.024	12.00	0.027	13.50	0.033	16.50
0.4	0.024	6.00	0.027	6.75	0.033	8.25
0.6	0.024	4.00	0.027	4.50	0.033	5.50
0.8	0.024	3.00	0.027	3.36	0.033	4.13
1.0	0.024	2.40	0.027	2.70	0.033	3.30
1.2	0.024	2.00	0.027	2.25	0.033	2.75
1.4	0.024	1.71	0.027	1.93	0.033	2.36
1.6	0.024	1.50	0.027	1.69	0.033	2.06
1.8	0.024	1.33	0.027	1.50	0.033	1.83
2.0	0.024	1.20	0.027	1.35	0.033	1.65

1. ΔT represents $\Delta\theta$ or $\Delta\theta_w$

C. Vapour Pressure

Vapour pressure was evaluated from the psychrometer equation

$$e = e_s(\theta_w) - \gamma D \qquad (A2.7)$$

in which $D = \theta - \theta_w$ and $e_s(\theta_w) = a' \exp\left[B'\theta_w/(\theta_w+\phi')\right]$.

Therefore:

$$\delta e_{rms} = \left\{\left[\left[\frac{a'B'\phi'}{(\theta_w+\phi')^2} \exp\left[B'\theta_w/(\theta_w+\phi')\right]\right] \delta T_{rms}\right]^2 + \left[-\gamma\left[2(\delta T_{rms})^2\right]^{\frac{1}{2}}\right]^2\right\}^{\frac{1}{2}} . \qquad (A2.8)$$

Tabulations of δe_{rms} are listed in Table A2.3.

D. Vapour Pressure Difference

Vapour pressure differences were evaluated from

$$\Delta e = e_{z_1} - e_{z_2} . \qquad (A2.9)$$

Hence

$$\delta \Delta e_{rms} = \left[2(\delta e_{rms})^2\right]^{\frac{1}{2}} . \qquad (A2.10)$$

Tabulations of $\delta \Delta e_{rms}$ are listed in Table A2.4.

TABLE A2.3. Errors in Vapour Pressure.

e (Pa)	D = 0.0 K		D = 1.0 K	
	δe_{rms} (Pa)	$\delta e_{rms}/e$ (%)	δe_{rms} (Pa)	$\delta e_{rms}/e$ (%)
500	1.58	0.32	1.60	0.32
1000	1.86	0.19	1.91	0.19
1500	2.31	0.15	2.39	0.16
2000	2.87	0.14	2.94	0.15
2500	3.48	0.14	3.57	0.14
3000	4.14	0.14	4.23	0.14

e (Pa)	D = 2.0 K		D = 5.0 K	
	δe_{rms} (Pa)	$\delta e_{rms}/e$ (%)	δe_{rms} (Pa)	$\delta e_{rms}/e$ (%)
500	1.62	0.32	1.74	0.35
1000	1.97	0.20	2.15	0.22
1500	2.45	0.16	2.67	0.18
2000	3.02	0.15	3.27	0.16
2500	3.65	0.15	3.92	0.16
3000	4.32	0.14	4.60	0.15

e (Pa)	D = 10.0 K	
	δe_{rms} (Pa)	$\delta e_{rms}/e$ (%)
500	1.99	0.40
1000	2.48	0.25
1500	3.05	0.20
2000	3.69	0.18
2500	4.36	0.17
3000	5.06	0.17

TABLE A2.4. Errors in Vapour Pressure Differences

D = 5.0 K

Δe (Pa)	e = 1000 Pa $\delta\Delta e_{rms}$ (Pa)	e = 1000 Pa $\delta\Delta e_{rms}/\Delta e$ (%)	e = 1500 Pa $\delta\Delta e_{rms}$ (Pa)	e = 1500 Pa $\delta\Delta e_{rms}/\Delta e$ (%)
0	3.04	-	3.78	-
20	3.04	15.20	3.78	18.90
40	3.04	7.60	3.78	9.45
60	3.04	5.07	3.78	6.30
80	3.04	3.80	3.78	4.73
100	3.04	3.04	3.78	3.78
120	3.04	2.53	3.78	3.15
140	3.04	2.17	3.78	2.70
160	3.04	1.90	3.78	2.36
180	3.04	1.69	3.78	2.10
200	3.04	1.52	3.78	1.89

Δe (Pa)	e = 5000 Pa $\delta\Delta e_{rms}$ (Pa)	e = 5000 Pa $\delta\Delta e_{rms}/\Delta e$ (%)	e = 7500 Pa $\delta\Delta e_{rms}$ (Pa)	e = 7500 Pa $\delta\Delta e_{rms}/\Delta e$ (%)
0	4.62	-	5.54	-
20	4.62	23.10	5.54	27.70
40	4.62	11.55	5.54	13.85
60	4.62	7.70	5.54	9.23
80	4.62	5.78	5.54	6.93
100	4.62	4.62	5.54	5.54
120	4.62	3.85	5.54	4.62
140	4.62	3.30	5.54	3.96
160	4.62	2.89	5.54	3.46
180	4.62	2.57	5.54	3.08
200	4.62	2.31	5.54	2.77

e = 2000 Pa

Δe (Pa)	D = 1.0 K δe_{rms} (Pa)	D = 1.0 K $\delta e_{rms}/\Delta e$ (%)	D = 2.0 K δe_{rms} (Pa)	D = 2.0 K $\delta e_{rms}/\Delta e$ (%)
0	4.16	-	4.27	-
20	4.16	20.80	4.27	21.35
40	4.16	10.40	4.27	10.68
60	4.16	6.93	4.27	7.12
80	4.16	5.20	4.27	5.34
100	4.16	4.16	4.27	4.27
120	4.16	3.47	4.27	3.56
140	4.16	2.97	4.27	3.05
160	4.16	2.60	4.27	2.67
180	4.16	2.31	4.27	2.37
200	4.16	2.08	4.27	2.14

Δe (Pa)	D = 5.0 K δe_{rms} (Pa)	D = 5.0 K $\delta e_{rms}/\Delta e$ (%)	D = 10.0 K δe_{rms} (Pa)	D = 10.0 K $\delta e_{rms}/\Delta e$ (%)
0	4.62	-	5.22	-
20	4.62	23.10	5.22	26.10
40	4.62	11.55	5.22	13.05
60	4.62	7.70	5.22	8.70
80	4.62	5.78	5.22	6.53
100	4.62	4.62	5.22	5.22
120	4.62	3.85	5.22	4.35
140	4.62	3.30	5.22	3.73
160	4.62	2.89	5.22	3.26
180	4.62	2.57	5.22	2.90
200	4.62	2.31	5.22	2.61

E. Net Radiation Flux Density

The reduction equation for net radiation flux density is

$$Q^* = cm \quad . \tag{A2.11}$$

Hence:

$$\delta Q^*_{rms} = \left[(c\delta m)^2 + (m\delta c)^2\right]^{\frac{1}{2}} \quad . \tag{A2.12}$$

Therefore δQ^*_{rms} depends upon the resolution in the reading of the sensor output (±0.29 mV) and the calibration error of the sensor. The latter was set at ±5%, a liberal estimate for this type of sensor (Latimer (1972), Sinclair et al. (1975); Fuchs and Tanner (1970)). Table A2.5 indicates a relative error of approximately ±5%, with greater error for $Q^* < 200\ Wm^{-2}$.

F. Soil Heat Flux Density

In this experiment, an error of ±5% was assigned to Q_G. This estimate agrees well with that presented by other workers (Fuchs and Tanner (1970); Sinclair et al. (1975)).

G. Latent Heat Flux Density

Latent heat flux density was evaluated using the Bowen ratio approach:

$$\lambda Q_E = \frac{Q^*-Q_G}{1+\beta} = \frac{Q^*-Q_G}{1+\gamma \frac{\Delta\theta}{\Delta e}} \quad . \tag{A2.13}$$

TABLE A2.5. Errors in Net Radiation Flux Density

Q^* (Wm^{-2})	δQ^*_{rms} (Wm^{-2})	$\delta Q^*_{rms}/Q^*$ (%)
0	6.33	-
50	6.80	13.60
100	8.06	8.06
200	11.84	5.92
300	16.28	5.43
400	20.98	5.25
500	25.78	5.16
600	30.66	5.11
700	35.57	5.08

Hence

$$\delta\lambda Q_{E_{rms}} = \left[\left(\frac{\partial \lambda Q_E}{\partial Q^*} \delta Q^* \right)^2 + \left(\frac{\partial \lambda Q_E}{\partial Q_G} \delta Q_G \right)^2 + \left(\frac{\partial \lambda Q_E}{\partial \Delta\theta} \delta \Delta\theta \right)^2 + \left(\frac{\partial \lambda Q_E}{\partial \Delta e} \delta \Delta e \right)^2 \right]^{\frac{1}{2}} \quad \text{(A2.14)}$$

in which:

$$\frac{\partial \lambda Q_E}{\partial Q^*} = \left(1 + \gamma \frac{\Delta\theta}{\Delta e}\right)^{-1} , \quad \text{(A2.15)}$$

$$\frac{\partial \lambda Q_E}{\partial Q_G} = -\left(1 + \gamma \frac{\Delta\theta}{\Delta e}\right)^{-1} , \quad \text{(A2.16)}$$

$$\frac{\partial \lambda Q_E}{\partial \Delta\theta} = - \frac{Q^* - Q_G}{\left(1 + \gamma \frac{\Delta\theta}{\Delta e}\right)^2} \cdot \frac{\gamma}{\Delta e} \quad \text{(A2.17)}$$

and

$$\frac{\partial \lambda Q_E}{\partial \Delta e} = \frac{Q^* - Q_G}{\left(1 + \gamma \frac{\Delta\theta}{\Delta e}\right)^2} \cdot \gamma \frac{\Delta\theta}{\Delta e^2} . \quad \text{(A2.18)}$$

A sample tabulation of $\lambda Q_{E_{rms}}$ is presented in Table 3.2. When humidity differences are large ($\Delta e > 25$ Pa), λQ_E is estimated with relative errors between ±5% and ±12%. At smaller Δe values, the errors in λQ_E become very large.

The results of the error analysis presented herein for λQ_E find approximate agreement with the findings of Fritschen (1965), McCaughey and Davies (1975) and Sinclair et al. (1975).

APPENDIX THREE

SOLUTIONS FOR $r_{ST}(P)$ ERROR ANALYSIS EQUATIONS

Leaf adaxial and abaxial conductances, $1/r_{AD}$ and $1/r_{AB}$ respectively, visualized as parallel conductors of water vapour, can be weighted by leaf area index LAI to estimate bulk stomatal resistance $r_{ST}(P)$:

$$\frac{1}{r_{ST}(P)} = \frac{LAI}{r_{AD}} + \frac{LAI}{r_{AB}} \quad . \tag{A3.1}$$

Hence:

$$r_{ST}(P) = \left\{ LAI \left[\frac{1}{r_{AD}} + \frac{1}{r_{AB}} \right] \right\}^{-1} \quad . \tag{A3.2}$$

The sensitivity of $r_{ST}(P)$ to LAI error is

$$\frac{\partial r_{ST}(P)}{\partial LAI} = \frac{\partial}{\partial LAI} \left\{ LAI \left[\frac{1}{r_{AD}} + \frac{1}{r_{AB}} \right] \right\}^{-1} \tag{A3.3}$$

and after differentiation, $\partial r_{ST}(P)$ is

$$\partial r_{ST}(P) = - r_{ST}(P) \ \frac{\partial LAI}{LAI} \quad . \tag{A3.4}$$

Hence, the relative error in $r_{ST}(P)$ is

$$\frac{\partial r_{ST}(P)}{r_{ST}(P)} = - \frac{\partial LAI}{LAI} \quad . \tag{A3.5}$$

The sensitivity of $r_{ST}(P)$ to leaf conductance error is

$$\frac{\partial r_{ST}(P)}{\partial \left[\frac{1}{r_{AD}} + \frac{1}{r_{AB}}\right]} = \frac{\partial}{\partial \left[\frac{1}{r_{AD}} + \frac{1}{r_{AB}}\right]} \left\{ LAI \left[\frac{1}{r_{AD}} + \frac{1}{r_{AB}}\right] \right\}^{-1} \tag{A3.6}$$

and after differentiation, $\partial r_{ST}(P)$ is

$$\partial r_{ST}(P) = - r_{ST}(P) \frac{\partial \left[\frac{1}{r_{AD}} + \frac{1}{r_{AB}}\right]}{\left[\frac{1}{r_{AD}} + \frac{1}{r_{AB}}\right]} \quad . \tag{A3.7}$$

Hence, the relative error in $r_{ST}(P)$ is

$$\frac{\partial r_{ST}(P)}{r_{ST}(P)} = - \frac{\partial \left[\frac{1}{r_{AD}} + \frac{1}{r_{AB}}\right]}{\left[\frac{1}{r_{AD}} + \frac{1}{r_{AB}}\right]} . \tag{A3.8}$$

The relative error in r_{ST} arising from both LAI and leaf conductance error is obtained by summing equations A3.5 and A3.8:

$$\frac{\delta r_{ST}(P)}{r_{ST}(P)} = - \left\{ \frac{\partial LAI}{LAI} + \frac{\partial \left[\frac{1}{r_{AD}} + \frac{1}{r_{AB}}\right]}{\left[\frac{1}{r_{AD}} + \frac{1}{r_{AB}}\right]} \right\} \quad . \tag{A3.9}$$

APPENDIX FOUR

SOLUTIONS FOR r_{ST}(CM) AND r_{ST}(OLA) ERROR ANALYSIS EQUATIONS

A. r_{ST}(OLA) Error Analysis Equations

r_{ST}(OLA) was evaluated from

$$r_{ST}(OLA) = \frac{\rho Cp}{\gamma} \frac{\left[e_s\left[\theta(L)\right] - e(z)\right]}{\lambda Q_E} - r_{aVH} \qquad (A4.1)$$

As such

$$\delta r_{ST}(OLA)_{rms} = \left\{ \left(\frac{\partial r_{ST}(OLA)}{\partial \left[e_s\left[\theta(L)\right] - e(z)\right]} \delta\left[e_s\left[\theta(L)\right] - e(z)\right] \right)^2 + \left(\frac{\partial r_{ST}(OLA)}{\partial r_{aVH}} \delta r_{aVH} \right)^2 + \left(\frac{\partial r_{ST}(OLA)}{\partial \lambda Q_E} \delta \lambda Q_E \right)^2 \right\}^{\frac{1}{2}} \qquad (A4.2)$$

in which

$$\frac{\partial r_{ST}(OLA)}{\partial \left[e_s\left[\theta(L)\right] - e(z)\right]} = \frac{\rho Cp}{\gamma \lambda Q_E} , \qquad (A4.3)$$

$$\frac{\partial r_{ST}(OLA)}{\partial r_{aVH}} = -1 \qquad (A4.4)$$

and

$$\frac{\partial r_{ST}(OLA)}{\partial \lambda Q_E} = -\frac{\rho Cp}{\gamma} \frac{\left[e_s\left[\theta(L)\right] - e(z)\right]}{\lambda Q_E^2} . \qquad (A4.5)$$

B. r_{ST}(CM) Error Analysis Equations

r_{ST}(CM) was evaluated from

$$r_{ST}(CM) = \frac{r_{aVH}\left[S(Q^*-Q_G-\lambda Q_E) - \gamma\lambda Q_E\right] + \rho Cp\left[e_s\left[\theta(z)\right] - e(z)\right]}{\gamma\lambda Q_E}. \quad (A4.6)$$

As such

$$\delta r_{ST}(CM)_{rms} = \left\{\left(\frac{\partial r_{ST}(CM)}{\partial r_{aVH}}\,\delta r_{aVH}\right)^2 + \left(\frac{\partial r_{ST}(CM)}{\partial Q^*}\,\delta Q^*\right)^2 + \left(\frac{\partial r_{ST}(CM)}{\partial Q_G}\,\delta Q_G\right)^2 + \left(\frac{\partial r_{ST}(CM)}{\partial \lambda Q_E}\,\delta \lambda Q_E\right)^2 + \left(\frac{\partial r_{ST}(CM)}{\partial S}\,\delta S\right)^2 + \left(\frac{\partial r_{ST}(CM)}{\partial\left[e_s\left[\theta(z)\right] - e(z)\right]}\,\delta\left[e_s\left[\theta(z)\right] - e(z)\right]\right)^2\right\}^{\frac{1}{2}} \quad (A4.7)$$

in which

$$\frac{\partial r_{ST}(CM)}{\partial r_{aVH}} = \frac{S(Q^*-Q_G-\lambda Q_E) - \gamma\lambda Q_E}{\gamma\lambda Q_E}, \quad (A4.8)$$

$$\frac{\partial r_{ST}(CM)}{\partial Q^*} = \frac{S\, r_{aVH}}{\gamma\lambda Q_E}, \quad (A4.9)$$

$$\frac{\partial r_{ST}(CM)}{\partial Q_G} = -\frac{S\, r_{aVH}}{\gamma\lambda Q_E}, \quad (A4.10)$$

$$\frac{\partial r_{ST}(CM)}{\partial S} = \frac{r_{aVH}}{\gamma\lambda Q_E}\,(Q^*-Q_G-\lambda Q_E), \quad (A4.11)$$

$$\frac{\partial r_{ST}(CM)}{\partial\left[e_s\left[\theta(z)\right] - e(z)\right]} = \frac{\rho Cp}{\gamma \lambda Q_E} \qquad (A4.12)$$

and

$$\frac{\partial r_{ST}(CM)}{\partial \lambda Q_E} = \frac{r_{aVH}\, S(Q_G - Q^*) - \rho Cp\left[e_s\left[\theta(z)\right] - e(z)\right]}{\gamma\, \lambda Q_E^{\,2}} . \qquad (A4.13)$$

C. Evaluation of δQ^*, δQ_G, $\delta \lambda Q_E$, δS, $\delta\left[e_s\left[\theta(L)\right] - e(z)\right]$, $\delta\left[e_s\left[\theta(z)\right] - e(z)\right]$, δr_{aVH} –

1. δQ^*

δQ^* can be evaluated from equation A2.12

$$\delta Q^*_{rms} = \left[(c\ \delta m)^2 + (m\ \delta c)^2\right]^{\frac{1}{2}} \qquad (A4.14)$$

in which c = 21.82 Wm^{-2}/mV, δc = 1.091 Wm^{-2}/mV and δm = 0.29 mV.

2. δQ_G –

In this experiment, a relative error of ±5% was assigned to Q_G. Hence:

$$\delta Q_G = Q_G \frac{\delta Q_G}{Q_G} = 0.05\ Q_G \qquad (A4.15)$$

3. $\delta \lambda Q_E$ –

$\delta \lambda Q_E$ can be evaluated from equation A2.14

$$\delta \lambda Q_{E_{rms}} = \left\{\left(\frac{\partial \lambda Q_E}{\partial Q^*}\,\delta Q^*\right)^2 + \left(\frac{\partial \lambda Q_E}{\partial Q_G}\,\delta Q_G\right)^2 + \left(\frac{\partial \lambda Q_E}{\partial \Delta\theta}\,\delta \Delta\theta\right)^2 + \left(\frac{\partial \lambda Q_E}{\partial \Delta e}\,\delta \Delta e\right)^2\right\}^{\frac{1}{2}} . \qquad (A4.16)$$

in which δQ^* and δQ_G are calculated from equations A4.14 and A4.15 and $\delta\Delta\theta$ and $\delta\Delta e$ can be assessed from equations A2.6 ($\delta\Delta\theta_{rms}$) and A2.10 ($\delta\Delta e_{rms}$).

4. $\underline{\delta S}$

S is given by

$$S = \frac{a' B' \phi'}{(\theta(z)+\phi')^2} \exp\left[B'\theta(z)/(\theta(z)+\phi')\right] \qquad (A4.17)$$

As such

$$\delta S = \frac{\partial S}{\partial \theta(z)} \delta\theta(z) \qquad (A4.18)$$

in which

$$\frac{\partial S}{\partial \theta(z)} = a'B'\phi' \left\{ \frac{\exp\left[B'\theta(z)/(\theta(z)+\phi')\right] \left[B'\phi' - 2(\theta(z)+\phi')\right]}{\left[\theta(z) + \phi'\right]^4} \right\}. \qquad (A4.19)$$

In equation A4.18, $\delta\theta(z)$ can be evaluated from equation A2.4.

5. $\underline{\delta\left[e_s\left[\theta(L)\right] - e(z)\right]}$

$\left[e_s\left[\theta(L)\right] - e(z)\right]$ can be expanded to

$$\left[e_s\left[\theta(L)\right] - e(z)\right] = a' \exp\left[B'\theta(L)/(\theta(L)+\phi')\right] - \left[(a' \exp\left[B'\theta_w(z)/\right.\right.$$

$$\left.\left.\theta_w(z)+\phi')\right] - \gamma(\theta(z)-\theta_w(z))\right] . \qquad (A4.20)$$

As such

$$\delta\left[e_s\left[\theta(L)\right] - e(z)\right]_{rms} = \left\{\left(\frac{\partial\left[e_s\left[\theta(L)\right] - e(z)\right]}{\partial\theta(z)}\ \delta\theta(z)\right)^2 + \left(\frac{\partial\left[e_s\left[\theta(L)\right] - e(z)\right]}{\partial\theta(L)}\ \delta\theta(L)\right)^2 + \left(\frac{\partial\left[e_s\left[\theta(L)\right] - e(z)\right]}{\partial\theta_w(z)}\ \delta\theta_w(z)\right)^2\right\}^{\frac{1}{2}} \quad (A4.21)$$

in which:

$$\frac{\partial\left[e_s\left[\theta(L)\right] - e(z)\right]}{\partial\theta(z)} = \gamma \quad (A4.22)$$

$$\frac{\partial\left[e_s\left[\theta(L)\right] - e(z)\right]}{\partial\theta_w(z)} = \frac{-a'B'\phi'}{(\theta_w(z)+\phi)^2}\ \exp\left[B'\theta_w(z)/(\theta_w(z)+\phi')\right] - \gamma \quad (A4.23)$$

and

$$\frac{\partial\left[e_s\left[\theta(L)\right] - e(z)\right]}{\partial\theta(L)} = \frac{a'B'\phi'}{(\theta(L)+\phi')^2}\ \exp\left[B'\theta(L)/(\theta(L)+\phi')\right] \quad (A4.24)$$

In equation A4.21, $\delta\theta(z)$ and $\delta\theta_w(z)$ can be evaluated from equation A2.4. $\delta\theta(L)$ also can be evaluated from equation A2.4 with c = 2.71025 K mV^{-1}, $\delta c = \pm 0.00792$ K and $\delta m = 0.003$ mV.

6. $\delta\left[e_s\left[\theta(z)\right] - e(z)\right]$ / $\left[e_s\left[\theta(z)\right] - e(z)\right]$ can be expanded to

$$\left[e_s\left[\theta(z)\right] - e(z)\right] = a' \exp\left[B'\theta(z)/(\theta(z)+\phi')\right] - \left[\left(a' \exp\left[B'\theta_w(z)/(\theta_w(z)+\phi')\right] - \gamma(\theta(z)-\theta_w(z))\right]\right. \quad (A4.25)$$

As such

$$\delta\left[e_s\left[\theta(z)\right] - e(z)\right] = \left\{\left(\frac{\partial\left[e_s\left[\theta(z)\right] - e(z)\right]}{\partial\theta(z)}\,\delta\theta(z)\right)^2 + \left(\frac{\partial\left[e_s\left[\theta(z)\right] - e(z)\right]}{\partial\theta_w(z)}\,\delta\theta_w(z)\right)^2\right\}^{\frac{1}{2}} \quad (A4.26)$$

in which:

$$\frac{\partial\left[e_s\left[\theta(z)\right] - e(z)\right]}{\partial\theta(z)} = \frac{a'B'\theta'}{(\theta(z)+\phi')^2}\exp\left[B'\theta(z)/(\theta(z)+\phi')\right] + \gamma \quad (A4.27)$$

and

$$\frac{\partial\left[e_s\left[\theta(z)\right] - e(z)\right]}{\partial\theta_w(z)} = -\frac{a'B'\theta'}{(\theta_w(z)+\phi')^2}\exp\left[B'\theta_w(z)/(\theta_w(z)+\phi')\right] - \gamma \quad (A4.28)$$

In equation A4.26, $\delta\theta(z)$ and $\delta\theta_w(z)$ can be evaluated from equation A2.4.

7. $\underline{\delta r}_{aVH}$ –

r_{aVH} is defined by

$$r_{aVH} = r_{aM} + r_b \quad (A4.29)$$

in which

$$r_{aM} = \frac{\left[\ln\left(\frac{z-d+z_o}{z_o}\right) + \Phi_M\right]^2}{u(z)\,k^2} \quad (A4.30)$$

and

$$r_b = 6.266\,u^{*-2/3} = 6.266\left\{u(z)k\left[\ln\left(\frac{z-d+z_o}{z_o}\right) + \Phi_M\right]^{-1}\right\}^{-2/3} \quad (A4.31)$$

Hence:

$$\delta r_{aVH_{rms}} = \delta r_{aM_{rms}} + \delta r_{b_{rms}} \quad (A4.32)$$

$\delta r_{aM_{rms}}$ is given by

$$\delta r_{aM_{rms}} = \left\{ \left(\frac{\partial r_{aM}}{\partial u(z)} \delta u(z) \right)^2 + \left(\frac{\partial r_{aM}}{\partial z_o} \delta z_o \right)^2 + \left(\frac{\partial r_{aM}}{\partial d} \delta d \right)^2 \right\}^{\frac{1}{2}} \quad (A4.33)$$

in which:

$$\frac{\partial r_{aM}}{\partial u(z)} = - \frac{\left[\ln\left(\frac{z-d+z_o}{z_o} \right) + \Phi_M \right]^2}{k^2 \, u(z)^2} , \quad (A4.34)$$

$$\frac{\partial r_{aM}}{\partial z_o} = - \frac{2 \left[\ln\left(\frac{z-d+z_o}{z_o} \right) \right]}{u(z) \, k^2} \frac{(z-d)}{z_o (z-d+z_o)} \quad (A4.35)$$

and

$$\frac{\partial r_{aM}}{\partial d} = - \frac{2 \left[\ln\left(\frac{z-d+z_o}{z_o} \right) \right]}{u(z) \, k^2 \, (z-d+z_o)} \quad (A4.36)$$

$\delta r_{b_{rms}}$ is given by

$$\delta r_{b_{rms}} = \left\{ \left(\frac{\partial r_b}{\partial u(z)} \delta u(z) \right)^2 + \left(\frac{\partial r_b}{\partial z_o} \delta z_o \right)^2 + \left(\frac{\partial r_b}{\partial d} \delta d \right)^2 \right\}^{\frac{1}{2}} \quad (A4.37)$$

in which:

$$\frac{\partial r_b}{\partial u(z)} = -4.179 \, k \left\{ u(z) k \left[\ln \frac{z-d+z_o}{z_o} + \Phi_M \right]^{-1} \right\}^{-1.667} \cdot \left[\ln\left(\frac{z-d+z_o}{z_o} \right) + \Phi_M \right]^{-1} , \quad (A4.38)$$

$$\frac{\partial r_b}{\partial z_o} = -4.179\ u(z)k \left\{ u(z)k \left[\ln\left(\frac{z-d+z_o}{z_o}\right) + \Phi_M \right]^{-1} \right\}^{-1.667}$$

$$\cdot \left[\ln\left(\frac{z-d+z_o}{z_o}\right) + \Phi_M \right]^{-2} \frac{(z-d)}{z_o(z-d+z_o)} \qquad \text{(A4.39)}$$

and

$$\frac{\partial r_b}{\partial d} = -4.179\ \frac{u(z)k}{(z-d+z_o)} \left\{ u(z)k \left[\ln\left(\frac{z-d+z_o}{z_o}\right) + \Phi_M \right]^{-1} \right\}^{-1.667}$$

$$\cdot \left[\ln\left(\frac{z-d+z_o}{z_o}\right) + \Phi_M \right]^{-2} \qquad \text{(A4.40)}$$

Evaluation of equations A4.33 and A4.37 requires estimates of $\delta u(z)$, δz_o and δd. As these are difficult to assess with confidence, each has been set at a fixed relative error. Based upon the distribution of z_o and d values about predicted model estimates in Figures 4.5 and 4.6, both z_o and d have been assessed relative errors of 50%. Hence:

$$\delta z_o = z_o \frac{\delta z_o}{z_o} = 0.5\ z_o \qquad \text{(A4.41)}$$

and

$$\delta d \doteq d \frac{\delta d}{d} = 0.5\ d \qquad \text{(A4.42)}$$

A relative error of 1% was assigned for u(z). Hence:

$$\delta u(z) = u(z) \frac{\delta u(z)}{u(z)} = 0.01\ u(z)\ . \qquad (A4.43)$$

APPENDIX FIVE

SENSITIVITY OF EQUATION 4.6 AND 2.20 TO r_{ST} AND r_{aVH}

A. Sensitivity of Equation 4.6 to r_{ST} and r_{aVH}

Latent heat flux density from equation 4.6 is given by

$$\lambda Q_E = \frac{\rho Cp}{\gamma} \frac{\left[e_s[\theta(L)] - e(z)\right]}{r_{ST} + r_{aVH}} \quad (A5.1)$$

The sensitivity of this equation to r_{ST} error is

$$\frac{\partial \lambda Q_E}{\partial r_{ST}} = \frac{\partial}{\partial r_{ST}} \left[\frac{\rho Cp}{\gamma} \frac{\left[e_s[\theta(L)] - e(z)\right]}{r_{ST} + r_{aVH}} \right] \quad (A5.2)$$

and after differentiation, $\partial \lambda Q_E$ is

$$\partial \lambda Q_E = -\frac{\rho Cp}{\gamma} \frac{\left[e_s[\theta(L)] - e(z)\right]}{(r_{ST} + r_{aVH})^2} \cdot r_{ST} \cdot \frac{\partial r_{ST}}{r_{ST}} \quad (A5.3)$$

The sensitivity of equation 4.6 to r_{aVH} error is

$$\frac{\partial \lambda Q_E}{\partial r_{aVH}} = \frac{\partial}{\partial r_{aVH}} \left[\frac{\rho Cp}{\gamma} \frac{\left[e_s[\theta(L)] - e(z)\right]}{r_{ST} + r_{aVH}} \right] \quad (A5.4)$$

and after differentiation, $\partial \lambda Q_E$ is

$$\partial \lambda Q_E = -\frac{\rho Cp}{\gamma} \frac{\left[e_s[\theta(L)] - e(z)\right]}{(r_{ST} + r_{aVH})^2} \cdot r_{aVH} \cdot \frac{\partial r_{aVH}}{r_{aVH}} \quad (A5.5)$$

B. Sensitivity of Equation 2.20 to r_{ST} and r_{aVH}

Latent heat flux density from equation 2.20 is given by

$$\lambda Q_E = \frac{S\,(Q^* - Q_G) + \rho Cp \left[e_s\left[\theta(z)\right] - e(z)\right] / r_{aVH}}{S + \gamma + \gamma \dfrac{r_{ST}}{r_{aVH}}} \quad . \qquad (A5.6)$$

The sensitivity of this equation to r_{ST} error is

$$\frac{\partial \lambda Q_E}{\partial r_{ST}} = \frac{\partial}{\partial r_{ST}}\left[\frac{S(Q^*-Q_G) + \rho Cp\left[e_s\left[\theta(z)\right] - e(z)\right] / r_{aVH}}{S + \gamma + \gamma \dfrac{r_{ST}}{r_{aVH}}}\right] \qquad (A5.7)$$

and after differentiation, $\partial \lambda Q_E$ is

$$\partial \lambda Q_E = - \frac{\gamma \left[S(Q^*-Q_G) + \rho Cp\left[e_s\left[\theta(z)\right] - e(z)\right] / r_{aVH}\right]}{r_{aVH}\left[S + \gamma + \gamma \dfrac{r_{ST}}{r_{aVH}}\right]^2} \cdot r_{ST} \cdot \frac{\partial r_{ST}}{r_{ST}} \qquad (A5.8)$$

The sensitivity of equation 2.20 to r_{aVH} is

$$\frac{\partial \lambda Q_E}{\partial r_{aVH}} = \frac{\partial}{\partial r_{aVH}}\left[\frac{S(Q^*-Q_G) + \rho Cp\left[e_s\left[\theta(z)\right] - e(z)\right] / r_{aVH}}{S + \gamma + \gamma \dfrac{r_{ST}}{r_{aVH}}}\right] \qquad (A5.9)$$

and after differentiation, $\partial \lambda Q_E$ is

$$\partial \lambda Q_E = \left\{ \frac{\left[S(Q^* - Q_G) + \rho Cp \left[e_s\left[\theta(z)\right] - e(z)\right] / r_{aVH}\right] \left[\gamma \dfrac{r_{ST}}{r_{aVH}^2}\right]}{\left[S + \gamma + \gamma \dfrac{r_{ST}}{r_{aVH}}\right]^2} - \frac{\left[\rho Cp \left[e_s\left[\theta(z)\right] - e(z)\right] / r_{aVH}^2\right]}{\left[S + \gamma + \gamma \dfrac{r_{ST}}{r_{aVH}}\right]} \right\} \cdot r_{aVH} \cdot \frac{\partial r_{aVH}}{r_{aVH}} \qquad (A5.10)$$

APPENDIX SIX

LEAF AND BULK STOMATAL RESISTANCE

DATA SUMMARY

MORNING OBSERVATIONS

JULIAN DAY	TIME (EST)	r_{AD} (cm^{-1})	r_{AB} (cm^{-1})	r_L (cm^{-1})	LAI	$r_{ST}(T)$ (cm^{-1})	$r_{ST}(CH)$ (cm^{-1})	$\delta r_{ST}(CH)$ (cm^{-1})	$\frac{\delta r_{ST}(CH)}{r_{ST}(CH)}$ (%)	$r_{ST}(OLA)$ (cm^{-1})	$\delta r_{ST}(OLA)$ (cm^{-1})	$\frac{\delta r_{ST}(OLA)}{r_{ST}(O.A.)}$ (%)
174	0900	480.1	445.9	232.0	.04	3739.8	M	M	M	M	M	M
175	0900	407.0	361.8	191.5	.04	4788.4	33.2	37.4	112.7	M	M	M
176	0900	372.9	367.7	224.7	.05	4494.8	10.4	35.4	340.4	M	M	M
177	0900	392.6	255.0	171.4	.05	3427.2	15.7	38.6	245.9	M	M	M
178	0900	307.6	171.5	110.1	.06	1835.3	61.5	44.3	72.0	M	M	M
179	0900	349.2	210.6	131.4	.06	2189.5	75.8	69.0	81.8	M	M	M
182	0900	245.6	201.7	110.7	.10	1107.7	3.2	25.6	800.0	M	M	M
183	0900	963.9	200.1	113.8	.12	948.2	48.1	23.6	49.1	M	M	M
184	0900	126.7	112.6	99.6	.16	372.6	25.0	28.8	115.2	M	M	M
185	0900	139.4	98.5	57.7	.20	288.6	75.2	32.9	43.8	M	M	M
186	0900	167.9	132.7	76.1	.26	885.1	43.6	18.1	41.5	M	M	M
187	0900	276.1	137.9	92.0	.33	776.7	96.9	59.3	61.2	M	M	M
188	0900	217.2	129.4	81.1	.40	702.7	132.0	52.4	39.7	151.1	33.1	20.6
189	0900	276.9	143.7	94.6	.50	589.2	137.1	65.5	33.2	145.5	26.2	18.0
190	0900	138.8	105.9	66.0	.61	98.2	81.2	41.4	47.5	108.5	21.7	19.8
191	0900	54.8	42.9	24.0	.72	33.3	246.0	89.9	36.5	253.1	53.1	22.6
192	0900	183.3	85.9	58.5	.83	70.4	136.6	32.4	23.7	145.0	23.3	16.1
193	0900	166.6	84.6	56.1	.95	59.1	86.7	38.2	44.1	122.1	27.9	22.9
194	0900	148.4	122.7	67.2	1.00	67.2	124.5	33.3	26.7	150.4	22.2	14.8
195	0900	183.9	99.9	58.0	1.18	32.2	58.3	24.7	49.1	77.1	14.3	18.5
197	0900	235.1	145.5	82.7	1.34	69.1	43.1	22.9	53.1	75.1	19.1	25.4
198	1000	235.1	124.0	81.2	1.42	57.2	50.6	23.5	46.4	70.1	16.0	22.8
199	0900	128.9	66.5	43.9	1.51	39.1	M	M	M	M	M	M
200	1000	134.7	108.1	59.4	1.60	37.1	M	M	M	M	M	M
201	1000	367.5	361.3	111.1	1.67	66.5	M	M	M	M	M	M
202	0900	243.6	123.0	81.7	1.75	46.7	M	M	M	M	M	M
203	0900	275.3	148.6	95.7	1.83	52.3	M	M	M	M	M	M
208	1000	462.6	273.4	171.8	2.15	79.9	115.1	23.3	20.2	142.8	18.2	12.7
209	1000	828.2	563.4	335.3	2.21	151.7	225.3	36.1	16.0	277.7	30.3	10.9
211	1000	569.2	299.8	178.0	2.38	76.7	36.1	14.7	40.7	69.1	12.4	20.0
214	1000	245.2	143.9	90.7	2.49	36.4	55.0	16.3	29.6	86.8	14.0	14.4
215	1000	232.7	195.7	106.3	2.53	42.0	66.2	26.7	40.3	94.5	21.0	21.8
217	1000	338.7	261.4	140.9	2.63	53.6	36.4	12.8	35.2	46.4	10.3	25.3
218	1100	1183.0	461.4	332.8	2.66	124.8	188.9	44.5	23.6	283.2	42.9	15.1
219	1000	1216.9	597.3	400.6	2.69	148.9	204.5	50.5	24.7	265.0	40.0	15.1
222	1000	937.9	640.9	298.9	2.77	107.9	M	M	M	M	M	M
223	1000	1230.3	461.4	335.6	2.81	119.4	128.6	38.6	30.0	174.1	37.2	21.4
226	1000	692.1	287.8	203.3	2.86	71.1	97.8	13.4	23.2	119.9	15.2	12.7
230	1000	2027.8	684.1	513.5	2.92	175.2	295.6	124.8	42.2	417.8	154.4	40.0
231	1000	2185.4	684.4	521.2	2.92	178.5	M	M	M	M	M	M
233	0900	2335.1	948.6	303.0	2.92	103.8	147.3	60.3	40.9	243.7	50.5	20.7
234	1000	1155.9	532.3	364.5	2.91	125.3	242.9	103.4	42.6	312.3	101.5	32.5
236	1000	2041.0	367.4	311.4	2.90	107.4	232.3	83.2	36.0	377.5	99.5	26.4
238	1000	1285.0	443.3	329.6	2.87	114.8	267.1	75.2	30.4	416.5	88.5	21.2
239	1000	2601.3	365.6	320.5	2.85	112.5	379.0	178.6	47.1	454.8	187.5	41.2
240	1000	1740.8	381.3	312.8	2.83	110.5	226.8	66.5	29.3	320.6	72.5	22.1
244	1000	1001.8	318.5	241.7	2.80	86.3	288.1	66.2	32.8	286.8	65.7	22.9
245	1000	751.7	273.9	200.8	2.76	72.7	162.7	59.7	36.7	261.2	64.9	24.8
263	1000	1011.9	318.6	242.3	2.74	88.4	M	M	M	M	M	M
265	1000	1184.0	318.1	290.7	2.66	94.3	227.6	61.1	26.8	322.6	67.3	20.9
267	1000	2644.0	243.6	223.1	2.57	86.8	M	M	M	M	M	M
269	1000	1063.4	136.8	121.3	2.47	49.1	79.7	22.2	27.9	141.2	23.1	16.4
271	1000	895.6	221.3	177.5	2.36	73.8	108.5	26.3	24.2	144.9	23.8	16.4
272	1000	165.0	65.5	46.9	2.27	20.6	63.2	24.9	39.4	106.1	23.5	22.1
273	1000	276.8	52.7	44.3	2.23	19.8	81.6	31.1	38.1	135.4	28.3	20.9
274	1000	1134.9	52.7	50.4	2.15	23.4	91.0	64.7	71.1	167.8	73.5	43.8
276	1000	660.0	116.1	99.7	2.03	48.7	170.9	71.1	41.6	295.5	69.9	24.0
277	1000	919.8	304.3	228.6	1.95	117.2	114.8	24.4	21.3	172.7	27.2	15.7
278	1000	1384.8	277.7	231.3	1.88	123.0	135.0	39.3	25.8	164.4	35.2	21.4
279	1000	1246.4	291.1	236.8	1.80	131.1	102.9	15.6	13.2	144.1	16.6	11.5
280	1000	1153.5	437.1	317.0	1.72	184.3	105.5	35.0	33.2	146.1	36.6	25.1
282	1000	958.7	392.2	338.1	1.57	215.3	105.8	25.1	23.7	153.1	25.8	16.6

M denotes missing data

MIDDAY OBSERVATIONS

JULIAN DAY	TIME (EST)	r_{AB} (cm^{-1})	r_{AB} (cm^{-1})	r_L (cm^{-1})	LAI	$r_{ST}(P)$ (cm^{-1})	$r_{ST}(CN)$ (cm^{-1})	$\delta r_{ST}(CN)$ (cm^{-1})	$\frac{\delta r_{ST}(CN)}{r_{ST}(CN)}$ (%)	$r_{ST}(OLA)$ (cm^{-1})	$\delta r_{ST}(OLA)$ (cm^{-1})	$\frac{\delta r_{ST}(OLA)}{r_{ST}(OLA)}$ (%)
174	1400	537.2	253.1	171.6	.04	4290.2	M	M	M	M	M	M
176	1300	661.8	319.6	215.9	.05	4310.5	125.3	44.4	35.4	M	M	M
177	1300	584.7	372.9	227.7	.05	4553.8	141.4	49.5	35.0	M	M	M
178	1200	547.6	219.2	139.8	.06	2329.4	140.7	104.5	30.7	M	M	M
179	1300	319.7	175.8	113.4	.06	1800.6	479.7	143.2	29.9	M	M	M
181	1300	256.8	212.6	116.3	.08	1453.5	4.2	19.3	459.5	M	M	M
182	1300	220.6	152.6	90.2	.10	901.8	20.4	26.2	128.4	M	M	M
183	1300	110.5	106.2	54.2	.12	451.3	24.6	21.2	86.2	M	M	M
184	1400	149.1	108.9	63.0	.16	393.6	188.5	69.3	36.8	M	M	M
185	1300	236.5	164.7	96.0	.20	480.3	329.7	131.0	39.7	M	M	M
186	1300	283.8	183.4	101.2	.26	389.2	201.9	47.4	23.5	M	M	M
187	1300	304.8	171.3	112.2	.33	338.8	219.7	49.9	22.7	M	M	M
188	1300	232.9	180.5	101.7	.40	254.2	257.1	53.4	20.8	240.6	32.9	13.7
189	1300	228.6	169.2	106.4	.50	212.9	321.1	80.7	25.1	244.5	39.1	16.0
192	1200	188.0	77.5	54.9	.83	66.1	192.0	39.4	20.5	181.9	24.4	13.4
193	1300	239.3	132.3	83.9	.95	88.3	192.1	42.7	22.2	189.4	26.0	13.7
194	1300	265.5	149.9	97.9	1.00	98.9	159.4	35.4	22.2	165.8	19.3	11.2
195	1300	145.4	104.8	60.9	1.18	51.6	182.6	45.1	24.0	94.2	23.4	24.8
197	1300	185.0	121.0	73.2	1.34	54.6	93.4	21.5	40.3	56.5	15.0	26.5
198	1300	153.7	98.9	60.2	1.42	42.4	70.3	25.1	35.7	74.9	15.8	21.1
199	1300	172.0	92.4	60.1	1.51	39.8	M	M	M	M	M	M
200	1300	167.1	114.3	64.3	1.60	46.2	M	M	M	M	M	M
201	1300	205.7	143.7	95.6	1.67	57.3	M	M	M	M	M	M
202	1300	213.3	222.5	144.6	1.75	82.6	M	M	M	M	M	M
203	1300	403.5	233.2	157.3	1.83	86.0	M	M	M	M	M	M
206	1300	297.2	141.5	95.9	2.02	47.5	136.3	35.5	26.0	178.3	26.4	14.8
208	1400	691.0	472.0	288.4	2.15	130.4	343.1	86.9	25.3	356.4	66.6	18.7
209	1300	1192.5	693.4	438.5	2.21	198.4	443.3	93.6	21.0	501.8	75.0	14.9
211	1300	540.2	182.5	126.4	2.32	58.8	40.4	11.3	28.0	55.8	15.9	28.9
213	1300	316.7	191.1	119.3	2.42	49.3	39.1	13.9	35.5	60.9	11.2	18.4
214	1300	268.6	179.2	107.3	2.49	43.2	88.2	17.7	20.1	110.7	13.5	12.2
215	1300	295.0	161.9	90.5	2.53	35.8	M	M	M	M	M	M
217	1200	446.5	311.5	183.6	2.63	69.8	81.1	18.8	23.2	107.3	16.7	15.6
218	1200	1277.5	603.7	410.0	2.66	154.1	233.3	52.4	22.5	318.6	52.9	15.2
219	1300	1057.9	921.3	492.4	2.69	183.1	360.7	97.3	27.0	462.0	90.7	19.6
221	1300	573.7	235.2	167.0	2.75	60.7	M	M	M	M	M	M
222	1300	863.7	454.8	269.9	2.77	97.4	223.5	52.5	23.5	313.8	49.1	15.6
223	1300	876.0	399.7	255.0	2.81	90.8	238.1	111.8	47.0	316.0	119.4	37.8
226	1300	980.7	359.8	261.8	2.86	91.5	83.1	18.5	22.3	146.1	19.0	13.0
227	1200	368.9	234.3	140.2	2.87	48.8	214.8	63.0	29.3	375.1	65.5	17.5
230	1200	2305.2	536.8	435.4	2.92	149.1	240.1	123.0	51.2	392.4	154.4	39.3
231	1300	2055.4	1170.0	745.6	2.92	255.3	M	M	M	M	M	M
232	1300	1897.1	574.7	598.7	2.93	204.3	M	M	M	M	M	M
233	1200	1446.9	637.4	442.5	2.92	151.5	M	M	M	M	M	M
234	1300	1730.6	808.5	551.1	2.91	189.4	M	M	M	M	M	M
235	1300	1995.1	642.0	457.8	2.91	157.3	M	M	M	M	M	M
236	1300	3044.3	691.7	563.6	2.90	194.4	568.1	460.0	78.2	763.1	547.1	71.7
237	1300	2837.1	649.1	492.2	2.89	170.3	510.6	76.7	54.2	658.8	294.4	44.7
238	1300	2429.1	690.8	537.4	2.87	187.2	379.8	222.8	58.7	522.4	255.6	48.9
239	1300	2692.6	757.1	588.7	2.85	205.8	M	M	M	M	M	M
240	1300	2917.8	582.4	485.5	2.83	171.6	277.5	68.2	24.6	410.7	77.9	19.0
241	1300	2213.5	608.5	384.9	2.80	123.2	233.5	73.7	33.0	303.0	73.7	23.7
242	1300	2438.8	989.1	674.5	2.76	171.9	792.0	716.1	99.2	857.9	760.6	86.3
249	1300	1013.4	157.5	136.3	2.47	55.2	129.4	33.6	26.0	189.9	34.7	18.3
250	1300	1394.9	224.7	192.1	2.40	80.0	169.0	47.8	28.3	257.1	52.3	20.3
252	1300	1284.7	237.6	200.5	2.27	88.3	198.4	76.9	38.8	247.7	76.2	30.8
253	1300	1518.9	316.3	263.2	2.23	118.0	294.6	139.6	47.4	361.8	138.3	38.3
254	1300	947.1	126.3	103.9	2.15	48.3	101.7	53.8	52.9	159.7	55.6	34.8
257	1300	1752.3	311.1	264.3	1.95	139.5	M	M	M	M	M	M
258	1300	1227.3	765.3	471.7	1.88	262.1	320.5	69.1	21.6	438.4	75.2	17.2
260	1300	909.5	491.3	319.0	1.72	185.5	336.5	187.8	55.8	443.6	217.9	49.1
261	1300	1329.5	681.3	449.7	1.65	272.5	111.8	23.1	20.7	205.9	28.0	13.6
262	1300	1233.5	821.8	493.9	1.57	314.6	361.5	208.0	57.5	470.4	239.9	51.0

M denotes missing data

AFTERNOON OBSERVATIONS

JULIAN DAY	TIME (EST)	r_{AD} (cm^{-1})	r_{AB} (cm^{-1})	r_L (cm^{-1})	LAI	$r_{ST}(P)$ (cm^{-1})	$r_{ST}(CN)$ (cm^{-1})	$\delta r_{ST}(CN)$ (cm^{-1})	$\frac{\delta r_{ST}(CN)}{r_{ST}(CN)}$ (%)	$r_{ST}(OLA)$ (cm^{-1})	$\delta r_{ST}(OLA)$ (cm^{-1})	$\frac{\delta r_{ST}(OLA)}{r_{ST}(OLA)}$ (%)
178	1900	674.8	251.7	183.3	06	3054.9	231 *	101 0	43 6	M	M	M
179	1900	1059.4	295.6	231.1	.06	3852.1	349.1	160.7	46.0	M	M	M
180	1900	366.1	225.7	138.6	.08	1994 6	-29.6	46.7	157.8	M	M	M
181	1900	238.2	131.2	85.0	08	1062.9	M	M	M	M	M	M
182	1900	484.0	247 6	164.0	.10	1640.4	42 3	52 6	124 3	M	M	M
183	1900	229 5	117.4	77.7	.12	647.2	53.7	67.4	125.5	M	M	M
184	1900	241.5	159 4	96.0	.16	600.1	119.5	276 1	231.0	M	M	M
185	1800	721.7	294.5	209.2	.20	1045.9	349.5	210.9	60.3	M	M	M
186	1800	358.5	188 4	123.5	.26	475.0	303.8	69.3	22.8	M	M	M
187	1900	638.3	275.1	192.2	.33	582.5	422.6	85.6	20.3	M	M	M
188	1900	802.9	311.8	224.6	.40	561 4	436.3	94 3	21.6	339.9	31 8	15 2
189	1800	452.2	257.1	163 9	.50	327.8	422.1	94.5	22.4	362.9	67 2	18 5
190	1800	224.9	130.3	84 9	.61	139.1	193.5	153.4	79 3	218.3	101 0	46 3
191	1800	307.3	159.6	105.0	.72	145.9	363.9	57.6	15.8	335.5	41.5	12 4
192	1800	297.4	126.4	87.7	.83	105.7	223.4	45.4	20.3	219.6	32.2	14.7
193	1800	246.5	155.6	95.4	.95	100.4	240 4	43.6	18.1	224.4	30.4	13 5
194	1800	936.6	311 9	234.0	1.00	234.0	243.3	46.9	19 3	240.4	31.6	13.1
197	1800	746.8	237.5	179.6	1.34	134.0	195.8	60.7	31.1	193 5	40.3	20 8
199	1800	973.5	438.5	302.3	1.54	200.2	M	M	M	M	M	M
200	1800	768.6	463.5	290.0	1.60	181.2	M	M	M	M	M	M
201	1800	1141.9	412.6	303.1	1.67	181.5	M	M	M	M	M	M
202	1800	2025.0	613.0	383.6	1.75	219.2	M	M	M	M	M	M
203	1900	1736.6	783.2	539.8	1.83	295.0	M	M	M	M	M	M
205	1900	1599.2	558.0	413.7	1.95	212.1	151.0	158.1	104.7	201.2	95.9	47.7
206	1900	2082.8	571.2	448.3	2.02	221.9	187.0	209.7	122.8	347 7	202.9	58.1
207	1800	1483.0	449.1	344.7	2.09	164.9	M	M	M	M	M	M
208	1800	1489.5	1098.8	665.8	2.15	309.7	M	M	M	M	M	M
209	1800	2926.8	995.4	742.9	2.21	336.2	393.1	85.2	21.7	454 1	76.2	16 8
210	1900	3502.3	941.9	869.3	2.27	806.7	42.3	34.8	82.3	73.8	20.9	28.2
211	1800	5707.3	841.6	809.9	2.32	176.7	M	M	M	M	M	M
212	1800	2185.1	945.9	436.8	2.38	183.5	105.7	26.8	25.4	131.6	21.2	16.1
213	1800	3826.4	1246.7	941.6	2.42	389.1	141.6	57.7	40.8	170.9	47.7	27 9
214	1800	1087.7	517.1	350.5	2.49	140.8	138.1	77.2	55.9	190.5	58.6	30.8
215	1800	673.3	377.8	242.0	2.53	95.7	M	M	M	M	M	M
217	1800	742.5	725 7	367.0	2.63	139.5	163.6	37.8	23.1	197.4	31.5	16.4
218	1800	1845.0	852.3	582.7	2 66	219.1	259.6	56 0	21.6	281.2	40 5	14 4
219	1800	3151.4	1921 7	1193.8	2.69	443.8	537.6	993.9	171.9	658 8	554 2	121 0
221	1800	2639.8	806.7	617.5	2.75	224.5	219.1	299 5	136.7	211 3	258.1	122 1
222	1800	1902.2	676.8	499.2	2.77	180.2	116.1	46.1	39.7	80.5	27.8	34 5
223	1800	4264.5	810 2	680.8	2.81	242.3	M	M	M	M	M	M
224	1800	3152.5	521.2	391.5	2.83	103.0	M	M	M	M	M	M
225	1800	1650 3	479.3	371.4	2.85	130.3	M	M	M	M	M	M
226	1800	3671.0	565.5	486.3	2.86	170 0	331.2	94.3	28.5	417.4	92.9	22 3
227	1800	1760.7	906.5	586.1	2.87	207 7	342.6	76.9	22.4	411 4	70 3	17.1
228	1800	4484.3	809.4	685.6	2.88	230.1	381.4	149.3	39.1	430 2	139.6	32 0
230	1800	4146.0	766.4	646.8	2.92	221.5	544.7	231.5	42.5	587.1	223.9	37 5
232	1800	3944 0	756.8	613.6	2.93	209.4	M	M	M	M	M	M
234	1800	2215.0	615.0	481.4	2.91	165.4	M	M	M	M	M	M
236	1800	2342.3	602.5	479.2	2.90	165.3	M	M	M	M	M	M
238	1900	1690.1	679.1	481.1	2.87	167.6	M	M	M	M	M	M
239	1700	2095.8	398.4	334.8	2.85	117.5	414.4	577.1	139.3	546 1	625.3	121.2
240	1700	8824.3	1492.8	980.3	2.83	349.2	M	M	M	M	M	M
241	1800	2625.7	762.8	591.1	2.80	211.1	561.6	460.5	78 4	677.5	472.8	69 8
242	1800	3061.9	805.8	637.9	2.76	231.1	567.0	702.5	123.9	658.7	722.0	109.6
243	1800	4310.8	805.0	678.3	2.74	247.6	M	M	M	M	M	M
246	1700	2700.2	353.1	312.3	2.62	119.2	167.0	24.2	14.5	176 3	22 3	12 6
249	1700	1969.0	273.0	239.8	2.47	97.1	189.9	53.4	28.1	226.8	50 7	22.4
250	1700	1830.3	295 3	254.1	2.48	105.9	382.7	121.0	31.6	430.8	99.1	23.0
252	1800	1294.3	376.1	291.4	2.27	128 4	477.7	508 5	105.6	522.4	512.7	98 1
254	1700	1933.8	288.2	250.8	2.15	116.7	224.1	94.2	42.0	313.7	104.1	33 2
256	1700	2245.5	249.6	224.6	2.03	118.7	162.4	51.8	31 9	194.0	50.4	26.0
257	1700	1843.8	497.9	382.0	1.95	201.0	256.6	42.7	16.6	296.7	43.0	14.5
258	1700	3520.1	982.0	393.5	1.88	209.3	419.3	116.2	27.7	492.6	125.5	25 5
259	1700	8933.3	1037.4	708.4	1.80	393.5	M	M	M	M	M	M
261	1700	1448.9	537 8	382.2	1.65	237.7	189.7	51.9	26.0	327.6	60.5	18.5
262	1700	1736.5	1020.2	642.6	1.57	409.3	650.1	231.9	35.7	884.1	265 8	33 1

M denotes missing data

LEAF RESISTANCE, SOIL MOISTURE AND VAPOUR PRESSURE DEFICIT DATA FOR MORNING, MIDDAY AND AFTERNOON PERIODS WHEN LAI > 1

MORNING OBSERVATIONS				MIDDAY OBSERVATIONS				AFTERNOON OBSERVATIONS			
JULIAN DAY	r_L (sm^{-1})	MORNING X_w (cm^3H_2O/ cm^3soil)	$e_s[\theta(z)]$ - $e(z)$ (Pa)	JULIAN DAY	r_L (sm^{-1})	MORNING X_w (cm^3H_2O/ cm^3soil)	$e_s[\theta(z)]$ - $e(z)$ (Pa)	JULIAN DAY	r_L (sm^{-1})	AFTERNOON X_w (cm^3H_2O/ cm^3soil)	$e_s[\theta(z)]$ - $e(z)$ (Pa)
195	38.6	.101	1172	195	60.9	.101	1954	197	179.6	.113	649
197	92.7	106	751	197	73.2	.106	3594	199	302.3	.103	1132
198	88.2	.119	1226	198	60.2	.119	1468	200	290.0	.093	2284
199	43.9	.125	1087	199	60.1	.125	1509	201	303.1	.085	863
200	59.4	.127	910	200	64.3	.127	1368	203	539.8	.089	1157
202	81.7	.101	743	201	95.6	.104	1209	205	413.7	.063	852
203	95.7	.083	773	202	144.6	.101	1526	206	448.3	.074	785
208	171.8	.064	1149	203	197.3	.083	1736	207	344.7	.070	526
209	335.3	.065	2199	206	95.9	.077	870	208	665.8	.062	935
211	176.0	.169	685	208	280.4	.065	2363	209	742.9	.064	2746
214	90.7	.092	855	209	438.5	.065	2878	210	409.3	.152	1427
215	105.3	.074	509	211	136.4	.169	1113	212	436.8	.09	795
217	145.9	.072	567	213	119.1	.126	1151	213	941.6	.119	647
218	322.0	.067	1371	214	207.5	.092	1435	214	350.5	.074	1534
219	400.6	053	1279	215	90.5	.074	606	215	242.0	.087	1019
222	298.9	.066	955	217	183.6	.072	634	217	367.0	.071	979
223	335.6	054	850	218	410.0	.067	1596	218	582.7	.067	1358
226	203.3	.076	597	219	492.4	.053	1919	219	1193.8	.050	1479
230	511.5	.056	561	222	269.9	.066	1521	221	617.5	.066	791
231	52..	.048	1113	223	255.0	.054	1063	222	499.2	056	1248
233	303.0	.0.0	650	226	261.8	.076	981	223	680.8	.056	993
234	164.5	.044	1190	227	140.2	.063	1147	224	291.5	095	948
236	321.4	035	965	230	435.6	.056	1220	225	372.4	.077	982
238	329.6	.039	1140	231	744.6	.048	2303	226	486.3	.064	773
239	329.5	.030	1254	232	598.7	.042	2048	227	596.1	.056	1637
240	312.8	.038	1022	236	563.6	.035	1465	228	685.6	.053	1743
24.	241.7	.033	697	237	492.2	.031	1705	230	646.8	.051	1678
242	220.8	.040	665	238	517..	039	2030	232	613.6	.047	1870
243	242.3	.032	639	239	500.7	.030	1477	234	481.4	.047	1626
245	250.7	.038	785	240	485.5	.033	1499	238	481.1	.047	1328
247	223.	.102	878	241	344.9	.028	860	239	334.8	.034	914
249	221.3	.079	643	242	474.5	.040	1430	241	591.1	.030	972
251	177..	058	849	249	136.3	.079	1156	242	637.9	.038	1371
25.	40.9	.056	385	250	10. 1	.064	1205	243	675.3	035	1495
253	62..	...	...	252	100.5	.056	1130	246	713.9	032	1..
254	50.4	.050	810	253	263.2	.050	1339	249	839.3	.062	2146
256	98.7	.062	567	254	103.9	.050	479	250	234.1	.055	1206
257	228.6	.052	714	257	264.2	.052	874	252	291.4	.055	1152
258	231.3	.016	865	259	471.7	.047	1405	254	250.8	.047	690
259	2.5.0	047	647	260	319.0	043	1184	256	224.6	.051	844
260	317.0	048	613	261	449.7	.044	553	257	392.0	.042	-
262	315.1	042	612	262	493.9	042	1295	258	291.5	.045	1330
								259	708.4	049	1367
								26	394.2	.045	455
								262	642.6	.038	1774

APPENDIX SEVEN

HOURLY EVAPOTRANSPIRATION DATA SUMMARY

MORNING OBSERVATIONS

Julian Day	Time (EST)	Q^* (Wm^{-2})	G_0 (Wm^{-2})	θ (K)	θ(L)[1] (K)	e (Pa)	r_{aV} (sm^{-1})	r_{ST}(CM) (sm^{-1})	r_{ST}(OLA) (sm^{-1})	λQ_E (Wm^{-2})	$\delta\lambda Q_E$ (Wm^{-2})	$\frac{\delta\lambda Q_E}{\lambda Q_E}$ (%)	r_{ST}(P) (Wm^{-2})	λQ_E employing r_{ST}(P) in equation 20	[illegible]	[illegible]
														(---------- Wm^{-2}	----------	)
175	0900	360.	104.	16.91	M	1405.	111.1	33.2	M	196.	17.	8.7	4788.4	13.	M	4.
176	0900	356.	85.	17.16	M	1421.	110.6	10.4	M	201.	18.	9.0	4494.8	14.	M	4.
177	0900	316.	74.	17.77	M	1559	111.9	15.7	M	178.	16.	9.0	3427.2	16.	M	6.
178	0900	356.	105.	17.97	M	1431.	105.6	61.5	M	170.	16.	9.4	1835.3	30	M	12
179	0900	371.	111.	17.97	M	1550.	129.5	75.8	M	153.	18.	11.8	2189.5	27.	M	9.
182	0900	343.	80.	20.03	M	1613.	71.0	3 2	M	236.	21.	8.9	1107.7	41.	M	16.
183	0900	273.	70.	22.95	M	1685.	46.4	48.1	M	208.	31.	14.9	948.2	40.	M	28.
184	0900	271.	66.	24 20	M	2412.	49.3	25.0	M	185.	23.	*12.4	372.6	70.	M	54.
185	0900	343.	91.	25.56	M	2263.	34.9	75.2	M	198.	29.	14.6	288.6	99.	M	75.
186	0900	277.	38.	18.01	M	1715.	40.2	43.6	M	156.	16.	10.3	285.1	63.	M	41.
187	0900	316.	112.	13.66	M	1403.	116.3	96.9	M	138.	16.	11.6	278.7	98.	M	69.
188	0900	321.	115.	23.42	27.45	1665.	82.6	132.0	151.1	155.	16.	10.3	202.7	133.	121.	118
189	0900	306.	100.	25.04	27.46	1748.	63.7	137.1	145.5	165.	18.	10.9	169.2	145.	136	154.
190	0900	292.	91.	27.40	29.54	2351.	66.9	87.2	109.5	160.	17.	9.4	98.4	175.	193	234.
191	0900	103.	28.	22.85	24.26	2235.	72.7	246.0	233.1	47.	8.	17.0	33.3	82.	136.	193.
192	0900	321.	77.	17.30	21.37	1183.	44.7	136.6	145.0	133.	15.	11.3	70.4	177.	219.	176.
193	0900	277.	73.	16.93	23.88	1190.	87.2	86.7	122.1	156.	14.	9.0	59.1	169.	222.	206.
194	0900	271.	82.	23.03	25.16	12[illegible]	53.0	124.5	150.4	170.	16.	9.4	63.2	211.	297.	313.
195	0900	303.	70	26.62	28.50	2314.	48.3	50.3	77.1	225.	18.	8.0	32.2	243.	351.	387.
197	0900	343.	74.	17.44	22.38	1240.	65.8	43.1	75.1	203.	16.	7.9	69.1	183.	212.	206.
198	1000	367.	72.	21.64	22.84	1160.	55.8	50.6	70.1	257.	21.	8.2	57.2	250.	287.	256.
208	1000	378.	80.	25.48	28.93	2210.	26.5	115.1	142.8	200.	20.	10 0	79.9	238.	318.	275.
209	1000	391.	95.	26.12	31.36	1195.	36.2	225.3	277.7	194.	19.	9.3	15[illegible].7	243.	325.	278.
211	1000	410.	81.	20.62	24.70	1743.	35.3	36.1	67.1	257.	21.	8.2	7[illegible].7	203.	223.	174
214	1000	373.	69	20.64	28.12	2100.	28 8	55.0	96.9	245.	23.	9.4	36.4	277.	473.	436.
215	1000	102	28.	22.14	23.69	2138.	28 0	66.2	96.5	116.	16.	15.5	42 0	13[illegible].	206.	229.
217	1000	519.	43.	16.96	22.45	1624.	23.2	36.4	30.4	311.	30.	9.6	53.6	273.	246.	226.
218	1100	454	96.	23 19	31.36	1470.	31.7	188.9	283.2	179.	24.	13 4	124.8	296.	361.	31[illegible].
219	1100	395.	6[illegible].	24.00	30.68	1704.	39.4	204.5	265.0	161.	20.	12.4	148 9	19[illegible]	260.	2[illegible]6.
223	1100	350.	59.	24.74	27.09	1915.	18.6	128.6	174.1	157.	30.	19.1	119.4	165.	220.	212.
226	1000	391.	62.	19.46	25.80	1663.	25.4	57.6	119.9	210.	19.	9.0	71.1	191.	316.	327.
230	1000	401.	78.	20 02	32 45	1779.	35.9	295.6	417.8	123.	42.	34.1	175.2	173.	265.	237.
233	0900	227.	50.	24.39	29.78	2404.	53.0	147.3	243.7	109.	18.	16.5	103.8	124.	206.	220.
234	1000	293.	46.	24.95	29.58	1968.	24.8	242.9	3[illegible]2.3	116.	35.	30.2	125.3	178.	261.	218.
236	1000	371	57.	21.41	29 61	1534.	26.1	231.3	377.5	116.	28.	24.1	107.4	190.	350.	259.
238	1000	3[illegible].	72.	[illegible]	[illegible]	1[illegible]	29.2	247.1	416.5	117.	23.	19.7	114.8	166.	362.	3[illegible].
239	1000	164.	45.	25.33	27.45	1976.	18.2	379.0	454.8	64.	25.	39.1	112.5	157.	232.	242.
240	1000	319.	50.	19.88	26.42	1298.	27.2	226.8	328.6	111.	22.	19.8	110.5	176.	266.	277.
241	1000	192.	38.	18.94	23.46	1191.	39.7	202.1	286.8	79.	15.	19.0	86.3	123.	204.	213.
242	1000	251.	42.	19 94	25.55	1664.	31.2	162.7	261.2	101.	22.	21.8	72.7	154.	234.	269.
245	1000	190.	37.	15.81	20.56	1011.	33.7	227.6	322.6	74.	14.	18.9	94.3	126.	205.	204.
247	1000	325.	60.	18.34	24.00	1465.	31.8	79.7	141.2	162.	19.	11.7	49.1	196.	346.	363.
251	1000	265.	55.	20.02	23.34	1513.	28.5	108.5	144.9	143.	18.	12.6	75.8	171.	238.	303
252	1000	159.	40.	20.83	22.66	2075.	22.6	63.2	106.1	96.	17.	17.7	20.6	139.	286.	325.
253	1000	25[illegible].	53.	21.65	25.58	2130.	30.1	61.6	135.4	126.	20.	15.9	19.8	190.	419.	385.
254	1000	76.	19.	20.08	21.53	2139.	24.0	91.0	167.8	41.	16.	39.0	23 4	69.	166.	158.
256	1000	70.	20.	21.78	22.36	2041.	15.8	170.9	205.5	54.	17.	31.5	48.7	119.	187.	247.
257	1000	275.	38.	13.94	19.51	878.	30.7	114.8	172.7	128.	15.	11.7	117.2	126.	176.	214.
258	1000	308.	53.	18.04	21.20	1197.	12.3	125.0	164.4	139.	28.	20.1	123.0	141.	182.	186.
259	1000	327.	52.	14.31	18.77	933.	19.7	102.9	144.1	135.	13.	9.6	131.1	114.	147.	159.
260	1000	268.	56.	19.87	22.86	1706.	15.0	105.5	146.1	123.	28.	22.8	184.3	81.	99.	126.
262	1000	295.	77.	18.85	22.51	1564.	20.8	105.8	155.1	122.	17.	13.9	215.3	74.	91.	135.

M denotes missing data

1. Measured with thermocouple array
2. θ(L) measured with thermocouple array
3. θ(L) measured with porometer temperature sensor

MIDDAY OBSERVATIONS

Julian Day	Time (EST)	Q^* (Wm^{-2})	Q_g (Wm^{-2})	θ (K)	$\theta(L)^1$ (K)	e (Pa)	r_{aV} (sm^{-1})	r_{ST}(CM) (sm^{-1})	r_{ST}(OLA) (sm^{-1})	λQ_E (Wm^{-2})	$\delta\lambda Q_E$ (Wm^{-2})	$\frac{\delta\lambda Q_E}{\lambda Q_E}$ (%)	r_{ST}(P) (Wm^{-2})	λQ_E employing r_{ST}(P) in equation 2.20	6.4[2]	4.6[3]
														(Wm^{-2})		
176	1300	487.	70.	20.81	M	1512.	79.7	125.3	M	241.	24.	10.0	4310.5	20.	M	8.
[illegible]	[illegible]	535	130.	21.52	M	1460	92.0	141.[illegible]	M	243.	22.	9 1	4553 8	23.	M	10.
[illegible]	[illegible]	467.	130.	20.81	M	1440.	110.4	340.7	M	148.	19.	12.8	2329 4	39.	M	15.
179	13.0	524.	147.	23.00	M	1553	105.6	479.7	M	147.	21.	14.3	1890.6	56	M	28
181	1300	262.	-30.	20.77	M	1671.	63.3	4.2	M	236.	18.	7.6	1453.5	30.	M	17.
182	1300	618.	99.	25.04	M	1692.	73 5	20.4	M	447.	30.	6 7	901.8	115.	M	42.
183	1300	251.	25.	22 73	M	2223.	44 6	24.6	M	194.	24	12.4	451 3	58.	M	32.
184	1400	284.	78.	23 36	M	2554.	43.0	188.5	M	180.	32.	17 8	393 6	117.	M	170.
185	1300	526.	129.	29.49	M	2238.	37.4	329.7	M	170.	43.	25.3	480 3	131.	M	92.
186	1300	519.	123.	21.79	M	1473.	45.0	201 9	M	185.	21.	11 4	389 2	127.	M	70.
187	1400	512.	136.	23.50	M	1557.	49.0	249.7	M	183.	19.	10.4	339.8	141.	M	103.
188	1300	515.	115	27.16	32.13	1654.	38.6	257.1	240 6	201.	23.	11.4	254.2	202.	190.	170.
189	1300	485.	116.	30 94	34.52	1973.	53 9	521.1	244.5	207.	26	12.6	212.9	255.	232.	22[illegible]
192	1200	541.	120.	21.19	27.39	1097.	45.1	192.0	181.9	205.	20.	9.8	66.1	329.	419.	307.
193	1300	530.	165.	24.09	30.36	1189.	52.8	192.1	189.4	234.	22.	9.4	88.3	320.	401.	270.
194	1300	567.	117.	28.43	32.53	1487	50.5	159.4	145.8	310.	25.	8.1	87.6	381	440.	411.
195	1300	554.	116.	31.15	36 04	2076	78.0	106.6	94.2	346.	27.	7 8	51 6	367.	460.	504.
197	1300	598.	109	21.09	26 48	1041.	56.5	53.4	56.5	359.	28.	7.2	54 6	388.	396	460.
198	1300	387.	69	22.47	25.94	1431.	55.0	70.3	74.5	269.	21.	7 8	42.4	300.	359	443.
206	1300	530.	132.	23 22	30.31	1966.	31 4	136.3	178.3	203.	24.	11.8	47.5	317.	540.	420.
208	1400	543.	74	30.09	35.35	1501.	24.5	343 1	356.4	170.	31.	17.4	130.4	333.	435.	345
209	1400	509.	106	29 28	36 40	1169.	32.8	443.3	501.8	163.	23.	14.1	198.4	279.	377.	345.
21.	1200	529.	61	22 44	25 80	1602.	25.5	40.4	55.8	385.	29.	7.5	58 8	338	372.	364.
213	1200	491.	53.	22 76	26 27	1617	33 2	39.1	60.9	347.	25.	7.2	49 3	326.	396	466
214	1300	547.	79.	26 33	30.55	1693.	26 1	88 2	110.7	313.	26	8.3	43.2	407.	618	621.
217	1200	446.	49	19 18	22 86	1555	25 [illegible]	81 1	137.3	145	16	11 2	69 8	194.	200	146.
218	1200	539	95.	24 36	33 62	1492	25.1	233.3	348.6	182.	25.	13.7	154 1	240.	379.	284.
219	1300	541	90	26 02	34.78	1445.	27 1	360.7	462.0	151	28	18 5	183 1	242.	351.	293.
222	1300	546.	97.	24 36	32 90	1527	25 5	223 5	313.8	185.	26.	14.1	97 4	306.	511.	381
223	1300	509	58.	24.04	29 12	1927	18 7	259 1	316 0	114	41.	36.0	90 8	219.	348.	270
226	1300	468.	60.	21 55	29 28	1590	30 8	83 1	146 1	256.	23.	9 0	91 5	245.	370.	279
227	1400	332.	68	22 55	3. 23	1466	40 3	214 8	375 1	130.	20.	15 4	48 8	250	605.	5[illegible]
230	1400	493.	75	24 93	33 57	1934	2. 0	240.1	392 4	146	54.	37 0	149.1	204	355.	305
230	1300	474.	60	23 07	31.04	1796.	22.0	548.1	763 1	73.	51.	69 9	19[illegible] 4	175	265.	236.
232	1300	[illegible]	57	20 04	29 2	1867	37 6	500 6	668 8	73	21	42 5	170 3	152	243	221.
233	1300	440	63.	27 92	34 95	1731.	21.0	379 8	522 4	127	60.	47 2	187 2	215	332	290.
240	1400	358.	67	21.[illegible]	28 68	2061	27 1	817 5	410 7	121.	21.	17 4	17[illegible] 6	170	268.	246
241	1300	381.	20	19 93	24 39	1467	39.4	223 5	303 3	85.	17	20.0	127 2	119.	179.	157.
242	1400	389	62	23 80	31 61	1518.	34.9	722 0	857.9	63	53.	84 1	47. 9	180.	274	194
249	1400	[illegible]	75	20 70	27 43	1704	20.9	129 4	189 9	204.	33.	16.2	55 2	327.	565	553
250	1200	509	86	21 57	29 63	1764	22.1	169 0	257 1	182	34	18 7	80 0	286	495	489.
252	1400	558	68	24 06	28 [illegible]	1664	20.2	198 4	247.7	136.	39.	28 7	88 3	223.	337.	372.
253	1400	407	79	25 [illegible]	30.79	1881.	22.1	294.6	361 0	120	43	35.8	118 0	223	329	313
254	1200	194	36	21.[illegible]	24.42	2128.	20.1	102 7	159 7	94	29	30 9	48 3	141.	248	252
259	1300	-71	80.	18 42	26 56	713	21.1	320.5	438 4	111.	18.	16.2	260 1	131	180	182
260	1300	389.	71	2. 84	27.34	1433.	16.5	330 5	443 6	87	41	47.1	185 5	142.	199	183
261	1300	340	-6	13 20	20 91	964	30.3	121 8	205.9	120.	13	10 8	272.5	64	94.	101.
262	1200	424.	68	22.23	28 31	1482.	16.1	361.5	470.4	88.	43.	48.9	314.6	98.	129	126.

M denotes missing data

1 Measured with thermocouple array
2 $\theta(L)$ measured with thermocouple array
3 $\theta(L)$ measured with porometer temperature sensor

AFTERNOON OBSERVATIONS

Julian Day	Time (PST)	Q* (Wm^{-2})	Q_G (Wm^{-2})	θ (F)	θ(L)[1] (K)	e (Pa)	r_{aH} (sm^{-1})	r_{ST}(CP) (sm^{-1})	r_{ST}(OLK) (sm^{-1})	λQ_E (Wm^{-2})	$\delta\lambda Q_E$ (Wm^{-2})	$\delta\lambda Q_E / \lambda Q_E$ (%)	r_{ST}(P) (Wm^{-2})	λQ_E equation 2.10 (Wm^{-2})	4.23 (Wm^{-2})	4.6 (Wm^{-2})
175	1900	44.	-72.	20.34	M	1421.	112.7	231.8	M	78.	13.	16.1	3054.9	14.	M	7.
176	1900	[illegible]	-63.	19.45	M	[illegible]	131.9	349.1	M	38.	8.	21.1	[illegible]	7.	M	4
[illegible]	1900	65.	[illegible]	20.39	M	[illegible]	143.0	-29.6	M	117.	10.	8.5	1994.6	20.	M	12.
182	1900	67.	-4.	23.85	M	1409.	89.2	42.3	M	160.	20.	12.5	1643.4	30.	M	[illegible]
183	1900	65.	-3.	22.41	M	2123.	93.4	53.7	M	68.	11.	16.2	647.2	26.	M	22.
184	1900	65.	-25.	26.55	M	2353	46.3	219.5	M	129.	110.	85.3	600.1	52.	M	55.
185	1800	105.	-40.	28.32	M	2246.	37.0	349.5	M	91.	37.	40.7	1045.9	39.	M	76.
186	1800	172.	-32.	22.47	M	1420.	50.7	303.8	M	103.	14.	13.6	475.0	76.	M	57.
187	1900	44.	-49.	23.44	M	1290.	73.6	422.6	M	68.	8.	11.8	932.5	55.	M	54.
188	1900	93.	-46.	27.80	27.41	1256.	84.5	436.3	339.9	103.	12.	11.7	561.4	89.	67.	[illegible]
189	1800	80	-29.	28.21	29.36	2062.	48.6	422.1	362.9	79.	13.	16.5	327.8	85.	67	94.
190	1800	92.	-24.	25.78	29.32	2372.	48.9	192.5	226.3	[illegible]	43.	37.7	139.1	120.	[illegible]	[illegible]
191	1800	109.	-20.	26.00	26.60	1319.	47.6	363.9	335.5	102.	11.	10.8	145.9	162.	[illegible]	[illegible]
192	1800	[illegible]	-45.	20.61	22.84	1273.	59.2	273.4	249.6	103.	11.	10.7	105.7	142.	173.	162.
193	1800	115.	-30.	23.79	25.31	1394.	53.8	240.4	224.4	119.	12.	10.1	100.4	165.	215.	233.
194	1800	132.	-22.	26.54	27.12	1361.	47.3	243.3	240.4	139.	15.	10.8	220.8	146.	149.	177.
197	1800	89.	-35	22.54	23.49	1082.	65.3	195.1	193.5	127.	19.	15.0	134.0	139.	166.	195.
205	1900	56.	-41.	21.37	22.93	1852.	102.5	451.0	201.7	53.	16.	30.2	212.1	48.	51.	69
206	1900	0.	-23.	21.15	[illegible]	1724.	89.5	187.0	[illegible]	40.	18.	45.0	221.9	39.	56.	[illegible]
[illegible]	1900	170.	-1.	25.67	31.71	[illegible]	35.6	393.1	454.7	127.	19.	15.0	336.2	142.	167.	133
[illegible]	1900	431.	-23.	23.14	[illegible]	1606.	41.3	42.3	73.8	201.	32.	15.9	206.7	109.	93.	98
[illegible]	[illegible]	[illegible]	-1.	21.45	22.39	1756.	29.1	105.7	131.6	106.	13.	12.0	153.5	78.	61.	[illegible]
213	[illegible]	65.	-8.	21.35	21.98	1718.	29.6	141.4	170.9	64.	20.	23.8	309.1	[illegible]	40.	34.
214	1800	113.	[illegible]	26.36	27.31	1869.	30.5	138.1	190.5	135.	34.	25.2	140.8	134.	172.	176.
[illegible]	[illegible]	103.	7.	20.56	[illegible]	1441.	32.9	163.6	192.4	93.	12.	12.9	139.5	[illegible]	121.	140
[illegible]	[illegible]	[illegible]	[illegible]	22.51	23.33	1418.	55.5	259.6	281.2	75.	9.	11.5	219.1	88	95.	126
219	1800	50.	-3.	24.32	25.50	[illegible]	104.9	537.6	458.0	53.	52.	98.1	443.8	59.	54.	69.
221	1800	59.	-14.	22.42	23.32	1921.	50.1	219.1	211.3	71.	76.	107.0	224.5	61.	67.	95.
222	1800	327.	0.	23.95	26.43	1746.	58.0	116.1	80.5	222.	30.	13.5	180.2	186.	129.	127.
[illegible]	[illegible]	-6.	[illegible]	23.49	[illegible]	[illegible]	39.8	331.2	417.4	37.	8.	21.6	170.0	57.	81.	76.
[illegible]	[illegible]	57.	4.	22.55	24.71	1606.	45.3	342.6	411.4	56.	8.	14.3	207.7	77.	102.	95
[illegible]	[illegible]	93.	1	25.26	26.69	1673.	30.0	351.4	436.2	65.	19.	30.2	238.1	88	109.	[illegible]
[illegible]	[illegible]	129.	[illegible]	24.32	26.64	[illegible]	25.8	544.7	597.4	59.	21.	35.6	221.5	118.	148.	133
239	[illegible]	153.	8.	27.14	[illegible]	1552.	24.1	414.4	516.1	47.	54.	114.9	117.5	117.	179.	155
[illegible]	[illegible]	[illegible]	-5.	21.26	23.64	1554.	28.4	561.6	677.5	35.	24.	68.6	211.1	76.	104.	[illegible]
[illegible]	[illegible]	129.	11.	[illegible]	[illegible]	[illegible]	23.9	567.0	[illegible]	49.	52.	[illegible]	231.1	102.	131.	[illegible]
[illegible]	[illegible]	172.	[illegible]	[illegible]	17.27	[illegible]	34.5	167.0	176.5	92.	9.	9.9	119.2	105	125.	[illegible]
249	[illegible]	175.	[illegible]	19.59	20.09	1173.	24.0	159.0	236.8	109.	22.	20.2	97.1	167.	225.	[illegible]
250	1700	93.	5.	20.71	[illegible]	1216.	62.6	392.7	430.8	57.	11.	19.3	105.9	110.	167	214.
252	[illegible]	[illegible]	12	22.66	23.97	1744.	24.0	477.7	522.4	41.	39.	95.1	128.4	104.	147.	172
[illegible]	[illegible]	[illegible]	[illegible]	[illegible]	25.54	2231.	21.5	224.1	313.7	56.	17.	30.4	116.7	87.	136.	[illegible]
256	1700	[illegible]	-3.	16.72	20.04	[illegible]	18.5	162.4	194.0	89.	21.	23.6	110.7	116.	[illegible]	135.
257	1700	[illegible]	-2.	15.19	16.45	912.	23.0	296.6	296.7	56.	7.	12.5	201.0	68.	80.	59.
259	1700	66.	13.	14.92	21.23	1320.	26.4	419.3	492.6	43.	11.	25.6	209.3	78.	98.	100.
261	1700	61.	2.	13.82	17.00	1125.	52.5	199.7	327.6	40.	6.	15.0	237.7	36.	53.	79.
262	1700	109.	29.	22.62	25.44	971.	19.4	650.1	804.1	59.	16.	32.0	409.3	76.	97.	65.

M denotes missing data

Measured with thermocouple array
θ(L) measured with thermocouple array
θ(?) measured with porometer temperature sensor

APPENDIX EIGHT

DAYTIME ENERGY BALANCE DATA SUMMARY

Julian Day	Date	Daylight Interval	Q^*	Q_c	Q_s	λE_p	λQ_{PE}^1	λE_{ES}	α' (dimensionless)	Morning Volumetric Soil Moisture (0.00-0.25 m depth) (m^3 H_2O m^{-3} soil)
			(---------- MJ m^{-2} day^{-1} ----------)							
[illegible]	[illegible] June 09	[illegible]0-1400	15.019	[illegible]	[illegible]	4.696	12 098	9.602	0 42	0 133
[illegible]	June 10	0700-1800	9.696	1 037	[illegible]	2 [illegible]	7 961	6 318	0 45	0 140
162	June [illegible]	0700-1800	11 455	1.106	7 [illegible]	2.415	8 374	6.644	0 38	0 140
164	June 13	0700-1800	12 830	1.679	2 [illegible]	8 3.9	9.539	7 571	1 10	0 158
165	June 14	0700-1800	15.089	3 057	7 768	4.435	10.979	8.713	0 51	0 141
167	June 16	0700-1800	14 425	1 463	4 602	6 360	10.718	8.507	0 65	0 199
168	June 17	0700-1800	16 264	1 643	[illegible] 207	8 409	11.590	9.198	0 91	0 182
169	June 18	0700-1800	10 807	0 645	3 508	6 0x1	7 920	6.285	0.96	0 178
171	June 20	0700-1800	18 [illegible]85	2 807	4 [illegible]47	11 14[illegible]	14.370	11 405	0 98	0 209
174	[illegible] 23	0700-[illegible]	10 774	2 [illegible]29	[illegible] 105	10 [illegible]00	11 778	9 347	1 10	0 106
175	June [illegible]	0700-[illegible]	12 702	[illegible] 079	3 059	7 [illegible]82	8 923	7.052	1 02	0 153
[illegible]	June 26	[illegible]	[illegible]2 [illegible]29	2 [illegible]45	3 [illegible]75	0 [illegible]475	8.615	6.996	0 93	0 10[illegible]
178	June 27	0700-1800	[illegible]4 6[illegible]3	3 [illegible]39	5 [illegible]794	5.627	9 939	7 829	0 71	0 147
[illegible]	June 28	07[illegible]-[illegible]	13.[illegible]96	3 [illegible]65	5.716	[illegible] 075	9.563	7.590	0 67	0 156
183	June 29	0700-1800	8 611	1 10[illegible]	1 564	5.946	6 279	4.983	1 19	0 153
182	July 01	0700-1800	17 568	2 [illegible]49	1.400	13 019	13.791	10.945	1.24	0 187
183	July 02	07[illegible]-1800	[illegible] 650	1 [illegible]416	0 559	6 675	6 556	5 203	1 26	0 160
184	July 03	0700-1800	14 [illegible]29	2 709	3 [illegible]890	8.246	11 070	8 786	0 94	0 151
186	July 04	0700-1800	15.337	3 092	6 830	6 004	12 [illegible]21	9.540	0 83	0 152
187	July 05	0700-1800	15 207	2 662	6.389	6 [illegible]16	11 203	8.895	0 72	0 141
188	July 06	0700-[illegible]00	15 [illegible]4[illegible]	[illegible],189	5 508	6.[illegible]47	20.527	[illegible].347	[illegible] 73	0 [illegible]16
190	July 07	07[illegible]-1800	15 [illegible]87	[illegible].347	[illegible] 667	7 002	11 179	8 872	0 79	0 126
191	July 08	[illegible]-1800	14 [illegible]47	3 [illegible]45	3 [illegible]941	7.361	11 147	8 847	0 83	0 [illegible]34
190	July 09	[illegible]-1800	12 [illegible]30	2 [illegible]870	3 [illegible]341	7 375	10.338	8 205	0 90	0 127
191	July 10	0700-[illegible]0	[illegible].792	1.460	2.206	5.116	6 696	5.[illegible]73	0 94	0 126
192	July [illegible]	0700-1800	15 352	[illegible].632	6 039	6.681	11 159	8.856	0 75	0 [illegible]20
193	July 12	0700-1800	15 366	2 [illegible]92	4 226	8.203	11.305	8 972	0 91	0 128
194	July 13	[illegible]-1800	16 0[illegible]4	2 [illegible]55	3.604	9 [illegible]45	12.706	10 084	0 96	0 [illegible]70
197	July [illegible]	0700-[illegible]	16 [illegible]39	2 568	2.740	11 201	12 309	9.769	1 15	0 [illegible]16
[illegible]	July [illegible]	[illegible]	9 412	1 [illegible]40	0 [illegible]39	7 [illegible]33	7.191	5.707	1 27	0.119
199	July 26	[illegible]	13.671	1 [illegible]7[illegible]	0 981	10.976	11.295	8.964	1.22	0 125
[illegible]	July 21	07[illegible]-1800	16.029	2.[illegible]81	5.166	9.132	12.824	10.178	0 90	0.101
203	July 22	0700-1800	14 [illegible]27	2 318	4.332	7.768	11 016	8.820	0 88	0 [illegible]83
205	July 24	0700-1800	10 799	[illegible] 626	2 240	3.934	9.870	7.832	1 01	0 [illegible]8
206	July 25	0700-1800	11 [illegible]34	2.142	5.500	6.492	10.830	8.595	0.76	0 077
207	July 26	0700-1800	8 140	0 966	2.199	4.972	6.432	5.105	0 97	0 075
208	July 27	0700-1800	13 561	2.248	4.709	6.604	10.896	8 649	0 76	0.065

Julian Day	Date	Daylength Interval	Q^*	Q_G	Q_H	λQ_E	λQ_{PE}[1]	λQ_{ES}	α' (dimensionless)	Morning Volumetric Soil Moisture (0.00-0.25 m depth) (m^3 H_2O/m^3 soil)
			---------- MJ m^{-2} day^{-1} ----------							
[illegible]	July 28	0700-1500	15 339	2 610	6 41[illegible]	6 304	12.368	9.816	0.64	0.065
211	July 30	0700-1700	13.360	1 206	1.713	10.461	10 815	8.583	1 22	0 169
212	July 31	0700-1500	10 569	1 151	0 906	6.507	8.236	6 536	1 30	0 140
213	Aug 01	0700-1600	12.390	1 496	1.148	9.745	9 726	7.719	1 26	0 126
214	Aug 02	0700-1800	14 048	1.920	2.397	9 731	11 441	9.080	1 07	0.092
215	Aug 03	0700-1800	[illegible] 637	0 950	1 600	5 057	6 063	4 812	1.05	0.074
216	Aug 04	0700-1800	10 442	0.525	1 812	8 105	8.765	6.956	1 17	0 088
217	Aug 05	0700-1800	11 330	1 200	3 280	6 849	8 734	6.932	0 99	0 072
218	Aug 06	0700-1800	15 046	2 [illegible]6	6 [illegible]64	6.263	11.732	9.311	0.67	0 067
219	Aug 07	0700-1800	15 164	2 382	7 466	5.335	11.960	9.492	0.56	0 053
222	Aug 10	0700-1700	14 171	2 098	6 [illegible]53	5.460	10.921	8 667	0.63	0 046
223	Aug 11	0700-1800	11 062	1.670	5 253	4.139	8.633	6.851	0 60	0 054
226	Aug 14	0700-1800	12 060	1.537	3 709	6.815	9 213	7.312	0 93	0.076
227	Aug 15	0700-1703	11.626	1 836	5 0.3	4.775	8.771	6.961	0 69	0 063
228	Aug 16	0700-1800	13 679	2 081	7 219	4 376	10 624	8.590	0 51	0 058
229	Aug 18	0700-1600	13.977	2 .68	7 375	4 434	10 988	8.720	0.51	0.056
231	Aug 19	0700-1600	10 701	1 763	4 509	4 429	8 452	6 708	0 66	0 048
237	Aug 25	0700-1600	9.719	1 550	5 302	2 867	7.433	5.899	0.49	0 031
238	Aug 26	0700-1800	11.542	1 995	5 000	4.547	9.042	7.176	0 63	0 039
240	Aug 28	0700-1700	8.910	1.176	4 998	2 735	6.797	5.395	0 51	0.038
241	Aug 29	0700-1600	7 511	1 214	3 087	2 409	5 559	4.412	0 55	0 038
242	Aug 30	0700-1500	8 933	1 423	4 695	2.815	6 762	5 366	0.52	0.040
243	Aug 31	0700-1600	7 503	1.010	3 621	2 872	5 901	4 683	0 61	0 032
246	Sept 03	0700-1600	7 704	0.[illegible]7	2 [illegible]96	4 779	5 362	4.255	1 12	0 103
247	Sept 04	0700-1600	10 490	1.316	3.496	5 638	7 410	5.881	0 96	0 102
248	Sept 05	0700-1800	13 152	1 826	5 308	5 958	9.527	7 553	0 79	0.093
249	Sept 06	0700-1800	11 534	1 658	4 307	5 569	8.482	6.731	0 83	0.079
250	Sept 07	0700-1800	11 878	1 629	5.286	4.763	8 740	6.937	0 69	0.064
251	Sept 08	0700-1700	6 9 5	1 373	2 045	3 528	4 902	3.890	0 91	0 058
252	Sept 09	0700-1800	7.786	1 482	2 866	3 417	5.754	4.567	0 75	0.056
253	Sept 10	0700-1800	9 632	1.811	4 796	3 026	7.210	5.722	0 53	0 050
254	Sept 11	0700-1500	4 796	1.053	1.309	2 345	3.269	2 595	0.90	0 050
257	Sept 14	0700-1800	7.173	0 821	2.757	3.595	4.994	3.963	0.91	0 052
258	Sept 15	0700-1700	10 112	1 550	4.638	3.923	7.301	5.795	0.68	0.046
259	Sept 16	0700-1700	11.268	1.748	6.006	3.434	7.751	6.152	0.56	0 047
260	Sept 17	0700-1700	[illegible]8 210	1 544	3.887	2 779	5.863	4.654	0 60	0 048
261	Sept 18	0700-1700	6 796	0.860	29921	3 015	4 406	3.497	0.66	0 044
262	Sept 19	0700-1700	10 426	2 122	5.299	3.105	7.352	5 819	0.53	0.042

1 λQ_{PE} evaluated from Priestley and Taylor (1972) model (equation 2.40)

APPENDIX NINE

NET PYRRADIOMETER AND PYRANOMETER CHARACTERISTICS AND CALIBRATION SUMMARY

Characteristics of Net Pyrradiometer and Pyranometer

Characteristic	Swissteco Net Pyrradiometer Type S-1	Eppley Precision Spectral Pyranometer Model 2
Response: (approx.)	0.045mV/Wm^{-2} (at 293K)	0.009mV/Wm^{-2}
Linearity of response: (0-1.4kWm^{-2})	±1%	±1%
Temperature dependence: (253 to 313K)	-0.05% (per K)	±0.5%
Cosine response: (at 80° zenith angle)	±4.0%	±1.0%
Impedance: (nominal)	150-200 Ω	650-700 Ω
Time constant: 63.2%	5 S	1 S

NET PYRRADIOMETER AND PYRANOMETER CALIBRATION SUMMARY

Sensor	Calibration Constant[1] (mV/Wm^{-2})		
	Pre-Season	Post-Season	Adopted
Swissteco Net Pyrradiometer Type S-1 #6906	0.04550	0.04614	0.04582
Eppley Precision Spectral Pyranometer Model 2 #11665 F3	0.00921	0.00921	0.00921

1. Sensor calibrations were conducted by the National Atmospheric Radiation Centre, Atmospheric Environment Service, Toronto, Ontario. The pre-season calibrations were conducted on March 14, 1974 and the post-season calibrations on November 15, 1974.

APPENDIX TEN

CONVERSION OF DATE TO JULIAN DAY OF THE YEAR

Date	JAN	FEB	MAR	APR	MAY	JUNE	JULY	AUG	SEPT	OCT	NOV	DEC
1	1	32	60	91	121	152	182	213	244	274	305	335
2	2	33	61	92	122	153	183	214	245	275	306	336
3	3	34	62	93	123	154	184	215	246	276	307	337
4	4	35	63	94	124	155	185	216	247	277	308	338
5	5	36	64	95	125	156	186	217	248	278	309	339
6	6	37	65	96	126	157	187	218	249	279	310	340
7	7	38	66	97	127	158	188	219	250	280	311	341
8	8	39	67	98	128	159	189	220	251	281	312	342
9	9	40	68	99	129	160	190	221	252	282	313	343
10	10	41	69	100	130	161	191	222	253	283	314	344
11	11	42	70	101	131	162	192	223	254	284	315	345
12	12	43	71	102	132	163	193	224	255	285	316	346
13	13	44	72	103	133	164	194	225	256	286	317	347
14	14	45	73	104	134	165	195	226	257	287	318	348
15	15	46	74	105	135	166	196	227	258	288	319	349
16	16	47	75	106	136	167	197	228	259	289	320	350
17	17	48	76	107	137	168	198	229	260	290	321	351
18	18	49	77	108	138	169	199	230	261	291	322	352
19	19	50	78	109	139	170	200	231	262	292	323	353
20	20	51	79	110	140	171	201	232	263	293	324	354
21	21	52	80	111	141	172	202	233	264	294	325	355
22	22	53	81	112	142	173	203	234	265	295	326	356
23	23	54	82	113	143	174	204	235	266	296	327	357
24	24	55	83	114	144	175	205	236	267	297	328	358
25	25	56	84	115	145	176	206	237	268	298	329	359
26	26	57	85	116	146	177	207	238	269	299	330	360
27	27	58	86	117	147	178	208	239	270	300	331	361
28	28	59	87	118	148	179	209	240	271	301	332	362
29	29		88	119	149	180	210	241	272	302	333	363
30	30		89	120	150	181	211	242	273	303	334	364
31	31		90		151		212	243		304		365

REFERENCES

Benci, J.F., 1974: Soybean Stomatal Response to Environmental Conditions, Ph.D. Thesis, Univ. of Missouri-Columbia, 110pp.

Bindon, H.H., 1965: A critical review of tables and charts used in psychrometry. Humidity and Moisture, ed. A. Wexler, Vol. One, Principles and Methods of Measuring Humidity in Gases, Reinhold, New York, 3-15.

Black, T.A., C.B. Tanner and W.R. Gardner, 1970: Evapotranspiration from a snap bean crop. Agron. J., 62, 66-69.

Bradley, E.F., 1972: The influence of thermal stability on a drag coefficient measured close to the ground. Agr. Meteor., 9, 183-190.

Brady, R.A., S.M. Goltz, W.L. Powers and E.T. Kanemasu, 1975: Relation of soil water potential to stomatal resistance of soybean. Agron. J., 67, 97-99.

Carlson, J.B., 1973: Morphology. Soybeans: Improvement, Production and Uses, ed. B.E. Caldwell, Am. Soc. Agronomy, Madison, 17-95.

Cook, N.H. and E. Rabinowicz, 1963: Physical Measurement and Analysis. Addison-Wesley, Reading, Mass., 312pp.

Davies, J.A., 1972: Actual, potential and equilibrium evaporation for a beanfield in southern Ontario. Agr. Meteor., 10, 331-348.

Davies, J.A. and C.D. Allen, 1973: Equilibrium, potential and actual evaporation from cropped surfaces in southern Ontario. J. Appl. Meteor., 12, 649-657.

Deacon, E.L. and W.C. Swinbank, 1958: Comparison between momentum and water transfer. Proc. Symp. Arid Zone Res., UNESCO, Canberra, 38-41.

Denmead, O.T. and I.C. McIlroy, 1970: Measurements of non-potential evaporation from wheat. Agr. Meteor., 7, 285-302.

de Vries, D.A., 1963: Thermal properties of soils. Physics of Plant Environment, ed. W.R. van Wijk, North-Holland Publ. Co., Amsterdam, 210-235.

Dilley, A.C., 1968: On the computer calculation of vapor pressure and specific humidity gradients from psychrometric data. J. Appl. Meteor., 7, 717-719.

Dyer, A.J., 1967: The turbulent transport of heat and water vapour in an unstable atmosphere. Quart. J. R. Meteor. Soc., 93, 501-508.

Dyer, A.J., 1974: A review of flux-profile relationships. Boundary Layer Meteor., 7, 363-372.

Fogel, C.M., 1962: Introduction to Engineering Computations. Int. Textbooks Co., Scranton, 210pp.

Fritschen, L.J., 1965: Accuracy of evapotranspiration determinations by the Bowen ratio method. I.A.S.H. Bull., 10, 38-48.

Fuchs, M. and C.B. Tanner, 1968: Calibration and field test of soil heat flux plates. Soil Sci. Soc. Amer. Proc., 32, 326-328.

Fuchs, M. and C.B. Tanner, 1970: Error analysis of Bowen ratios measured by differential psychrometry. Agr. Meteor., 7, 329-334.

Gandar, P.W. and C.B. Tanner, 1976: Water vapor sorption by the walls and sensors of stomatal diffusion porometers. Agron. J., 68, 245-249.

Jury, W.A. and C.B. Tanner, 1975: Advection modification of the Priestley and Taylor evapotranspiration formula. Agron. J., 67, 840-842.

Kanemasu, E.T., L.R. Stone and W.L. Powers, 1976: Evapotranspiration model tested for soybean and sorghum. Agron. J., 68, 569-572.

Kanemasu, E.T., G.W. Thurtell and C.B. Tanner, 1969: Design, calibration and field use of a stomatal diffusion porometer. Plant Physiol., 44, 881-885.

Latimer, J.R., 1972: Radiation Measurement. Int. Field Year for the Great Lakes. Tech. Manual Ser., 2, 53pp.

Lemon, E.R., 1967: Aerodynamic studies of CO_2 exchange between the atmosphere and the plant. Harvesting the Sun, ed. A. San Pietro, F.A. Greer and T.J. Army, Academic Press, New York, 263-290.

Lourence, F.J. and W.O. Pruitt, 1969: A psychrometer system for micrometeorology profile determination. J. Appl. Meteor., 8, 492-498.

McCaughey, J.H. and J.A. Davies, 1975: Energy exchange in a corn canopy. Can. J. Plant Sci., 55, 691-704.

McNaughton, K.G. and T.A. Black, 1973: A study of evapotranspiration from a Douglas fir forest using the energy balance approach. Water Resources Res., 9, 1579-1590.

Monteith, J.L., 1965: Evaporation and environment. The State and Movement of Water in Living Organisms, ed. G.F. Fogg, Academic Press, New York, 205-234.

Monteith, J.L., 1973: Principles of Environmental Physics. Edward-Arnold, London, 241pp.

Monteith, J.L., G. Szeicz and P.E. Waggoner, 1965: The measurement and control of stomatal resistance in the field. J. Appl. Ecol., 2, 345-355.

Morrow, P.A. and R.O. Slatyer, 1971: Leaf resistance measurements with diffusion porometers: Precautions in calibration and use. Agr. Meteor., 8, 223-233.

Penman, H.L., 1948: Natural evaporation from open water, bare soil and grass. Proc. Roy. Soc., London, A193, 129-145.

Penman, H.L. and R.K. Schofield, 1951: Some physical aspects of assimilation and transpiration. Symp. Soc. Exp. Biol., 5, 115-129.

Priestley, C.H.B. and R.J. Taylor, 1972: On the assessment of surface heat flux and evaporation using large-scale parameters. Mon. Wea. Rev., 100, 81-92.

Rosenthal, W.D., E.T. Kanemasu, R.J. Raney and L.R. Stone, 1977: Evaluation of an evapotranspiration model for corn. Agron. J., 69, 461-464.

Rouse, W.R. and R.B. Stewart, 1972: A simple model for determining evaporation for high-latitude upland sites. J. Appl. Meteor., 11, 1063-1070.

Scarborough, J.B., 1962: Numerical Mathematical Analysis. John Hopkins Press, Baltimore, 594pp.

Šesták, Z., J. Čatský and P.G. Jarvis, 1971: Plant Photosynthetic Production: Manual of Methods. Dr. W. Junk N.V. Publishers, The Hague, 818pp.

Sinclair, T.R., L.H. Allen and E.R. Lemon, 1975: An analysis of errors in the calculation of energy flux densities above vegetation by a Bowen-ratio method. Boundary Layer Meteor., 8, 129-139.

Slatyer, R.O. and I.C. McIlroy, 1961: Practical Micrometeorology. UNESCO, Paris, 300pp.

Stanhill, G., 1969: A simple instrument for the field measurement of turbulent diffusion flux. J. Appl. Meteor., 8, 509-513.

Stewart, R.B. and W.R. Rouse, 1976(a): Simple models for calculating evaporation from dry and wet tundra surfaces. Arctic Alpine Res., 8, 263-274.

Stewart, R.B. and W.R. Rouse, 1976(b): A simple method for determining the evaporation from shallow lakes and ponds. Water Resources Res., 12, 623-628.

Swinbank, W.C., 1964: The exponential wind profile. Quart. J. R. Meteor. Soc., 90, 119-135.

Swinbank, W.C., 1968: A comparison between the predictions of dimensional analysis for the constant-flux layer and observations in unstable conditions. Quart. J. R. Meteor. Soc., 94, 460-467.

Swinbank, W.C. and A.J. Dyer, 1967: An experimental study in micrometeorology Quart. J. R. Meteor. Soc., 93, 494-500.

Szeicz, G. and I.F. Long, 1969: Surface resistance of crop canopies. Water Resources Res., 5, 622-633.

Szeicz, G., G. Endrodi and S. Tajchman, 1969: Aerodynamic and surface factors in evaporation. Water Resources Res., 5, 380-394.

Szeicz, G., C.H.M. van Bavel and S. Takami, 1973: Stomatal factor in the water use and dry matter production by sorghum. Agr. Meteor., 12, 361-389.

Tan, C.S. and T.A. Black, 1976: Factors affecting the canopy resistance of a Douglas fir forest. Boundary Layer Meteor., 10, 475-488.

Tanner, C.B., 1963: Basic instrumentation and measurements for plant environment and micrometeorology. Soils Bull., 6, University of Wisconsin.

Tanner, C.B. and M. Fuchs, 1968: Evaporation from unsaturated surfaces: a generalized combination method. J. Geophys. Res., 73, 1299-1304.

Tanner, C.B. and W.A. Jury, 1976: Estimating evaporation and transpiration from a row crop during incomplete cover. Agron. J., 68, 239-243.

Tanner, C.B. and W.L. Pelton, 1960: Potential evapotranspiration estimates by the approximate energy balance method of Penman. J. Geophys. Res., 65, 3391-3413.

Thom, A.S., 1972: Momentum, mass and heat exchange of vegetation. Quart. J. R. Meteor. Soc., 98, 124-134.

Thom, A.S., 1975: Momentum, mass and heat exchange of plant communities. Vegetation and the Atmosphere, ed. J.L. Monteith, Academic Press, New York, 57-109.

Van Wijk, W.R., 1965: Soil microclimate, its creation, observation and modification. Agricultural Meteorology, Meteor. Mono., 6, 59-73.

Wilson, R.G., 1971: Methods of Measuring Soil Moisture. Int. Field Year for the Great Lakes Tech. Manual Ser., 1, 20pp.

Wilson, R.G. and J.H. McCaughey, 1971: Soil heat flux divergence in a developing corn canopy. Clim. Bull., 9, 9-16.

Wilson, R.G. and W.R. Rouse, 1972: Moisture and temperature limits of the equilibrium evapotranspiration model. J. Appl. Meteor., 11, 436-442.